AAAS

Science



SNAP SHUT

Venus flytrap's fast cell wall softening allows rapid closure pp. 1127 & 1183

11 JUNE 2026

Climate may not kill the vital Atlantic 'conveyor belt' p. 1112

Science-inspired fiction for summer p. 1118

Metamaterials for strong and subtle sensing p. 1177

Science
AAAS

Unveiling the complexity of post-Roman polity formation using ancient DNA

Authors
Yijie Tian, István Koncz, Norbert Faragó, Corina Knipper, Ronny Friedrich, Deven N. Vyas, Levente Samu, Olga Spekker, Tamás Szeniczey, Tamás Hajdu, Balázs Gusztáv Mende, Péter Tomka, Ildikó Katalin Pap, Dávid Czigány, Rita Radzeviciute, Luca Traverso, Guido Alberto Gnecchi-Ruscone, Paolo Francalacci, Bernd Schöne, Gábor Tóth, Anna Szécsényi-Nagy, Petrus le Roux, Kurt W. Alt,, Zuzana Hofmanová, Walter Pohl, Johannes Krause, Tivadar Vida, Patrick J. Geary, and Krishna R. Veeramah, DOI https://doi.org/10.1126/science.aec2634

Corresponding authors. Email: krishna.veeramah@stonybrook.edu, geary@ias.edu and koncz.istvan@btk.elte.hu

Rights Retention Statement
This Author Accepted Manuscript (AAM) is made available under the terms of the Creative Commons Attribution 4.0 License (CC BY 4.0).
The definitive version was published in Science on 11 June 2026, DOI: https://doi.org/10.1126/science.aec2634

Title: Unveiling the complexity of post-Roman polity formation in Pannonia using ancient DNA

Authors: Yijie Tian[1,#], István Koncz[2,#,*], Norbert Faragó[2], Corina Knipper[3], Ronny Friedrich[3], Deven N. Vyas[1], Levente Samu[2], Olga Spekker[4], Tamás Szeniczey[5], Tamás Hajdu[5,6], Balázs Gusztáv Mende[7], Péter Tomka[8], Ildikó Katalin Pap[9], Dávid Czigány[8], Rita Radzeviciute[10], Luca Traverso[10], Guido Alberto Gnecchi-Ruscone[10,11,12], Paolo Francalacci[13], Bernd Schöne[14], Gábor Tóth[15], Anna Szécsényi-Nagy[7,16], Petrus le Roux[17], Kurt W. Alt[14,18], Zuzana Hofmanová[10,19], Walter Pohl[20], Johannes Krause[10], Tivadar Vida[2,7], Patrick J. Geary[21,*] and Krishna R. Veeramah[1,*]

Affiliations:
1. Department of Ecology and Evolution, Stony Brook University, Stony Brook, NY 11794, USA
2. Institute of Archaeological Sciences, Department of Humanities, Eötvös Loránd University, Budapest 1088, Hungary
3. Curt Engelhorn Center Archaeometry, 68159 Mannheim, Germany
4. Department of Biological Anthropology, Institute of Biology, University of Szeged, Szeged 6726, Hungary
5. Department of Biological Anthropology, Faculty of Science, Eötvös Loránd University
6. Centre for Applied Bioanthropology, Institute for Anthropological Research
7. Institute of Archaeogenomics, HUN-REN Research Centre for the Humanities, Budapest 1097, Hungary
8. Rómer Flóris Művészeti és Történeti Múzeum, Győr 9022, Hungary
9. Institute of Hungarian Research, Budapest 1062, Hungary
10. Department of Archaeogenetics, Max Planck Institute for Evolutionary Anthropology, Leipzig 04103, Germany
11. Archaeo- and Palaeogenetics, Institute for Archaeological Sciences, Department of Geosciences, University of Tübingen, Tübingen 72074, Germany
12. Senckenberg Centre for Human Evolution and Palaeoenvironment at the University of Tübingen, Tübingen 72074, Germany
13. Dipartimento di Scienze della Vita e dell'Ambiente, Università di Cagliari, Cagliari 09126, Italy
14. Institut für Geowissenschaften, Johannes Gutenberg-Universität Mainz, Mainz 55122, Germany
15. Department of Biology, Berzsenyi Dániel Teacher Training Centre, Savaria University Centre, Eötvös Loránd University, Szombathely 9700, Hungary
16. MTA-BTK Lendület 'Momentum' Bioarchaeology Research Group, Budapest, Hungary
17. Department of Geological Sciences, University of Cape Town, Rondebosch, South Africa
18. Danube Private University, Dept. Natural and Cultural Human History, Krems, A 3500, Austria
19. Department of Archaeology and Museology, Faculty of Arts, Masaryk University, Brno, Czechia
20. Institute for Medieval Research, Austrian Academy of Sciences; Institute for Austrian Historical Research, University of Vienna, Vienna 1020, Austria
21. School of Historical Studies, Institute for Advanced Study, Princeton, NJ 08540, USA
#. These authors contributed equally

*. Corresponding authors. Email: krishna.veeramah@stonybrook.edu, geary@ias.edu and koncz.istvan@btk.elte.hu

Abstract: The transformation of the Roman world (4th–9th centuries CE), culminating in the Western Roman Empire's fall, marked a fundamental transition in European history. Key questions persist regarding the regionally specific nature of this transformation. We generated a paleogenomic dataset to reconstruct post-Roman organizations in the Little Hungarian Plain at micro-regional resolution. Genetic and archaeological analyses of two Roman (n=68) and five post-Roman (n=246) sites reveal a rise in Northern European ancestry, reflecting large-scale population movements into this region. Moreover, despite post-Roman sites sharing similar genetic profiles, material culture, and burial practices, they show distinct social structures, especially regarding the role played by biological relatedness. These findings highlight local hierarchies and reveal the making of a post-Roman polity.

.

Main Text:

Introduction

The 4th-6th centuries CE marked a period of substantial demographic, cultural, and political change in Europe, coinciding with the Western Roman Empire's dissolution and the emergence of various post-Roman polities within and beyond its former territories (*1–3*). While contemporary authors ascribed agency in these processes to what they termed "barbarian" peoples and highlighted the role of migration in these changes, more recent historical research has attributed economic, social and cultural transformations to internal factors rather than population movements (*1*, *2*, *4*).

The Little Hungarian Plain (henceforth LHP), located along the Danube between the Alps and the Transdanubian Mountains (Fig. 1), provides an ideal case study for understanding these transformations. As part of the Pannonian provinces, by the 4th century CE it had become an important frontier zone of the Roman Empire, while also serving as an internal border region connecting the western and eastern halves of the empire. With major urban centers such as Savaria, Scarbantia, and Arrabona, the region was supported by a well-developed military and civic infrastructure. Main trade routes crossed the region along the Danube to the west and the Amber Road running north to south (*5–9*). Following the abandonment of the region by the Roman administration in the first half of the 5th century, the territory witnessed multiple political shifts. These included the short-lived rule of the Huns and the appearance of groups of Germanic origin, including the Langobards who established a kingdom in the area around 500 CE that lasted until their migration to Italy in 568 (*7*, *10–12*). While there is no clear evidence for the continuous habitation of Roman towns (*8*, *9*), the emergence of new communities and the high diversity of archaeological sites show the importance of the region during the 6th century, as it became one of the core territories of this emerging new polity (*11–14*).

Archaeological records show changes in settlement structure and material culture suggesting a major transformation affecting everyday life, burial customs, sustenance strategies, and political administration (*5*, *11*, *12*). During the Roman period, communities formed a dense infrastructural and collaborative network which provided the basis of both local and regional organization (*8*, *9*, *15–18*). The organization of post-Roman, early medieval polities however is more obscure. While 6th-century cemeteries display a picture of stratified communities and diverse long-distance cultural connections (*11–13*), the lack of contemporaneous settlements and the silence of detailed written sources indicate that these cemeteries represented small rural communities, providing little understanding of how they formed parts of larger structures (*11*, *12*).

To better understand the development of the LHP during these periods, we sequenced 314 ancient genomes dated between the 3rd and 6th centuries CE from seven completely sampled sites (Fig. 1). By integrating genetic, isotopic, and archaeological evidence, we sought to address two longstanding questions: First, to what extent do changes described in historical sources and observed in the LHP archaeological record reflect underlying large-scale population movements rather than internal cultural and political transformations? Second, what forms of community formation, development, and interactions could be observed among contemporaneous sites in a single region?

Dense sampling of the LHP

We chose cemeteries with available archaeological and osteological material and aimed to include all available individuals from seven sites (Fig. 1, Table S1, Supplementary Text S1). The Late Roman period is represented by two sites near the Roman town of Arrabona (today Győr, Hungary): Győr-Frigyes lkt. is a small burial group (n=2) dated to the 3rd century CE, while Győr-Széchenyi square belonged to a community (n=66) dated to 4th-5th century CE, the latest phase of the Roman town (*19*, *20*). Burial sites are rare in the middle/second half of the 5th century, the Hunnic period, when late Roman towns had lost their urban character and role in the region, but a series of newly founded cemeteries emerged around 500 CE (*5*, *12*). During the Langobard occupation in the 6th century, sites ranged from large (ca. 100 burials) and small (ca. 20-40 burials) cemeteries to burial groups with only a few graves (*11*, *13*). Therefore we sampled two large sites, Hegykő (n=74) and Szeleste (n=110), founded at the end of the 5th century and used until the second half of the 6th century (*21–23*), and three smaller sites, Gyirmót (n=32), Kóny (n=11) and Ménfőcsanak (n=19), each in use only for a few decades in the mid-6th century (*7*, *24*). All post-Roman sites are directly connected to late Roman infrastructure and/or earlier urban centers but represent rural communities living outside the former towns (*5*, *15*, *16*). They show similarities in their archaeological material, with shared artefact types (most notably brooches) and long-distance connections with Northern and Western Europe and the Mediterranean (*12*, *13*, *25–27*)**.**

Our comprehensive sampling strategy yielded 314 new ancient DNA genomes (Table S1, S2) from the Late Roman period (n=68, two sites) and the 6th century (n=246, five sites), along with additional $^{87}Sr/^{86}Sr$ (n=247, 5 sites), $\delta^{13}C$ and $\delta^{15}N$ (n=283, 5 sites) measurements and new radiocarbon dates (n=38, 6 sites, Table S1) (Table S1, Supplementary Text S2, Fig. S1-S13). Genomic libraries were prepared from petrous bone and underwent partial UDG treatment (*28*) followed by an in-solution capture targeting ~1.2M single nucleotide polymorphisms (SNPs) (*29*, *30*) (henceforth 1,240K capture) and Illumina sequencing. The average SNP coverage was ~1.95×. We estimated low contamination in all individuals (mean 1%) based on X chromosomes in males (as determined by relative X/Y reads) and mtDNA in all individuals. Samples were filtered according to the requirements of each downstream analysis (see Materials and Methods and Table S1).

Post-Roman influx of northern ancestry

Historical sources document multiple migratory events in the LHP between the middle of the 5th and 6th centuries that correspond with changes in the archaeological record (*5*). The scarcity of later 5th century sites and absence of evidence for the continuous use of late Roman towns have been interpreted as signs of depopulation, or even abandonment, of the area following the Roman period (*5*, *8*, *9*). The appearance of new communities around 500 CE and during the 6th century are generally attributed to the expansion of the Langobards into the region (*7*, *11*, *12*).

To examine evidence of migration through changes in genomic ancestry, we conducted principal component analyses (PCA), with the 3rd-5th (n=68) and 6th-century (n=246) individuals projected onto the modern European POPRES reference set (*31*). We observed changes in the ancestry composition between the two periods: 3-5th-century individuals displayed a unimodal distribution along PC1 (Silverman test, k=1: p=0.89), clustering primarily with modern southern European populations. In contrast, the 6th century individuals showed a bimodal distribution

(Silverman test, k=1: p=0; k=2: p=0.53) centered around both modern northern and southern European populations, the latter overlapping with the previous period. The 3rd-5th-century individuals also exhibited a greater variance along PC2 (*t*-test on variance, p<<0.001) (Fig. 2A, Fig. S14). The Roman and post-Roman period populations also demonstrated a significantly different pairwise F_{ST} (F_{ST}=0.0021, z-score=9.99).

We also applied two model-based analyses (fastNGSadmix (*32*) and qpAdm (*33*)) (Fig. 2B) to estimate individual genomic ancestry proportions based on a penecontemporary reference panel (See Table S3 column "fastNGSadmix and qpAdm_source") modified from Vyas, Koncz et al. (*34*), and consisting of n=219 4-8th CE individuals grouped into eight ancient populations representing contemporary Mediterranean Europe (MEDEU), Northern Germany/Britain (NGBI), Scandinavia/Estonia (SCAND), East Asia (EASIA), South Asia (SASIA), Central Asia (CASIA), North Africa (NAFRICA), and sub-Saharan Africa (SUBSAHARAN). FastNGSadmix results (Table S4, Figs. S15-S16) were consistent with the PCA: 3rd-5th-century sites exhibited a major contemporary Southern European (MEDEU) ancestry (64.5%), while 6th-century sites displayed a higher Northern European (NGBI+SCAND, 59.3%) compared with Southern ancestry (38.6%). Despite using modern reference populations, the PC1 values were significantly correlated with both ancient Northern and Southern European ancestry (Pearson's $r = -0.94$ and 0.94, respectively; both p<0.001). We also observed a higher proportion of non-European ancestry (CASIA, EASIA, NAFRICA, SASIA, and SUBSAHARAN) in the 3-5th-century sites compared to the 6th-century sites (mean=5.9% vs. 1.3%, *t*-test p=0.03). When using qpAdm (Table S5-S6 and Fig. S17-S18), 77% of LHP individuals could be modeled with one or two-source models (p>0.01), and yielded results that closely aligned with fastNGSadmix (estimated proportions of all eight ancestries, except SUBSAHARAN and SASIA, were significantly correlated (p<0.001)) (Figs. S19-S20). As a complementary approach, we performed unsupervised clustering (NGSadmix (*35*)) on unrelated samples. At K=2, the analysis recapitulated the North-South gradient observed in our supervised models (Fig. S21). The inferred ancestral components were highly correlated with the SCAND+NGBI and MEDEU components (R=0.929, p<<0.001 and R=-0.922, p<<0.001) (Fig. S22), demonstrating that our major inferences are robust to the specific choice of reference populations and are an emerging property of the LHP samples themselves.

We then applied qpWave (*33*) to test whether the Roman and post-Roman periods could be modeled using the same or distinct ancestral sources. We compiled published genomic data from European samples with median ages that predated or were contemporaneous with our two Roman-period LHP sites (*36–44*) and grouped them according to their sampling locations (Fig. S23), forming nine source populations (Table S3). For individuals from the 3rd-5th century, 43 out of 63 could be modeled using one of the penecontemporaneous sources (Fig. 3A, left, Table S7), amongst which only 12% (n=5) could be attributed to Northern European populations (either Northeast_Europe_1-4th c., Northern_Germany_3-8th c., or Scandinavia_3-8th c.).

When examining 6th century individuals, we incorporated two additional local source populations: the 3-5th century samples from the LHP (LHP_3-5th c.) and the previously published 5th-century Lake Balaton samples (Balaton_5th c.) (Table S1, S3, Fig. 3A, right) (*34*). In contrast to the previous period, of the 213 of 234 (91%) 6th-century individuals modeled with one source (Table S8), 41% (n=87) were attributed to Northern European populations (this increase in Northern European ancestry was seen at all four sites, with values ranging from 37-41%, Fig. 3B right). This increase (29%) suggests a possible influx of individuals from more

northern parts of Europe during the 6th century. However, we observed that 20% of individuals could also be modeled by "local" groups (LHP_3-5th c. and Balaton_5th c.), pointing also to some autochthonous continuity of the genetic profile in the post-Roman period.

As observed in the genomic analysis, $\delta^{13}C$ and $\delta^{15}N$ data (283 new measurements and 11 earlier published measurements, Supplementary Text S2) showed that adult individuals significantly differed between the Roman and post-Roman periods (Fig. 4A, Mann-Whitney test for stochastic equality - $\delta^{13}C$: z=5.462; p<0.0001; $\delta^{15}N$: z=8.292; p<0.0001), with higher $\delta^{15}N$ and $\delta^{13}C$ values generally attributed to the 4-5th-century individuals. These differences remained significant even after controlling for genetic ancestry using PC1 and PC2 as covariates in a PERMANOVA test (based on a $\delta^{13}C/\delta^{15}N$ distance matrix, with PC1, PC2, and Period as predictors; p=0.001 for Period). This suggests a change in subsistence strategies and nutrition between the two periods, though this may be linked to the different nature of the sites (for example urban vs rural contexts) rather than the direct result of a newly arriving population with a distinct diet. However, variation was also observed between the 6th-century sites (Fig. 4B, Table S9-S14). Moreover, multiple statistically significant correlations were observed between genetic ancestry and $\delta^{15}N/\delta^{13}C$ values (Fig. S24). For example, individuals with more Southern European ancestry showed higher $\delta^{13}C$ values in Hegykő (p=0.002) and Szeleste (p=0.009), suggesting that parts of the population in the 6th century communities might have retained a diet similar to the earlier period.

To explore individual-level mobility in the post-Roman period, we conducted $^{87}Sr/^{86}Sr$ analysis on all available individuals from the 6th-century sites (n=201, Fig 4C, Table S1, S15, Supplementary Text S2). We defined possible 'local' ranges based on environmental samples, measurements from bone (Table S16), and values of non-adult individuals. The Sr isotope values showed that the ratio of the individuals outside of ranges identified as possibly 'local' varied site by site, between 43 to 74%. These were mostly adult males and females (above 90%), with the exception of Hegykő which included 35.3% non-adult individuals. Adult males and females possessed similar ranges across sites other than Gyirmót, while adults and nonadults demonstrated similar ranges except for Hegykő. Local versus non-local Sr isotope values showed no correlation with genetic ancestry (p>0.05). Thus, while there was a broad influx of a population with predominantly Northern European genomic ancestry into the region, mobility was apparently not restricted by this population-level process, and individuals with southern ancestry that more likely represented the continuity of the Roman period local population were also moving between regions and into these communities as they formed and developed.

Finally, HapROH (*45*) identified only 17 out of 314 individuals with at least one Run of Homozygosity segment longer than 5cM (max - 53cM, mean=12cM), and of those 17, none were enriched at any particular site from both the Roman and post-Roman periods (Table S1). This aligns with broad genomic surveys of ancient Eurasia, which have demonstrated the rarity of close-kin unions during the medieval period (*45*).

Genetics supports Langobard migration

The post-Roman increase in northern genomic ancestry and dietary shift in the LHP indicate the possibility of a migratory event that could be reflected by an enrichment of recent genealogical links between 6th-century individuals in the LHP and specific external regions. Therefore we applied ancIBD (*46*) to detect Identity By Descent (IBD) segments indicative of shared ancestry

up to the 6th degree between individuals in the LHP and 861 penecontemporaneous individuals (Table S3) across Eurasia and Africa.

Given the large number of pairwise comparisons (n=111,930), we found few IBD connections (240, ~0.21%) >12cMs between post-Roman LHP individuals and contemporaneous populations. A similar proportion was found for the Roman period individuals (n=26,691 pairwise comparisons, 41 connections or 0.16%) (Tables S17-S18, Supplementary Text S3). Of the connections observed with post-Roman individuals, those with Northern European individuals predominate (82/116, 71%). Of note, while no UK sites connected with 3rd–5th century LHP individuals, 12 connected with 6th-century sites; similarly, connections with sites in Germany increased from 2 (Roman period) to 6 (post-Roman).

However, these links should be interpreted with caution as a) Northern European individuals are dominant in the reference set (303/861, 35%), b) the highest frequency of connections for both periods was observed in the same location (Groningen, Netherlands), suggesting a consistent background pattern and c) the highest number of external IBD connections observed for the Roman period also involved northern European individuals (13/27, 48%). Thus, our data does not indicate a specific 6th-century migratory event associated with the movement of the Langobards into LHP from a particular area in Europe, but rather a more general regional southward expansion into the (former) Western Roman Empire that was possibly accelerated after its fall (indeed, the presence of Northern European ancestry at the late 5th century Lake Balaton sites pre-dating the Langobard expansion further south (*34*) points to this broader demographic trend). In addition, the increased IBD connections with northern European populations may simply reflect the smaller effective population size associated with this genomic ancestry.

In comparison, when focusing on the historically documented route of the Langobard migration into northern Italy in 568, we observed markedly different patterns before and after the presumed migration. For sites pre-dating the attested migration—Győr-Széchenyi square (4-5th century), 5th century sites in Lake Balaton (*34*), and 5-7th century sites at Bardonecchia and Torino Lavazza in northern Italy (*34*)—we only identified two IBD connections (Fig. 3D_top). However, when focusing on the post-Roman sites along the same route—the 6th-century LHP sites, Szólád and the 6-8th-century site of Collegno—we observed multiple connections that significantly shaped a network constructed from IBD connections between sites from the LHP, Lake Balaton, and Northern Italy (Fig. 3C, 3D_bottom). The network was also primarily structured around individuals with predominantly Northern European ancestry based on fastNGSadmix estimates (Fig. S25). Similarly, when inferring local ancestry with FLARE (*47*) using reference populations from the 1000 Genomes Project, we found that the distribution of IBD segments associated with northern ancestry was significantly larger than that based on southern ancestry (Wilcoxon rank-sum test, $p<0.001$) (Fig. S26-S27).

Altogether, we find a substantial increase in Northern European genetic ancestry between the 3rd–5th and 6th centuries in the LHP, most likely driven by the movement of groups from outside the former Empire. The rarity of sites in the late 5th century suggests that this large-scale demographic shift occurred around 500 CE, coinciding with the emergence of new communities. However, the genomic data do not support a model of complete population replacement. Instead, they point to the persistence and cohabitation of earlier, locally mobile populations from the Roman period alongside incoming groups. These changes could be understood as the results of

the expansion of the Langobard Kingdom into the region, described in detail by written sources (*10*, *12*, *48*, *49*), which is further supported by IBD links between multiple regions that align with the historically inferred route of Langobard migration from the Middle Danube region to Italy (*48*, *49*).

Diverse post-Roman community formation

The Langobards appeared in the Lower Austrian Danube at the end of the 5th century, having already settled in today's Moravia, Czechia. Soon after 500 CE they established their kingdom in the Middle Danube region (*12*, *49*, *50*). The LHP became a core territory of the Langobard Kingdom, evidenced by the emergence of a series of new communities throughout this period. This region placed the Langobards on the European political stage for the first time and served as a crucial staging ground before their migration and eventual conquest of Italy (*12*, *48*, *49*). Archaeological research has described different types of cemeteries in Pannonia based on their chronology, size, and cultural contacts (*11–13*). Hegykő and Szeleste were founded around 500 CE, and the smaller sites, Gyirmót, Ménfőcsanak and Kóny, in the mid 6th century (*7*, *12*, *13*, *24*). While all sites show similar burial customs, including grave design and funerary representation, archaeological material demonstrates this chronological difference, as certain phenomena that are generally found in 5th century contexts, such as artificial cranial deformation, brick-structure graves or polyhedral earrings with garnet inlays, are only present in the earlier sites (*14*, *23*, *51*). Artifact types dated to the middle of the 6th century, such as S-brooches and rosette-shaped disc brooches are found in all 6th-century sites, while similarities in female dress and weaponry show cultural contacts that suggest that these communities were part of the same distribution networks (*13*, *27*).

The largest pairwise F_{ST} amongst the four 6th-century sites with sample sizes >=10 was between Hegykő and Ménfőcsanak (F_{ST} =8.8x10^{-4}), with none being significantly different (z-scores<3). Based on the results from fastNGSadmix, qpAdm, and PCA (Fig. S28), all sites had similar profiles of predominantly Northern and Southern European ancestry, resembling previously published data from nearby Szólád at Lake Balaton (*52*). Similarly, the analysis of uniparental markers showed no significant differences in Y-chromosome or mitochondrial DNA haplotype distributions across the sites (Supplementary Text S4, Tables. S19-S20).

We examined pairwise biological relatedness up to third-degree within the 6th century sites using lcMLkin (*53*) and KIN (*54*) (Table S21-S22, Fig. S29, Supplementary Text S5). Hegykő demonstrated the highest ratio of relatedness, with 67% of all individuals being part of one of the 10 inferred pedigrees. There were three pedigrees with more than four individuals, with the largest consisting of 13 individuals. In contrast, at Szeleste only 34% of the individuals belonged to the 14 pedigrees, only two of which contained more than 4 individuals (maximum 5). Gyirmót (n=32) contained one third-degree related pair (6%), Kóny (n=11) two parent-offspring pairs (36%), and Ménfőcsanak (n=19) had no individuals related up to the third-degree. We thenn tested for differences in the amount of biological relatedness using a resampling approach that controlled for sample size across all 6th-century sites. The results supported a clear division between the 6th-century sites, where Hegykő and the earlier published Szólád possessed significantly more biological relatedness than Szeleste, Gyirmót and Ménfőcsanak (Table S23). Differences in the patterns of more distant biological relatedness (up to 6th degree) were also evident from the ancIBD analysis for samples with 1240k coverage >=1x (n=130) (Fig. 3C). In Hegykő, multiple pedigrees, including all the larger ones, formed a tightly interconnected cluster.

In contrast, Szeleste exhibited a more fragmented structure with very few connections between pedigrees.

The role of biological relatedness in forming these neighboring communities appears to vary, with three general patterns emerging (Fig. 5). At Hegykő (as well as the previously published Szólád), pedigrees tended to only include members of one predominant genetic ancestry, with the larger pedigrees dominated by Northern European genetic ancestry. Members of these extended pedigrees were also buried together in the same area of the site (Fig. S30), indicating that these biological connections were socially meaningful, driving a significant relationship between genetic ancestry and burial proximity (Mantel test, $p<0.0001$). Moreover, the exclusive presence of weapons among members of these pedigrees suggested that they had elevated social and/or economic status in the community (*12*, *49*, *55*), and due to their predominantly Northern European genetic ancestry, there is significant correlation between genetic ancestry and the presence of weapons ($p<0.0001$). While these communities were not strictly patrilocal, as multi-generational female lines also exist, these correlations between biological relatedness and grave goods are observed only for male burials, suggesting a clear difference in burial representation between the two sexes. The elevated social status of the male members of the large pedigrees is also supported by observed differences in nutrition, as they showed higher $\delta^{15}N$ values, suggesting more access and intake of animal proteins (Fig. 4B).

In contrast, the smaller pedigrees at Szeleste and Kóny are more genomically heterogeneous. Only core families (i.e. parent-offspring sets) are buried together, while more distantly related individuals are buried separately in other parts of the cemeteries. Weapons are no longer restricted to pedigrees and also do not show significant correlation with any genetic ancestry. Moreover, no dietary differences are observed between various groups, indicating a less stratified community.

Further, Ménfőcsanak and Gyirmót exhibit little or no biological relatedness (less than 10%) and again there is no correlation between genetic ancestry and spatial organization of the sites or any aspect of burial customs. They also contain a lower ratio of weapons (10% and 13.3% among adult males respectively compared to 57.2% at Hegykő or 41.9% at Szeleste) and female burials with gilded jewelry (0% and 16.7% compared to 28% or 21.7%). However, Hegykő and Szólád were affected to a lesser extent by the grave disturbances characteristic of sixth-century Pannonia than the other three cemeteries examined, possibly leading to an inflation in the level of apparent differences between these two sets of sites.

A post-Roman polity in the making?

Contemporaneous written sources describe the gradual expansion of the Langobard settlement area in the Middle Danube region, though its extent, nature, and political context remain debated (*11*, *12*, *49*, *50*). Based on genomic ancestry, the five 6th-century LHP sites appear statistically indistinguishable. However, the integration of pairwise relatedness, burial practices, and historical-archaeological context reveals that multiple modes of community formation were shaped by interactions between incoming groups with higher proportions of Northern European ancestry and local populations with predominantly Southern European ancestry. However, genomic ancestry did not necessarily correspond with social differences. Rather than existing as separate entities, these groups cohabited and mixed in varying ways across sites, generating diverse community structures that might suggest a hierarchical relationship among sites. These

communities expressed cultural connections through their burial customs and grave goods, were spatially linked through the use of late Roman infrastructure, and were biologically connected as shown by the IBD links between them. This multi-layered network and possible hierarchy between the sites could have served as the basis of regional-level formation and development of an emerging post-Roman polity.

Correlations between weapons, grave organization, and pedigrees suggest that status inheritance was already established early in the 6th century in communities such as Hegykő, and that biological relatedness helped shape social kinship. Dominant lineages exhibit elevated social status that could indicate emerging elite communities of local or even regional importance. In contrast, at nearby Szeleste—archaeologically similar in burial style and material culture—such factors played a more limited role, highlighting the parallel emergence of distinct social models within the region. Notably, these cemeteries were previously viewed as representing the same rural community type, underscoring the added multi-dimensional resolution genomic data brings.

This mosaic of socioculturally diverse communities likely formed the basis of a new regional post-Roman polity. Written sources describe the Langobard Kingdom's involvement in dynastic marital alliances as well as extensive wars with its neighbors, and by the middle of the 6th century it had become a defining regional power with the occupation of Southern Pannonia (*49*). At the same time, settlement density increased, and new communities like those of Gyirmót, Kóny, and Ménfőcsanak emerged, making great use of surviving late Roman infrastructure, especially roads (*15*, *16*). One explanation of these communities is that they were not constituted through (biological) kinship relations, but instead emerged under the influence of external organizational forces. It is conceivable that (political or military) elites created them to secure control over strategically important locations or consolidate power through the strengthening of the networks. A similar situation is described by Paul the Deacon (*56*) in the case of the conquest of Cividale in Italy, when the dux of the city handpicked his followers to settle and defend the city. The term *fara*, attested in several written sources, may refer to either extended kin groups or mobile military units (*57–59*). Our genomic results suggest that the emerging Langobard society had begun to expand from primarily biological kinship-based structures to more diverse forms of social cohesion and community organization. Alternatively, the disrupted kinship structure in later cemeteries may reflect broader demographic shocks, such as the Justinianic Plague (*60*).

Concurrently, new artefact types emerged which could be understood as local productions (*27*). This process is especially visible in the case of S-shaped brooches, one of the most common and fast-changing jewelry types in all Western Europe during the period. While not completely replacing imported types, their widespread adoption suggests the presence of a strong communication network and shared cultural preferences (*27*). These developments, together with the appearance of new communities and expansion of the settlement area, indicate the emergence of a shared identity and the consolidation of Langobard political power. Rather than a loose collection of rural settlements, our data suggest a hierarchically structured network of communities.

Materials and Methods

Data Generation and Bioinformatic Processing

Various types of bones (Table S1) were sampled from all individuals dated to the Late Roman period (n = 68, from two sites) and the 6th century (n = 246, from five sites). Sample preparation was carried out in the dedicated ancient DNA laboratory facilities at the HUN-REN RCH Institute of Archaeogenomics in Budapest, Hungary. Bone surfaces were decontaminated using UV-C light and mechanically cleaned. Approximately 25–50 mg of bone powder was obtained by drilling or grinding and subsequently transferred to the Max Planck Institute for Evolutionary Anthropology (MPI-EVA) in Leipzig, Germany. DNA extraction and single-stranded library preparation (ssLib) were performed at the MPI-EVA Core Unit. This included the application of the partial UDG (UDG half) protocol to remove most of the ancient DNA damage from DNA fragments while preserving the typical C-to-T substitutions at the terminal nucleotides (*28*). In the same facility, two rounds of 1240k in-solution capture were performed (*30*), then sequencing was conducted using the Illumina HiSeq 4000 platform, generating 75-cycle single-end reads. Each library was sequenced to a depth of approximately 20 million reads.

The software pipeline nf-core/eager v2.3.2 was employed for the following further processing of the raw reads (*61*): adapters were removed from the sequenced reads with the AdapterRemoval (*62*); BWA v0.7.17 was employed to map the reads to the human reference genome with “bwa aln” (with the parameters: -n 0.01 -l 1024) and BWA samse (in case of single-end reads) or BWA sampe (paired-end) (*63*); reads with <30 phred mapping quality were discarded with Samtools v1.9 (*64*). PCR Duplicate reads were removed with Picard tools MarkDuplicates v.2.26.0 (https://github.com/broadinstitute/picard). A measure of the duplication rate, ClusterFactor (the ratio of total reads to unique reads at a given locus) was calculated for every sample (Table S1). To estimate the amount of C to T taphonomic deamination at the ends of the mapped fragments we used mapDamage v2.0 (*65*) run on a subset of 100,000 q30-reads.

Genotypes were called using an in-house indent caller that excluded the first and last five bases of each read (www.github.com/kveeramah). The resulting VCF files contained diploid genotypes and genotype likelihoods. Coverage for autosomal 1240K SNPs and the mitochondrial genome was assessed for all individuals using GATK v4.2 DepthOfCoverage (*66*). The number of autosomal 1240K SNPs covered by at least one read with mapping and base quality scores of 30 or higher was determined for each BAM file using samtools depth (*67*). Genetic sex was inferred using the Sex.DetERRmine pipeline, which evaluates relative X and Y chromosome coverage (https://github.com/TCLamnidis/Sex.DetERRmine). Nuclear contamination rates in genetic males were estimated with ANGSD based on the hemizygous X chromosome (*68*), while mitochondrial contamination rates for all individuals were assessed using Schmutzi (*69*).

We ran hapROH to estimate runs of homozygosity (ROH) in all 314 individuals from the LHP. The pseudohaploid PLINK files were converted to EIGENSTRAT format using Convertf (https://github.com/argriffing/eigensoft/tree/master/CONVERTF). We used the default global dataset from the 1000 Genomes Project (5008 haplotypes from 2504 individuals) as a reference panel, filtered to include only biallelic 1240K SNPs. The analysis was performed using the settings: min_cm=[4, 8, 12, 20], snp_cm=50, gap=0.5, min_len1=1.0, and min_len2=4.0. We counted all ROH segments longer than 5 cM.

Mitochondrial and Y Chromosome Haplotype Analysis

For mitochondrial DNA analysis, BAM files from the newly sequenced individuals were filtered to retain only reads mapping to the mitochondrial genome, which were then converted to FASTQ format using samtools (*67*). Mitochondrial genomes were assembled for individuals with more than 1,500 mitochondrial reads using the Mapping Iterative Assembler (*70*), a tool specifically designed for ancient mitochondrial genome assembly. Haplotype assignment was then performed with MitoTool 1.1.2 (*71*) to determine mitochondrial haplogroups. We only reported mtDNA haplogroups for individuals with greater than 2x average mitochondrial coverage (Table S1, column W). All downstream uniparental marker analyses are based on this filtered dataset.

Y chromosome haplotypes were estimated based on the 1240K Y chromosome SNPs. Y chromosome VCF files were compiled in Excel, and the phylogenetic position of each Y chromosome SNP was determined using information from published databases (https://isogg.org/, accessed on 08/31/2023) and the ISOGG repository (International Society of Genetic Genealogy, consulted on December 20, 2025) (*72–75*). To ensure long-term reproducibility despite frequent changes in ISOGG nomenclature, we adopted a mutation-based classification strategy following Ravasini et al. (*76*). This allowed for the identification of NRY haplogroups, named according to the terminal SNPs identified and the updated ISOGG nomenclature. For each sample, we have reported both the alphanumeric haplogroup label and the specific diagnostic SNPs (main branch and terminal mutations) in Table S2. Previously unclassified SNPs were assigned to haplogroups using a cladistic approach, accounting for the non-recombining nature of the NRY. Singletons were excluded unless already present in the referenced public databases.

Principal Component Analysis (PCA)

PCA was conducted by projecting target ancient samples onto a modern reference dataset using a 'leave-one-out' (or 'drop-one-in') procedure (*77*). First, the LHP diploid 1240K VCF files were converted to pseudohaploid plink datasets using a custom, in-house script. For this conversion, heterozygous genotype calls were resolved by selecting the allele with the higher read depth; in cases where allele depths were equal, an allele was chosen at random. The modern reference panel was integrated from the POPRES (*31*) datasets in its imputed form (*78*). The final analysis was based on 32,9302 SNPs overlapping between the LHP individuals and the reference dataset.

The PCA was performed using SmartPCA (*79*, *80*) on one ancient individuals at a time onto the reference panel. (https://github.com/ShyamieG/misc_scripts/blob/master/Procrustes_transform_PCA.py). To unify these results, we employed a Procrustes transformation (using a custom script) to merge all LHP individuals with at least 10,000 overlapping SNPs into a single PCA space. The individual with the highest SNP count (Hegyko_06) served as the fixed basis for this transformation; consequently, the variance explained by PC1 and PC2 is derived from the Hegyko_06 PCA. Finally, we visualized the results using theeaborn.kdeplot (*81*) function (default setting) to generate the Kernel Density Estimation contours.

Model-Based Clustering Analyses

Model-based clustering analysis was conducted using fastNGSadmix (*32*), applying a penecontemporaneous reference panel including 8 populations that developed from a previously published panel (*34*), supplemented with an additional CASIA panel representing Central Asia. The Beagle PL files were generated using vcftools (*82*) for all the 314 individuals at 1,082,095 autosomal sites for use by fastNGSadmix. The analysis was run separately for each individual using default parameters 30 times with random seeds, and the run with the highest likelihood chosen as the final result. The admixture plots shown in Fig. 2B utilize the point estimates given by the best run.

In order to assess the reliability of our fastNGSadmix admixture coefficients, we implemented a simple block bootstrapping procedure to estimate confidence intervals. A block bootstrap approach was chosen in order to incorporate the potentially inflated error arising from the correlation structure of neighboring SNPs being in linkage disequilibrium. Bootstrapping was performed over 10Mb non-overlapping blocks (as such the genome is divided into 300 discrete blocks across all autosomes), where 300 blocks are sampled randomly with replacement. We ran 50 bootstrap iterations for each individual and plotted the 90% confidence intervals (ranging from the 5th to the 95th quantile estimates) and the 50% confidence intervals (ranging from the 25th to the 75th quantile estimates) for each ancestry component across all 314 individuals. The mean SD for the eight ancestries are 0.2552% (SUBSAHARAN), 0.3274% (NAFRICA), 0.3840% (EASIA), 0.8138% (SASIA), 0.9026% (CASIA), 7.333% (MEDEU), 9.018% (SCAND) and 13.72% (NGBI). Non-Europeans ancestries had much smaller SDs. (Fig. S15-S16).

Unsupervised Clustering analysis

In addition to the supervised analysis, we also conducted an unsupervised model-based clustering analysis to determine how dependent our results were on the choice of reference populations. For this we used NGSadmix (*35*), which accounts for genotype uncertainty in low-coverage sequencing data by working directly with genotype likelihoods. The analysis was performed on a filtered dataset of 314 unrelated individuals (See Table S1 column “Used in analyses removing relatives”). We converted the genotype likelihoods into Beagle format and ran NGSadmix for K ancestral populations ranging from 2 to 8. For each K value, we performed 10 independent replicates with random seeds to ensure convergence to the global maximum likelihood. The results for K=2 through K=4 are presented alongside the fastNGSadmix results in Fig. S21. Results for higher K values are excluded as they lacked clear biological resolution and large variation across runs.

At K=2 the unsupervised analysis recapitulates the general North-South signal identified in our supervised analyses and that is the dominant ancestry component across all our LHP samples and drives most of our ancestry-related inferences. Indeed one unsupervised component demonstrated a strong and significant correlation with the Northern European reference populations (defined as the sum of NGBI and SCAND ancestry proportions; $r = 0.929$, p-val $<<0.001$). Similarly, the second component correlated strongly with the southern MEDEU

component (r = 0.922, p << 0.001). For values of K> =2, the inferred components provided no obvious additional informative population structure and varied considerably across replicate runs. For instance, when K=3, the additional component only contributes to about 10% of the total ancestry proportion, and varies considerably from run to run (twice to four times the variances of the major components across runs). This suggests that the unsupervised approach lacks sufficient power to make useful inferences beyond K=2 . This is unsurprising, as the low F_{ST} between the two northern and southern components is already close to the likely inference limit of unsupervised model-based clustering analysis, especially for low coverage data such as these, making inference of further population structure for minor components not well represented in the samples an extremely difficult analytical problem. This supports the primary use of supervised analysis when interpreting population structure in our ancient data.

qpAdm and qpWave analysis

We performed qpWave/qpAdm (v. 1520) analyses(part of the ADMIXTOOLS package) (*33*) to model ancestry of target samples to sets of penecontemporary reference samples. To prepare the data, a random read-indent caller, which excluded the first and last eight bases of each read (https://github.com/kveeramah/aDNA_GenoCaller), was applied in the analysis for all target, source, and reference populations. For our LHP individuals (target), we kept the ones that had more than 0.01x coverage. For the reference populations (right populations), we adopted 72 prehistoric individuals (*29*, *83–92*) used in a previous study (*34*), which comprised Anatolian_Neolithic (EEF, n = 26), Steppe_Eneolithic (SA, n = 18), Western Hunter-Gatherer (WHG, n = 15), Iran_Neolithic (Iran_N, n = 9), and Morocco_Iberomaurusian (MIM, n = 4) populations.

qpAdm was performed to validate the results obtained from fastNGSadmix. In this analysis, the source populations were the same as the reference populations used in the fastNGSadmix analysis. For every test, we used a single individual from the LHP as the target. We first tested a one-source model, then progressively added up to three source populations in a stepwise manner. The process was finalized once the tail probability exceeded 0.01.

For qpAdm results using the same number of source reference populations (one, two, or three), each individual modeled with n different combinations was assigned a weight of 1/n per combination. The final ancestry proportion for each reference population was calculated as the sum of its contributions across all combinations. For example, if an individual can be modeled using only one source reference population—either NGBI or SCAND—the resulting ancestry is assigned equally: 0.5 NGBI and 0.5 SCAND. In a different case with two reference populations, suppose an individual is modeled with two two-source combinations, such as NGBI (0.3) / MEDEU (0.7) and SCAND (0.2) / MEDEU (0.8). Then, the final ancestry proportions would be 0.15 NGBI, 0.75 MEDEU, and 0.1 SCAND. The raw output of qpAdm is reported in Table S5, Fig. S17 and Fig. S18 and the final summary of genetic ancestry are reported in Table S6 and illustrated in Fig. 2B.

To evaluate whether fastNGSadmix and qpAdm produced comparable results, we assessed the correlation between ancestry proportions estimated by the two methods (Fig. S19). We first removed all unmodeled individuals identified by qpAdm, as well as individuals with coverage lower than 0.01×. Each ancestry component was then compared separately.

Using Pearson's correlation and linear regression in R, we found that for the non-European components, SASIA and SUBSAHARAN did not exhibit significant correlations between the two methods. This is likely due to the very small number of individuals with detectable levels of these ancestries, as well as the extremely low estimated proportions—conditions under which correlation analysis is not meaningful. In contrast, CASIA, EASIA, and NAFRICA all showed significant correlations, suggesting greater consistency between the two methods. However, the regression slopes (covariates) deviate from the expected value of ~1, likely due to the small number of individuals carrying these non-European ancestries.

For the European components, MEDEU showed a strong correlation between fastNGSadmix and qpAdm, with a regression slope of 1.1, indicating a high degree of similarity. NGBI and SCAND also showed significant correlations, but with regression slopes closer to 0.5. This may reflect the difficulty in distinguishing between these two ancestries. When NGBI and SCAND were combined into a single component, the regression slope increased to 1.1 (Fig. S20), suggesting a more consistent and reliable estimation when these ancestries are not separated

We also employed qpWave specifically to model the source of our LHP target individuals using Eurasian source populations (Table S3), and for the right populations, we used the same groups used in qpAdm which consists of 72 prehistory individuals, and we also used a cutoff of 0.01 to accept the model. We prepared the source population by collecting previously published penecontemporaneous individuals, and grouped them based on their periods and geographic locations (Table S3, Fig. S23). To minimize biases related to sample size, we retained a maximum of 10 individuals per population and ensured all individuals were unrelated. Nine penecontemporaneous Eurasian reference populations are used to model the Roman period LHP individuals (n = 63 after removing low coverage individuals). For the Post-Roman period individuals (n=234 after removing low coverage individuals), besides the nine sources used in modeling the Roman period individuals, we incorporated the Roman-period LHP populations (10 high coverage unrelated individuals, see Table S1, column 'used as qpWave source (LHP_3-5th c.)') and the Lake Balaton populations as two additional sources. The qpWave results of the Roman and post-Roman individuals can be found in Table S7 and Table S8.

We used two complementary approaches to visualize the qpWave results. In the first approach (map interpolation), we excluded individuals who could not be modeled with any of the sources. For each remaining individual, we determined how many sources they could be modeled with and assigned equal proportions to each source (e.g., if an individual can be modeled with both Austria_2–5th c. and Balkans_1–6th c., each source received 0.5). We conducted this analysis for every single individual in both the Roman and post-Roman period (not including the low coverage individuals). Then, to obtain the overall ancestry contribution of a specific source population to the target population (i.e. Roman or post-Roman LHP), we averaged the estimated proportions across all individuals within the period.

For example, consider a Roman population of three individuals. If Ind1 is modeled equally by Austria_2–5th c. and Balkans_1–6th c. (50% each); Ind2 is modeled solely by France_4-6th c. (100%); and Ind3 is modeled by four sources including France_4-6th c., Balkans_1-6th c., Austria_2–5th c., and Central Italy_2-6th c. (25% each), the final population averages would be: 41.7% France_4-6th c.; 25% Austria_2–5th c.; 25% Balkans_1–6th c.; and 8.3% Central Italy_2-6th c.

To visualize the spatial distribution of ancestry, we mapped the geographic coordinates of each source individual, marking the center of each source population with a black dot. We used the modeling results to assign specific ancestry proportions to each source group (e.g., 25% Balkans 1–6th c., 25% Austria 2–5th c., 41.7% France 4–6th c., and 8.3% Central Italy 2–6th c.). We performed Inverse Distance Weighting (IDW) interpolation using the gstat (*93*) package to visualize the spatial distribution of modeled ancestry proportions across mainland Europe. This interpolation utilized the coordinates of every individual to estimate the gradient of ancestry components (as exemplified by the Balkans, Austria, France, and Italy distributions). The resulting maps are shown in Fig. 3A.

In the second approach (heatmap), we calculated the proportion of individuals at each site who could be modeled with a given source, excluding Győr-Frigyes and Kóny due to their small sample sizes (n<15). These site-level results are visualized in Fig. 3B; for instance, if 35% of Roman-period individuals can be modeled using the 'Balkans 1–6th c.' source, this frequency is represented as 35% in the heatmap.

F_{ST} analysis

We estimated F_{ST} using SmartPCA (*79*, *80*), with the following parameters enabled: inbreed, fastonly, fsthiprecision, and fstz. To ensure the independence of our samples, we first excluded relatives up to the fourth degree (defined as pi-hat >= 0.0625). In cases where related pairs were identified, we retained the individual with the highest sequencing coverage. Following this quality control, the final dataset included 232 individuals from the following sites: Győr-Széchenyi square: 54, Szeleste: 84, Hegykő: 40, Győrmót: 26, Ménfőcsanak: 18, Kóny: 8 and Győr-Frigyes lkt: 2. Consistent with our qpAdm and qpWave protocols, we employed a random read-intent caller to minimize biases arising from variation in coverage amongst samples, excluding the first and last eight bases of each read (https://github.com/kveeramah/aDNA_GenoCaller). For the final analysis, individuals were grouped based on their archaeological site or chronological period. Specifically, we grouped all post-Roman sites together for comparison against the Roman period for the inter-period comparison, whereas intra-period comparisons were conducted by grouping individuals according to their specific archaeological sites.

Biological relatedness

We utilized a customized version of the lcMLkin software package, which incorporated external allele frequency data, following an approach similar in a previous study (*52*), to identify close biological relationships (within the third degree) among individuals at each site. The analysis was performed using genotype likelihood data from 1,076.758 autosomal 1240K sites.

Allele frequency data from the 1000 Genomes CEU and TSI populations were used as outside population frequencies since the new individuals in this study are of predominately European ancestry. Relationships involving low-coverage individuals with fewer than 10,000 shared SNPs in an lcMLkin analysis were excluded (14% of the related pairs are removed), as they were likely

to be spurious rather than indicative of genuine biological relatedness. To validate the lcMLkin results, we also conducted an independent analysis using KIN (*54*). The analysis was run with default parameters, with the -cnt parameter set to 0. The comparison between KIN and lcMLkin results can be found in Table S22 column "lcMLkin_compare" and supplementary Text S5, and detailed description of pedigree reconstruction methods can be found in Supplementary Text S5.

IBD analysis

We implemented ancIBD (*46*) to understand the identical-by-descent haplotype sharing pattern between individuals in the LHP and other contemporaneous populations (Table S3) across Eurasia and Africa (*34*, *37*, *42–44*, *52*, *78*, *94–105*).

Genotypes were called from whole-genome data and imputed for all diploid, dinucleotide sites within the 1000 Genomes Project Phase 3 v5a VCF files using GLIMPSE v1.1 (*106*), with the 1000 Genomes Project data serving as the imputation reference (*75*). The dataset was then filtered down to the 1,240K positions. Following the steps outlined in ancIBD, we converted VCF files to HDF5 format and identified IBD segments using default parameters. To enhance result reliability, we applied three filtering steps: first, excluding individuals with genomic coverage below 1×, and second, removing those with a GP99 ratio lower than 0.7, as recommended by the original study, finally, we only kept the connections with at least one shared IBD segments longer than 12cM.

In the analysis focused on IBD sharing patterns among individuals from the Roman period, we have individuals from the LHP (n=31), 5th century sites of Fonyód, Hács and Balatonszemes around the Lake Balaton (*34*) (n=26), and Bardonecchia/Torino-Lavazza (*34*) (n=11).

For the post-Roman period, we have individuals from the LHP (n=130), Szólád (*52*) (n=24), and Collegno (*52*, *104*) (n=27). To construct the IBD network for post-Roman period individuals, we used Gephi v0.9.7 (*107*), applying the ForceAtlas2 (*108*) algorithm with "Prevent Overlap" enabled, an Edge_Weight_influence of 0.4, and Gravity set to 6. Edges were weighted by the adjusted Pi-hat value (calculated by dividing the sum_IBD by the total CM of the genome) and rescaled on a scale of 1 to 5. Node sizes were assigned based on rank, ranging from 10 to 30. Individuals with no IBD connections (degree=0) were excluded from the final network visualization.

Local ancestry inference

We applied FLARE (*47*) to infer local ancestry of individuals in the IBD network. We used modern populations from the 1000 Genomes Project (*75*)—CEU, GBR, TSI, AFR, EAS, and SAS—as reference populations for inferring local ancestry. To simplify analysis, we grouped the European populations into Northern European (nEUR, including CEU and GBR) and Southern European (TSI). We then analyzed raw IBD data generated by ancIBD (*46*), filtering out segments with a density lower than 220/cM or shorter than 12 cM. For each remaining segment, we determined the ancestry status of both individuals using FLARE. At each SNP, we assigned a status based on the degree of ancestry matching between the two individuals across four chromosomes: (a) 1.0 if all four chromosomes share the same ancestry, (b) 0.5 if three

chromosomes match (c), 0.25 if only one chromosome from each individual matches. For each segment, we iterated through all SNPs, recording the lengths associated with each ancestry and their corresponding status. This process was repeated across all segments, with the final ancestry length for each segment calculated as length × status. To visualize the results, we merged all IBD segments for each ancestry and constructed ancestry-specific networks using Gephi (*107*). Fig. S27 presents the resulting networks for nEUR and sEUR.

To assess the reliability of Local Ancestry Inference using FLARE, we compared its global ancestry estimates with those from fastNGSadmix using Pearson's correlation and linear regression in R. The analysis (Fig. S26) included all LHP individuals with coverage ≥1x, consistent with the threshold used in the IBD analysis. The results indicate that both Northern (nEUR) and Southern (sEUR) European ancestries are highly correlated between the two methods ($p < 0.0001$ for both). However, FLARE tends to estimate ancestry proportions more conservatively—rarely reaching exact values of 0 or 1—whereas fastNGSadmix often assigns these boundary values. We also observed a significant correlation for non-European ancestries; however, the regression fit was weaker compared to that of Northern and Southern ancestries, likely due to their low representation within the population.

Pairwise Kinship Density Resampling

To rigorously compare kinship density between 6th century sites (including Szólad) while controlling for differences in sample size, we performed a pairwise permutation analysis. We utilized counts of biological relatedness estimates generated by lcMLkin (p>=0.125, third degree) for each site as our test statistic. For every pair of sites, we downsampled the dataset of the larger site to match the sample size of the smaller site. Within this random subsample, we calculated the count of close relatives. This resampling procedure was repeated 1,000 times to generate a null distribution of expected relatedness counts for that sample size. We then calculated empirical p-values by comparing the observed number of related pairs in the smaller site against the distribution generated from the larger site. This allowed us to determine whether the frequency of biological relatedness differed significantly between populations while accounting for sample size. The results can be found in Table S23.

Mantel test of burial distance and genetic distance

We performed a Mantel test (*109*) in R to assess the relationship between burial distance and genetic distance. Burial distance was calculated using geographic coordinates, while genetic distance was estimated based on pairwise differences in PC1 values, treated as a proxy for genetic proximity.

Strontium isotope ($^{87}Sr/^{86}Sr$) analysis

Tooth enamel used for the Sr analysis was extracted in the laboratory of the Institute of Archaeogenomics, Budapest. For the extraction, first cleaning of the surface of the teeth was required for which a Dremel tool with an abrasion tip was used, followed by a ten-minute

ultrasonic bath. After that, the enamel was carefully powdered with the help of a diamond-coated dental drill bit attached to the Dremel tool, until ca. 25–40 mg material was obtained. Approximately 20-30 mg of material from each sample was processed for strontium (Sr) isotope analysis in the MC-ICP-MS Facility, Department of Geological Sciences, University of Cape Town following routine procedures (*110*). Enamel powder was weighed in Savillex PFA beakers, covered with 2 ml of concentrated HNO_3 and closed beakers were placed on a hot plate at 140ºC for an hour until complete dissolution. Beakers were opened, dried down and material redissolved in 1.5 ml 2M HNO_3. Elemental Sr was isolated from these solutions using Triskem Sr.Spec resin and chemical protocols after Pin et al (*111*). The isolated Sr fractions from each sample was diluted to 200 ppb Sr in 0.2% HNO_3 and analysed on a Nu Instruments NuPlasma HR MC-ICP-MS, with reported $^{87}Sr/^{86}Sr$ data referenced to bracketing analyses of the international standard reference NIST SRM987 using an $^{87}Sr/^{86}Sr$ value of 0.710255 (*112*). All Sr isotope data were corrected for Rb interference at 87 amu using the measured ^{85}Rb signal and the natural $^{85}Rb/^{87}Rb$ abundance ratio. Instrumental mass fractionation was corrected using the exponential law and an $^{86}Sr/^{88}Sr$ value of 0.1194. Results of repeat analyses of both an in-house carbonate reference material NM95 ($^{87}Sr/^{86}Sr$ 0.708897±0.000017 2s; n=5) and international reference material NIST SRM1400 ($^{87}Sr/^{86}Sr$ 0.713134±0.000037 2s; n=4) analysed as unknowns with samples during this study agree with long-term results from this facility (NM95 $^{87}Sr/^{86}Sr$ 0.708909±0.000038 2s; n=932, SRM1400 $^{87}Sr/^{86}Sr$ 0.713122±0.000036 2s; n=53) and limited published data (SRM1400 $^{87}Sr/^{86}Sr$ 0.71308-0.7134; GeoReM database). Elemental Sr measured in total procedural blanks were typical for this facility at < 250 pg and therefore negligible.

Carbon and Nitrogen isotope analyses

C and N isotope analysis (δ13C, δ15N) was conducted on collagen preferably from ribs, if those were not available on long bones (humerus, femur, tibia, or fibula) at the Curt Engelhorn Centre Archaeometry in Mannheim, Germany or at the Department of Applied and Analytical Palaeontology, Institute of Geosciences at the University Mainz, Germany. Bone samples were cleaned, chemically treated and collagen extracted using a modified Longin method (*113*) with modifications as described in Knipper et al. (*114*). C and N contents and the stable isotopic compositions were determined in triplicates using a Thermo Flash 2000 Organic Elemental Analyzer coupled to a Thermo Finnigan Mat 253 mass spectrometer or a vario PYRO cube CNSOH elemental analyzer (Elementar) and a precisION isotope ratios mass spectrometer (Isoprime) depending on the lab. Then the raw data were calibrated against the international Standards.

Radiocarbon dating

A total of 38 human bone samples were radiocarbon dated to provide absolute chronological anchors for the individuals analyzed. All samples were prepared and measured at the Curt-Engelhorn-Center Archaeometry in Mannheim, Germany (*115*). Collagen was extracted following a modified Longin protocol with an additional ultrafiltration step to remove low-molecular-weight contaminants (*116*). Quality control criteria included collagen yield, elemental composition (%C, %N), and atomic C:N ratio. All samples yielded sufficient collagen

for AMS measurement, with C:N atomic ratios falling within the accepted range for well-preserved collagen (2.9–3.6; (*117*)). Accepted collagen extracts were combusted in an Elementar VarioMicro elemental analyzer interfaced with either an in-house semi-automated graphitization system (MAG) or a commercial AGE3 system (Ionplus AG). The resulting graphite was measured on one of two MICADAS accelerators. Radiocarbon measurements were normalized using Oxalic Acid II (NIST SRM 4990C) as the primary standard. Each batch additionally included process blanks and quality control samples of known radiocarbon age—typically IAEA reference materials or well-characterized bone material routinely used in the laboratory—to monitor background levels, instrument stability, and measurement accuracy. The resulting conventional radiocarbon ages were corrected for isotopic fractionation and normalized to a $\delta^{13}C$ value of –25‰. Radiocarbon ages were calibrated using the IntCal20 calibration curve (*118*) in OxCal v4.4.4 (*119*).

Radiocarbon dating was primarily used to validate archaeological dating of the sites. Due to a plateau on the calibration curve, radiocarbon dating in the 5th-6th centuries CE is generally less accurate than typochronology based on the grave goods. Our results confirmed the general archaeological dating of the sites in all cases. One measurement from Hegykő_073 (sample HMU045) showed a much earlier dating (cal 258-410 CE) than the expected 6th century as supported by the other 14 measurements from the site. Hegykő_073 contained a male individual buried with spatha, shield and spear - all characteristic forms to the 6th and unknown to the 4th century CE. We consider this measurement as an anomaly, as according to the relevant study from Bronk Ramsey (*120*), outliers for various reasons show up once in every 20 measurements. Moreover, Hegykő_073 shows elevated $\delta^{15}N$ values suggesting that a reservoir effect could also affect the radiocarbon dating results. Unfortunately the impact of the freshwater diet's reservoir effect on radiocarbon data is not predictable and could result in variations from zero to six thousand years between the calibrated and real age (*121*, *122*). As such, despite the outlying radiocarbon date of Hegykő_073 we assume that the burial is contemporary to the rest of the site, as suggested by the deposition of the burial as well as the dating of its grave goods.

Provenance

The archaeological material of the investigated sites are stored and available for viewing in the following institutions: Rómer Flóris Művészeti és Történeti Múzeum in Győr (Gyirmót, Győr-Széchenyi square, Győr-Frigyes lkt., Ménfőcsanak), Sopron Museum in Sopron (Hegykő), Hungarian National Museum in Budapest (Hegykő grave 18), and in Savaria Megyei Hatókörű Városi Múzeum in Szombathely (Szeleste). The osteological material is stored in the Rómer Flóris Művészeti és Történeti Múzeum in Győr (Gyirmót, Győr-Széchenyi square, Győr-Frigyes lkt., Ménfőcsanak), Hungarian natural History Museum in Budapest (Hegykő), and in Savaria Megyei Hatókörű Városi Múzeum in Szombathely (Szeleste). These institutions are named partners of the HistoGenes project and cooperate with it through formal collaboration agreements.

All samples used for aDNA analyses were collected in the framework of the HistoGenes project, ERC SynGrant grant 856453 ERC-2019-SyG between 2020-2022 from the maintained collections of the aforementioned institutions by Balázs Gusztáv Mende and István Koncz in close collaboration with colleagues of the local museums who are also authors on the study.

Sample preparation was done in the ELTE RCH Institute of Archaeogenomics, Budapest, while the analyses were done at the facilities of the MPI Leipzig/Jena and Stony Brook University - all partner institutes of the project.

Isotope sampling was done in the framework of various projects. Hegykő and Gyirmót was sampled in the framework of BMBF project grant number: 01 UA 0806B by Corina Knipper in 2012; Szeleste in the framework of OTKA-NKFI project grant number: NN113157 by Corina Knipper and István Koncz in 2016; Kóny in the framework of the HistoGenes project, ERC SynGrant grant 856453 ERC-2019-SyG by Balázs Gusztáv Mende and István Koncz in 2022.

Prior to sampling, the materials from the sites were subjected to a condition assessment and revision. In all cases, samples were collected in the presence of an osteologist in order to minimize potential mixing. Sampling followed the national protocol recommended for destructive sampling for biological anthropological remains (*123*) as well as inhouse rules of the hosting institutions to minimize the invasive nature of the sampling and preserve the osteological material. The dating of the sampled sites is based on archaeological chronology; however, in every case this has also been verified through radiocarbon analyses, see Table S1 below for more detail on each individual site.

References

1. G. Halsall, *Barbarian Migrations and the Roman West, 376-568* (Cambridge University Press, Cambridge, England, 2007)*Cambridge medieval textbooks*.

2. C. Wickham, *Framing the Early Middle Ages: Europe and the Mediterranean, 400-800* (OUP Oxford, 2006).

3. M. Meier, *Die Geschichte der Völkerwanderung: Europa, Asien und Afrika vom 3. bis zum 8. Jahrhundert n.Chr. 7. Auflage* (C.H.Beck, Munich, Germany, 2021)*Historische Bibliothek der Gerda Henkel Stiftung*.

4. B. Ward-Perkins, *The Fall of Rome: And the End of Civilization* (OUP Oxford, 2006).

5. T. Vida, “Die Zeit zwischen dem 4. und dem 6. Jahrhundert im mittleren Donauraum aus archäologischer Sicht” in *Römische Legionslager in Den Rhein- Und Donauprovinzen - Nuclei Spätantik-Frühmittelalterlichen Lebens?*, C. Witschel, M. Konrad, Eds. (Bayerischen Akademie der Wissenschaften bei C.H.Beck, München, 2011)*Abhandlungen. Bayerische Akademie der Wissenschaften, phil.-hist. Klasse / NF 138*, pp. 615–650.

6. M. Hardt, “Pannonien im Spannungsfeld zwischen Römer- und Völkerwanderungszeit - eine geschichtliche Einführung” in *Keszthely-Fenékpuszta Im Kontext Spätantiker Kontinuitätsforschung Zwischen Noricum Und Moesia*, O. Heinrich-Tamáska, Ed. (Verlag Marie Leidorf, Rahden, Westf., 2011)*Castellum pannonicum pelsonense 2*, pp. 15–28.

7. P. Tomka, “Langobardenforschung in Nordwestungarn” in *Die Langobarden. Herrschaft*

Und Identität. Ergebnisse Eines Vom 2. Bis 4. November 2001 in Wien Abgehaltenen Internationalen Symposiums., W. Pohl, P. Erhart, Eds. (Verlag der österreichischen Akademie der Wissenschaften, Vienna, 2005)*Forschungen zur Geschichte des Mittelalters, 9 Denkschriften der philosophisch-historischen Klasse, 329*, pp. 247–264.

8. P. Tomka, "Kulturwechsel der spätantiken Bevölkerung eines Auxiliarcastells: Fallbeispiel Arrabona" in *Zentrum Und Peripherie – Gesellschaftliche Phänomene in Der Frühgeschichte*, H. Friesinger, A. Stuppner, Eds. (Verlag der österreichischen Akademie der Wissenschaften, Vienna, 2004)*Mitteilungen der Prähistorischen Kommission 57*, pp. 389–409.

9. P. Tomka, "Eine römische Stadt und ihre barbarische Peripherie: Scarbantia" in *Romania Gothica II. The Frontier World. Romans, Barbarians and Military Culture*, T. Vida, Ed. (Martin Optiz Kiadó, Budapest, 2015), pp. 587–615.

10. W. Pohl, "Migration und Ethnogenesen der Langobarden aus Sicht der Schriftquellen" in *Kulturwandel in Mitteleuropa: Langobarden, Awaren, Slawen. Akten Der Internationalen Tagung in Bonn Vom 25. Bis 28. Februar 2008*, J. Bemmann, M. Schmauder, Eds. (Habelt, R, Bonn, Germany, 2008)*Kolloquien zur Vor- und Frühgeschichte 11*, pp. 1–12.

11. T. Vida, "Aufgaben und Perspektiven der Langobardenforschung in Ungarn nach István Bóna" in *Kulturwandel in Mitteleuropa : Langobarden, Awaren, Slawen : Akten Der Internationalen Tagung in Bonn Vom 25. Bis 28. Februar 2008*, M. Schmauder, J. Bemmann, Eds. (Deutsches Archäologisches Institut. Römisch-Germanische Kommission (Berlin) by Habelt, Bonn, 2008)*Kolloquien zur Vor- und Frühgeschichte : 11. Bd*, pp. 343–362.

12. I. Bóna, "A langobardok története és régészeti emlékei" in *Hunok - Gepidák - Langobardok*, I. Bóna, J. Cseh, M. Nagy, P. Tomka, Á. Tóth, Eds. (JATE Magyar Őstörténeti Kutatócsoport, Szeged, 1993), pp. 102–162.

13. I. Koncz, A hegykői 6. Századi temető időrendje és kapcsolatrendszere. *Archaeol. Ért.* **139**, 71–98 (2014).

14. T. Bendeguz, K. Wiltschke-Schrotta, M. Binder, The Langobardian period cemetery of Vienna-Mariahilfer Gürtel. With a contribution to artificial cranial deformation in the western Carpathian Basin. *Jahrbuch des Römisch-Germanischen Zentralmuseums Mainz* **57** (2014).

15. T. Vida, Late Roman territorial organisation and the settlement of the barbarian gentes in Pannonia. *Hortus Artium Mediev.* **13**, 319–331 (2007).

16. R. Virágos, Tájrégészeti megközelítések a dunántúli 5-6. századi régészeti lelőhelyek értelmezésében. *Archaeol. Ért.* **133**, 199–221 (2008).

17. A. Wilson, A. Bowman, *Trade, Commerce, and the State in the Roman World* (Oxford University Press, London, England, 2017)*Oxford Studies on the Roman Economy*.

18. D. Hagmann, A system of ups and downs: Roman rural landscapes in Northern Noricum. *J.*

Rom. Archaeol. **38**, 79–116 (2025).

19. T. Hajdu, E. Fóthi, I. Kovári, M. Merczi, A. Molnár, G. Maász, P. Avar, A. Marcsik, L. Márk, Bone tuberculosis in Roman Period Pannonia (western Hungary). *Mem. Inst. Oswaldo Cruz* **107**, 1048–1053 (2012).

20. S. Bíró, P. Tomka, "Über die mysteriöse 'schwarze Schicht' und das sog. 'hunnenzeitliche Gräberfeld' von Győr-Széchenyi Platz" in *Na Hranicích Impéria = Extra Fines Imperii: Jaroslavu Tejralovi K 80. Narozeninám* (Masarykova univerzita – Archeologický ústav AV ČR, Brno, Brno, 2017), pp. 53–72.

21. I. Koncz, 568 — A historical date and its archaeological consequences. *Acta Archaeol.* **66**, 315–340 (2015).

22. G. Tóth, I. K. Pap, "Germán temető a Nyugat-Dunántúlon" in *Trendek és Eredmények a Biológiai Kutatás és Oktatás Terén*, M. Nagy, J. Poráčová, Eds. (J. Selye University, Komarno, 2016), pp. 22–27.

23. I. K. Pap, Savaria keleti temetője és a szelestei germán temető épített és tegulás sírjai (Savaria's eastern cemetery and the built and tegula tombs of the Szeleste Langobard cemetery). *Savaria* **38**, 91–105 (2016).

24. A. Vaday, The Langobard cemetery at Ménfőcsanak. *Antaeus* **33**, 163–242 (2015).

25. T. Vida, "Spätantike Buntmetallgefäβe im langobardenzeitlichen Pannonien" in *Macht Des Goldes, Gold Der Macht. Herrschafts Und Jenseitsrepräsentation Zwischen Antike Und Frühmittelalter Im Mittleren Donauraum. Aktend Des 23. Internationalen Symposiums Der Grundprobleme Der Frühgeschichtlichen Entwicklung Im Mittleren Donauraum, Tengelic, 16.-19.11.2011.*, M. Hardt, O. Heinrich-Tamáska, Eds. (Verlag Bernhard Albert Greiner, Weinstadt, 2013)*Forschungen zu Spätantike und Mittelalter 2*, pp. 339–360.

26. E. Horváth, Gemstone and glass inlaid fine metalwork from the Carpathian Basin: the Hunnic and Early Merovingian Periods. *Diss. archaeol. ex Inst. Archaeol. Univ. Rolando Eötvös Nomin.*, 275–302 (2013).

27. I. Koncz, About brooches and networks: Some remarks on the female dress in 6th century Pannonia. *Diss. archaeol. ex Inst. Archaeol. Univ. Rolando Eötvös Nomin.*, 163–176 (2018).

28. N. Rohland, E. Harney, S. Mallick, S. Nordenfelt, D. Reich, Partial uracil-DNA-glycosylase treatment for screening of ancient DNA. *Philos. Trans. R. Soc. Lond. B Biol. Sci.* **370**, 20130624 (2015).

29. I. Mathieson, I. Lazaridis, N. Rohland, S. Mallick, N. Patterson, S. A. Roodenberg, E. Harney, K. Stewardson, D. Fernandes, M. Novak, K. Sirak, C. Gamba, E. R. Jones, B. Llamas, S. Dryomov, J. Pickrell, J. L. Arsuaga, J. M. B. de Castro, E. Carbonell, F. Gerritsen, A. Khokhlov, P. Kuznetsov, M. Lozano, H. Meller, O. Mochalov, V. Moiseyev, M. A. R. Guerra, J. Roodenberg, J. M. Vergès, J. Krause, A. Cooper, K. W. Alt, D. Brown, D. Anthony, C. Lalueza-Fox, W. Haak, R. Pinhasi, D. Reich, Genome-wide patterns of selection in 230 ancient Eurasians. *Nature* **528**, 499–503 (2015).

30. Q. Fu, M. Meyer, X. Gao, U. Stenzel, H. A. Burbano, J. Kelso, S. Pääbo, DNA analysis of an early modern human from Tianyuan Cave, China. *Proc. Natl. Acad. Sci. U. S. A.* **110**, 2223–2227 (2013).

31. M. R. Nelson, K. Bryc, K. S. King, A. Indap, A. R. Boyko, J. Novembre, L. P. Briley, Y. Maruyama, D. M. Waterworth, G. Waeber, P. Vollenweider, J. R. Oksenberg, S. L. Hauser, H. A. Stirnadel, J. S. Kooner, J. C. Chambers, B. Jones, V. Mooser, C. D. Bustamante, A. D. Roses, D. K. Burns, M. G. Ehm, E. H. Lai, The Population Reference Sample, POPRES: a resource for population, disease, and pharmacological genetics research. *Am. J. Hum. Genet.* **83**, 347–358 (2008).

32. E. Jørsboe, K. Hanghøj, Albrechtsen, fastNGSadmix: Admixture proportions and principal component analysis of a single NGS sample. *Bioinformatics* **33**, 3148–3150 (2017).

33. N. Patterson, P. Moorjani, Y. Luo, S. Mallick, N. Rohland, Y. Zhan, T. Genschoreck, T. Webster, D. Reich, Ancient admixture in human history. *Genetics* **192**, 1065–1093 (2012).

34. D. N. Vyas, I. Koncz, A. Modi, B. G. Mende, Y. Tian, P. Francalacci, M. Lari, S. Vai, P. Straub, Z. Gallina, T. Szeniczey, T. Hajdu, L. Pejrani Baricco, C. Giostra, R. Radzevičiūtė, Z. Hofmanová, S. Évinger, Z. Bernert, W. Pohl, D. Caramelli, T. Vida, P. J. Geary, K. R. Veeramah, Fine-scale sampling uncovers the complexity of migrations in 5th-6th century Pannonia. *Curr. Biol.* **33**, 3951–3961.e11 (2023).

35. L. Skotte, T. S. Korneliussen, A. Albrechtsen, Estimating individual admixture proportions from next generation sequencing data. *Genetics* **195**, 693–702 (2013).

36. I. Olalde, P. Carrión, I. Mikić, N. Rohland, S. Mallick, I. Lazaridis, M. Mah, M. Korać, S. Golubović, S. Petković, N. Miladinović-Radmilović, D. Vulović, T. Alihodžić, A. Ash, M. Baeta, J. Bartík, Ž. Bedić, M. Bilić, C. Bonsall, M. Bunčić, D. Bužanić, M. Carić, L. Čataj, M. Cvetko, I. Drnić, A. Dugonjić, A. Đukić, K. Đukić, Z. Farkaš, P. Jelínek, M. Jovanovic, I. Kaić, H. Kalafatić, M. Krmpotić, S. Krznar, T. Leleković, M. M de Pancorbo, V. Matijević, B. Milošević Zakić, A. J. Osterholtz, J. M. Paige, D. Tresić Pavičić, Z. Premužić, P. Rajić Šikanjić, A. Rapan Papeša, L. Paraman, M. Sanader, I. Radovanović, M. Roksandic, A. Šefčáková, S. Stefanović, M. Teschler-Nicola, D. Tončinić, B. Zagorc, K. Callan, F. Candilio, O. Cheronet, D. Fernandes, A. Kearns, A. M. Lawson, K. Mandl, A. Wagner, F. Zalzala, A. Zettl, Ž. Tomanović, D. Keckarević, M. Novak, K. Harper, M. McCormick, R. Pinhasi, M. Grbić, C. Lalueza-Fox, D. Reich, A genetic history of the Balkans from Roman frontier to Slavic migrations. *Cell* **186**, 5472–5485.e9 (2023).

37. I. Lazaridis, S. Alpaslan-Roodenberg, A. Acar, A. Açıkkol, A. Agelarakis, L. Aghikyan, U. Akyüz, D. Andreeva, G. Andrijašević, D. Antonović, I. Armit, A. Atmaca, P. Avetisyan, A. İ. Aytek, K. Bacvarov, R. Badalyan, S. Bakardzhiev, J. Balen, L. Bejko, R. Bernardos, A. Bertsatos, H. Biber, A. Bilir, M. Bodružić, M. Bonogofsky, C. Bonsall, D. Borić, N. Borovinić, G. Bravo Morante, K. Buttinger, K. Callan, F. Candilio, M. Carić, O. Cheronet, S. Chohadzhiev, M.-E. Chovalopoulou, S. Chryssoulaki, I. Ciobanu, N. Čondić, M. Constantinescu, E. Cristiani, B. J. Culleton, E. Curtis, J. Davis, T. I. Demcenco, V. Dergachev, Z. Derin, S. Deskaj, S. Devejyan, V. Djordjević, K. S. Duffett Carlson, L. R. Eccles, N. Elenski, A. Engin, N. Erdoğan, S. Erir-Pazarcı, D. M. Fernandes, M. Ferry, S.

Freilich, A. Frînculeasa, M. L. Galaty, B. Gamarra, B. Gasparyan, B. Gaydarska, E. Genç, T. Gültekin, S. Gündüz, T. Hajdu, V. Heyd, S. Hobosyan, N. Hovhannisyan, I. Iliev, L. Iliev, S. Iliev, İ. İvgin, I. Janković, L. Jovanova, P. Karkanas, B. Kavaz-Kındığılı, E. H. Kaya, D. Keating, D. J. Kennett, S. Deniz Kesici, A. Khudaverdyan, K. Kiss, S. Kılıç, P. Klostermann, S. Kostak Boca Negra Valdes, S. Kovačević, M. Krenz-Niedbała, M. Krznarić Škrivanko, R. Kurti, P. Kuzman, A. M. Lawson, C. Lazar, K. Leshtakov, T. E. Levy, I. Liritzis, K. O. Lorentz, S. Łukasik, M. Mah, S. Mallick, K. Mandl, K. Martirosyan-Olshansky, R. Matthews, W. Matthews, K. McSweeney, V. Melikyan, A. Micco, M. Michel, L. Milašinović, A. Mittnik, J. M. Monge, G. Nekhrizov, R. Nicholls, A. G. Nikitin, V. Nikolov, M. Novak, I. Olalde, J. Oppenheimer, A. Osterholtz, C. Özdemir, K. T. Özdoğan, N. Öztürk, N. Papadimitriou, N. Papakonstantinou, A. Papathanasiou, L. Paraman, E. G. Paskary, N. Patterson, I. Petrakiev, L. Petrosyan, V. Petrova, A. Philippa-Touchais, A. Piliposyan, N. Pocuca Kuzman, H. Potrebica, B. Preda-Bălănică, Z. Premužić, T. D. Price, L. Qiu, S. Radović, K. Raeuf Aziz, P. Rajić Šikanjić, K. Rasheed Raheem, S. Razumov, A. Richardson, J. Roodenberg, R. Ruka, V. Russeva, M. Şahin, A. Şarbak, E. Savaş, C. Schattke, L. Schepartz, T. Selçuk, A. Sevim-Erol, M. Shamoon-Pour, H. M. Shephard, A. Sideris, A. Simalcsik, H. Simonyan, V. Sinika, K. Sirak, G. Sirbu, M. Šlaus, A. Soficaru, B. Söğüt, A. Sołtysiak, Ç. Sönmez-Sözer, M. Stathi, M. Steskal, K. Stewardson, S. Stocker, F. Suata-Alpaslan, A. Suvorov, A. Szécsényi-Nagy, T. Szeniczey, N. Telnov, S. Temov, N. Todorova, U. Tota, G. Touchais, S. Triantaphyllou, A. Türker, M. Ugarković, T. Valchev, F. Veljanovska, Z. Videvski, C. Virag, A. Wagner, S. Walsh, P. Włodarczak, J. N. Workman, A. Yardumian, E. Yarovoy, A. Y. Yavuz, H. Yılmaz, F. Zalzala, A. Zettl, Z. Zhang, R. Çavuşoğlu, N. Rohland, R. Pinhasi, D. Reich, R. Davtyan, A genetic probe into the ancient and medieval history of Southern Europe and West Asia. *Science* **377**, 940–951 (2022).

38. I. Olalde, S. Mallick, N. Patterson, N. Rohland, V. Villalba-Mouco, M. Silva, K. Dulias, C. J. Edwards, F. Gandini, M. Pala, P. Soares, M. Ferrando-Bernal, N. Adamski, N. Broomandkhoshbacht, O. Cheronet, B. J. Culleton, D. Fernandes, A. M. Lawson, M. Mah, J. Oppenheimer, K. Stewardson, Z. Zhang, J. M. Jiménez Arenas, I. J. Toro Moyano, D. C. Salazar-García, P. Castanyer, M. Santos, J. Tremoleda, M. Lozano, P. García Borja, J. Fernández-Eraso, J. A. Mujika-Alustiza, C. Barroso, F. J. Bermúdez, E. Viguera Mínguez, J. Burch, N. Coromina, D. Vivó, A. Cebrià, J. M. Fullola, O. García-Puchol, J. I. Morales, F. X. Oms, T. Majó, J. M. Vergès, A. Díaz-Carvajal, I. Ollich-Castanyer, F. J. López-Cachero, A. M. Silva, C. Alonso-Fernández, G. Delibes de Castro, J. Jiménez Echevarría, A. Moreno-Márquez, G. Pascual Berlanga, P. Ramos-García, J. Ramos-Muñoz, E. Vijande Vila, G. Aguilella Arzo, Á. Esparza Arroyo, K. T. Lillios, J. Mack, J. Velasco-Vázquez, A. Waterman, L. Benítez de Lugo Enrich, M. Benito Sánchez, B. Agustí, F. Codina, G. de Prado, A. Estalrrich, Á. Fernández Flores, C. Finlayson, G. Finlayson, S. Finlayson, F. Giles-Guzmán, A. Rosas, V. Barciela González, G. García Atiénzar, M. S. Hernández Pérez, A. Llanos, Y. Carrión Marco, I. Collado Beneyto, D. López-Serrano, M. Sanz Tormo, A. C. Valera, C. Blasco, C. Liesau, P. Ríos, J. Daura, M. J. de Pedro Michó, A. A. Diez-Castillo, R. Flores Fernández, J. Francès Farré, R. Garrido-Pena, V. S. Gonçalves, E. Guerra-Doce, A. M. Herrero-Corral, J. Juan-Cabanilles, D. López-Reyes, S. B. McClure, M. Merino Pérez, A. Oliver Foix, M. Sanz Borràs, A. C. Sousa, J. M. Vidal Encinas, D. J. Kennett, M. B. Richards, K. Werner Alt, W. Haak, R. Pinhasi, C. Lalueza-Fox, D. Reich, The genomic history of the Iberian Peninsula over the past 8000 years. *Science* **363**, 1230–1234 (2019).

39. C. Posth, V. Zaro, M. A. Spyrou, S. Vai, G. A. Gnecchi-Ruscone, A. Modi, A. Peltzer, A. Mötsch, K. Nägele, Å. J. Vågene, E. A. Nelson, R. Radzevičiūtė, C. Freund, L. M. Bondioli, L. Cappuccini, H. Frenzel, E. Pacciani, F. Boschin, G. Capecchi, I. Martini, A. Moroni, S. Ricci, A. Sperduti, M. A. Turchetti, A. Riga, M. Zavattaro, A. Zifferero, H. O. Heyne, E. Fernández-Domínguez, G. J. Kroonen, M. McCormick, W. Haak, M. Lari, G. Barbujani, L. Bondioli, K. I. Bos, D. Caramelli, J. Krause, The origin and legacy of the Etruscans through a 2000-year archeogenomic time transect. *Sci. Adv.* **7**, eabi7673 (2021).

40. M. L. Antonio, Z. Gao, H. M. Moots, M. Lucci, F. Candilio, S. Sawyer, V. Oberreiter, D. Calderon, K. Devitofranceschi, R. C. Aikens, S. Aneli, F. Bartoli, A. Bedini, O. Cheronet, D. J. Cotter, D. M. Fernandes, G. Gasperetti, R. Grifoni, A. Guidi, F. La Pastina, E. Loreti, D. Manacorda, G. Matullo, S. Morretta, A. Nava, V. Fiocchi Nicolai, F. Nomi, C. Pavolini, M. Pentiricci, P. Pergola, M. Piranomonte, R. Schmidt, G. Spinola, A. Sperduti, M. Rubini, L. Bondioli, A. Coppa, R. Pinhasi, J. K. Pritchard, Ancient Rome: A genetic crossroads of Europe and the Mediterranean. *Science* **366**, 708–714 (2019).

41. I. Stolarek, M. Zenczak, L. Handschuh, A. Juras, M. Marcinkowska-Swojak, A. Spinek, A. Dębski, M. Matla, H. Kóčka-Krenz, J. Piontek, Polish Archaeogenomics Consortium Team, M. Figlerowicz, Genetic history of East-Central Europe in the first millennium CE. *Genome Biol.* **24**, 173 (2023).

42. J. Gretzinger, D. Sayer, P. Justeau, E. Altena, M. Pala, K. Dulias, C. J. Edwards, S. Jodoin, L. Lacher, S. Sabin, Å. J. Vågene, W. Haak, S. S. Ebenesersdóttir, K. H. S. Moore, R. Radzeviciute, K. Schmidt, S. Brace, M. A. Bager, N. Patterson, L. Papac, N. Broomandkhoshbacht, K. Callan, É. Harney, L. Iliev, A. M. Lawson, M. Michel, K. Stewardson, F. Zalzala, N. Rohland, S. Kappelhoff-Beckmann, F. Both, D. Winger, D. Neumann, L. Saalow, S. Krabath, S. Beckett, M. Van Twest, N. Faulkner, C. Read, T. Barton, J. Caruth, J. Hines, B. Krause-Kyora, U. Warnke, V. J. Schuenemann, I. Barnes, H. Dahlström, J. J. Clausen, A. Richardson, E. Popescu, N. Dodwell, S. Ladd, T. Phillips, R. Mortimer, F. Sayer, D. Swales, A. Stewart, D. Powlesland, R. Kenyon, L. Ladle, C. Peek, S. Grefen-Peters, P. Ponce, R. Daniels, C. Spall, J. Woolcock, A. M. Jones, A. V. Roberts, R. Symmons, A. C. Rawden, A. Cooper, K. I. Bos, T. Booth, H. Schroeder, M. G. Thomas, A. Helgason, M. B. Richards, D. Reich, J. Krause, S. Schiffels, The Anglo-Saxon migration and the formation of the early English gene pool. *Nature* **610**, 112–119 (2022).

43. A. Margaryan, D. J. Lawson, M. Sikora, F. Racimo, S. Rasmussen, I. Moltke, L. M. Cassidy, E. Jørsboe, A. Ingason, M. W. Pedersen, T. Korneliussen, H. Wilhelmson, M. M. Buś, P. de Barros Damgaard, R. Martiniano, G. Renaud, C. Bhérer, J. V. Moreno-Mayar, A. K. Fotakis, M. Allen, R. Allmäe, M. Molak, E. Cappellini, G. Scorrano, H. McColl, A. Buzhilova, A. Fox, A. Albrechtsen, B. Schütz, B. Skar, C. Arcini, C. Falys, C. H. Jonson, D. Błaszczyk, D. Pezhemsky, G. Turner-Walker, H. Gestsdóttir, I. Lundstrøm, I. Gustin, I. Mainland, I. Potekhina, I. M. Muntoni, J. Cheng, J. Stenderup, J. Ma, J. Gibson, J. Peets, J. Gustafsson, K. H. Iversen, L. Simpson, L. Strand, L. Loe, M. Sikora, M. Florek, M. Vretemark, M. Redknap, M. Bajka, T. Pushkina, M. Søvsø, N. Grigoreva, T. Christensen, O. Kastholm, O. Uldum, P. Favia, P. Holck, S. Sten, S. V. Arge, S. Ellingvåg, V. Moiseyev, W. Bogdanowicz, Y. Magnusson, L. Orlando, P. Pentz, M. D. Jessen, A. Pedersen, M. Collard, D. G. Bradley, M. L. Jørkov, J. Arneborg, N. Lynnerup, N. Price, M. T. P. Gilbert, M. E. Allentoft, J. Bill, S. M. Sindbæk, L. Hedeager, K. Kristiansen, R. Nielsen, T. Werge, E.

Willerslev, Population genomics of the Viking world. *Nature* **585**, 390–396 (2020).

44. M. L. Antonio, C. L. Weiß, Z. Gao, S. Sawyer, V. Oberreiter, H. M. Moots, J. P. Spence, O. Cheronet, B. Zagorc, E. Praxmarer, K. T. Özdoğan, L. Demetz, P. Gelabert, D. Fernandes, M. Lucci, T. Alihodžić, S. Amrani, P. Avetisyan, C. Baillif-Ducros, Ž. Bedić, A. Bertrand, M. Bilić, L. Bondioli, P. Borówka, E. Botte, J. Burmaz, D. Bužanić, F. Candilio, M. Cvetko, D. De Angelis, I. Drnić, K. Elschek, M. Fantar, A. Gaspari, G. Gasperetti, F. Genchi, S. Golubović, Z. Hukeľová, R. Jankauskas, K. J. Vučković, G. Jeremić, I. Kaić, K. Kazek, H. Khachatryan, A. Khudaverdyan, S. Kirchengast, M. Korać, V. Kozlowski, M. Krošláková, D. Kušan Špalj, F. La Pastina, M. Laguardia, S. Legrand, T. Leleković, T. Leskovar, W. Lorkiewicz, D. Los, A. M. Silva, R. Masaryk, V. Matijević, Y. M. S. Cherifi, N. Meyer, I. Mikić, N. Miladinović-Radmilović, B. Milošević Zakić, L. Nacouzi, M. Natuniewicz-Sekuła, A. Nava, C. Neugebauer-Maresch, J. Nováček, A. Osterholtz, J. Paige, L. Paraman, D. Pieri, K. Pieta, S. Pop-Lazić, M. Ruttkay, M. Sanader, A. Sołtysiak, A. Sperduti, T. Stankovic Pesterac, M. Teschler-Nicola, I. Teul, D. Tončinić, J. Trapp, D. Vulović, T. Waliszewski, D. Walter, M. Živanović, M. E. M. Filah, M. Čaušević-Bully, M. Šlaus, D. Borić, M. Novak, A. Coppa, R. Pinhasi, J. K. Pritchard, Stable population structure in Europe since the Iron Age, despite high mobility. *Elife* **13**, e79714 (2024).

45. H. Ringbauer, J. Novembre, M. Steinrücken, Parental relatedness through time revealed by runs of homozygosity in ancient DNA. *Nat. Commun.* **12**, 5425 (2021).

46. H. Ringbauer, Y. Huang, A. Akbari, S. Mallick, I. Olalde, N. Patterson, D. Reich, Accurate detection of identity-by-descent segments in human ancient DNA. *Nat. Genet.* **56**, 143–151 (2024).

47. S. R. Browning, R. K. Waples, B. L. Browning, Fast, accurate local ancestry inference with FLARE. *Am. J. Hum. Genet.* **110**, 326–335 (2023).

48. W. Pohl, "Alboin und der Langobardenzug nach Italien. Aufstieg und Fall eines Barbarenkönigs" in *Sie Schufen Europa. Historische Portraits von Konstantin Bis Karl Dem Großen*, M. (hrsg). Meier, Ed. (C.H.Beck, München, 2007), pp. 216–227.

49. N. Christie, *The Lombards: The Ancient Longobards* (Wiley, 1999).

50. J. Jarnut, *Geschichte der Langobarden* (Kohlhammer, Stuttgart, Germany, 1982).

51. C. Knipper, I. Koncz, J. G. Ódor, B. G. Mende, Z. Rácz, S. Kraus, R. van Gyseghem, R. Friedrich, T. Vida, Coalescing traditions-Coalescing people: Community formation in Pannonia after the decline of the Roman Empire. *PLoS One* **15**, e0231760 (2020).

52. C. E. G. Amorim, S. Vai, C. Posth, A. Modi, I. Koncz, S. Hakenbeck, M. C. La Rocca, B. Mende, D. Bobo, W. Pohl, L. P. Baricco, E. Bedini, P. Francalacci, C. Giostra, T. Vida, D. Winger, U. von Freeden, S. Ghirotto, M. Lari, G. Barbujani, J. Krause, D. Caramelli, P. J. Geary, K. R. Veeramah, Understanding 6th-century barbarian social organization and migration through paleogenomics. *Nat. Commun.* **9**, 3547 (2018).

53. M. Lipatov, K. Sanjeev, R. Patro, K. R. Veeramah, Maximum Likelihood Estimation of Biological Relatedness from Low Coverage Sequencing Data, *bioRxiv* (2015)p. 023374.

54. D. Popli, S. Peyrégne, B. M. Peter, KIN: a method to infer relatedness from low-coverage ancient DNA. *Genome Biol.* **24**, 10 (2023).

55. J. Jarnut, “Langobardische Eliten in der sozialen Praxis” in *Théorie et Pratiques Des élites Au Haut Moyen Âge. Conception, Perception et Réalisation Sociale*, F. Bougard, H.-W. Goetz, R. Le Jan, Eds. (Brepols, 2011)vol. 13 of *Haut Moyen Âge*, pp. 283–290.

56. G. Waitz, Ed., *Monumenta Germaniae Historica. Scriptores Rerum Langobardicarum et Italicarum Saec VI- IX* (Hannover, 1878).

57. G. P. Bognetti, *L’influsso Delle Istituzioni Militari Romane Sulle Istituzioni Longobarde Del Secolo VI E La Natura Della “fara”* (Milano, 1967)*L’età longobarda 3*.

58. A. C. Murray, *Germanic Kinship Structure. Studies in Law and Society in Antiquity and in the Early Middle Ages* (Pontifical Institute of Medieval Studies, Toronto, 1983).

59. W. Haubrichs, »Leudes, fara, faramanni und farones«: Zur Semantik der Bezeichnungen für einige am Konsenshandeln beteiligte Gruppen. doi: 10.11588/VUF.2017.0.71813 (2020).

60. L. K. Little, Ed., *Plague and the End of Antiquity* (Cambridge University Press, Cambridge, England, 2006).

61. J. A. Fellows Yates, T. C. Lamnidis, M. Borry, A. Andrades Valtueña, Z. Fagernäs, S. Clayton, M. U. Garcia, J. Neukamm, A. Peltzer, Reproducible, portable, and efficient ancient genome reconstruction with nf-core/eager. *PeerJ* **9**, e10947 (2021).

62. M. Schubert, S. Lindgreen, L. Orlando, AdapterRemoval v2: rapid adapter trimming, identification, and read merging. *BMC Res. Notes* **9**, 88 (2016).

63. H. Li, R. Durbin, Fast and accurate short read alignment with Burrows-Wheeler transform. *Bioinformatics* **25**, 1754–1760 (2009).

64. H. Li, B. Handsaker, A. Wysoker, T. Fennell, J. Ruan, N. Homer, G. Marth, G. Abecasis, R. Durbin, 1000 Genome Project Data Processing Subgroup, The Sequence Alignment/Map format and SAMtools. *Bioinformatics* **25**, 2078–2079 (2009).

65. H. Jónsson, A. Ginolhac, M. Schubert, P. L. F. Johnson, L. Orlando, mapDamage2.0: fast approximate Bayesian estimates of ancient DNA damage parameters. *Bioinformatics* **29**, 1682–1684 (2013).

66. A. Mckenna, The genome analysis toolkit: A mapreduce framework for analyzing nextgeneration DNA sequencing data. *Genome Res* **20**, 1297–1303 (2010).

67. P. Danecek, J. K. Bonfield, J. Liddle, J. Marshall, V. Ohan, M. O. Pollard, A. Whitwham, T. Keane, S. A. McCarthy, R. M. Davies, H. Li, Twelve years of SAMtools and BCFtools. *Gigascience* **10** (2021).

68. T. S. Korneliussen, A. Albrechtsen, R. Nielsen, ANGSD: Analysis of next generation sequencing data. *BMC Bioinformatics* **15**, 356 (2014).

69. G. Renaud, V. Slon, A. T. Duggan, J. Kelso, Schmutzi: estimation of contamination and endogenous mitochondrial consensus calling for ancient DNA. *Genome Biol.* **16**, 224 (2015).

70. A. W. Briggs, J. M. Good, R. E. Green, J. Krause, T. Maricic, U. Stenzel, C. Lalueza-Fox, P. Rudan, D. Brajkovic, Z. Kucan, I. Gusic, R. Schmitz, V. B. Doronichev, L. V. Golovanova, M. de la Rasilla, J. Fortea, A. Rosas, S. Pääbo, Targeted retrieval and analysis of five Neandertal mtDNA genomes. *Science* **325**, 318–321 (2009).

71. L. Fan, Y.-G. Yao, An update to MitoTool: using a new scoring system for faster mtDNA haplogroup determination. *Mitochondrion* **13**, 360–363 (2013).

72. P. Francalacci, Low-pass DNA sequencing of 1200 Sardinians reconstructs European Ychromosome phylogeny. *Science* **341**, 565–569 (2013).

73. M. Karmin, L. Saag, M. Vicente, M. A. Wilson Sayres, M. Järve, U. G. Talas, S. Rootsi, A.-M. Ilumäe, R. Mägi, M. Mitt, L. Pagani, T. Puurand, Z. Faltyskova, F. Clemente, A. Cardona, E. Metspalu, H. Sahakyan, B. Yunusbayev, G. Hudjashov, M. DeGiorgio, E.-L. Loogväli, C. Eichstaedt, M. Eelmets, G. Chaubey, K. Tambets, S. Litvinov, M. Mormina, Y. Xue, Q. Ayub, G. Zoraqi, T. S. Korneliussen, F. Akhatova, J. Lachance, S. Tishkoff, K. Momynaliev, F.-X. Ricaut, P. Kusuma, H. Razafindrazaka, D. Pierron, M. P. Cox, G. N. N. Sultana, R. Willerslev, C. Muller, M. Westaway, D. Lambert, V. Skaro, L. Kovačevic, S. Turdikulova, D. Dalimova, R. Khusainova, N. Trofimova, V. Akhmetova, I. Khidiyatova, D. V. Lichman, J. Isakova, E. Pocheshkhova, Z. Sabitov, N. A. Barashkov, P. Nymadawa, E. Mihailov, J. W. T. Seng, I. Evseeva, A. B. Migliano, S. Abdullah, G. Andriadze, D. Primorac, L. Atramentova, O. Utevska, L. Yepiskoposyan, D. Marjanovic, A. Kushniarevich, D. M. Behar, C. Gilissen, L. Vissers, J. A. Veltman, E. Balanovska, M. Derenko, B. Malyarchuk, A. Metspalu, S. Fedorova, A. Eriksson, A. Manica, F. L. Mendez, T. M. Karafet, K. R. Veeramah, N. Bradman, M. F. Hammer, L. P. Osipova, O. Balanovsky, E. K. Khusnutdinova, K. Johnsen, M. Remm, M. G. Thomas, C. Tyler-Smith, P. A. Underhill, E. Willerslev, R. Nielsen, M. Metspalu, R. Villems, T. Kivisild, A recent bottleneck of Y chromosome diversity coincides with a global change in culture. *Genome Res.* **25**, 459–466 (2015).

74. G. D. Poznik, B. M. Henn, M.-C. Yee, E. Sliwerska, G. M. Euskirchen, A. A. Lin, M. Snyder, L. Quintana-Murci, J. M. Kidd, P. A. Underhill, C. D. Bustamante, Sequencing Y chromosomes resolves discrepancy in time to common ancestor of males versus females. *Science* **341**, 562–565 (2013).

75. 1000 Genomes Project Consortium, A. Auton, L. D. Brooks, R. M. Durbin, E. P. Garrison, H. M. Kang, J. O. Korbel, J. L. Marchini, S. McCarthy, G. A. McVean, G. R. Abecasis, A global reference for human genetic variation. *Nature* **526**, 68–74 (2015).

76. F. Ravasini, H. Kabral, A. Solnik, L. de Gennaro, F. Montinaro, R. Hui, C. Delpino, S. Finocchi, P. Giroldini, O. Mei, M. A. Beck De Lotto, E. Cilli, M. Hajiesmaeil, L. Pistacchia, F. Risi, C. Giacometti, C. L. Scheib, K. Tambets, M. Metspalu, F. Cruciani, E. D'Atanasio, B. Trombetta, The genomic portrait of the Picene culture provides new insights into the Italic Iron Age and the legacy of the Roman Empire in Central Italy. *Genome Biol.* **25**, 292

(2024).

77. K. R. Veeramah, A. Tönjes, P. Kovacs, A. Gross, D. Wegmann, P. Geary, D. Gasperikova, I. Klimes, M. Scholz, J. Novembre, M. Stumvoll, Genetic variation in the Sorbs of eastern Germany in the context of broader European genetic diversity. *Eur. J. Hum. Genet.* **19**, 995–1001 (2011).

78. K. R. Veeramah, A. Rott, M. Groß, L. van Dorp, S. López, K. Kirsanow, C. Sell, J. Blöcher, D. Wegmann, V. Link, Z. Hofmanová, J. Peters, B. Trautmann, A. Gairhos, J. Haberstroh, B. Päffgen, G. Hellenthal, B. Haas-Gebhard, M. Harbeck, J. Burger, Population genomic analysis of elongated skulls reveals extensive female-biased immigration in Early Medieval Bavaria. *Proc. Natl. Acad. Sci. U. S. A.* **115**, 3494–3499 (2018).

79. A. L. Price, N. J. Patterson, R. M. Plenge, M. E. Weinblatt, N. A. Shadick, D. Reich, Principal components analysis corrects for stratification in genome-wide association studies. *Nat. Genet.* **38**, 904–909 (2006).

80. N. Patterson, A. L. Price, D. Reich, Population structure and eigenanalysis. *PLoS Genet.* **2**, e190 (2006).

81. M. Waskom, seaborn: statistical data visualization. *J. Open Source Softw.* **6**, 3021 (2021).

82. P. Danecek, A. Auton, G. Abecasis, C. A. Albers, E. Banks, M. A. DePristo, R. E. Handsaker, G. Lunter, G. T. Marth, S. T. Sherry, G. McVean, R. Durbin, 1000 Genomes Project Analysis Group, The variant call format and VCFtools. *Bioinformatics* **27**, 2156–2158 (2011).

83. I. Lazaridis, D. Nadel, G. Rollefson, D. C. Merrett, N. Rohland, S. Mallick, D. Fernandes, M. Novak, B. Gamarra, K. Sirak, S. Connell, K. Stewardson, E. Harney, Q. Fu, G. Gonzalez-Fortes, E. R. Jones, S. A. Roodenberg, G. Lengyel, F. Bocquentin, B. Gasparian, J. M. Monge, M. Gregg, V. Eshed, A.-S. Mizrahi, C. Meiklejohn, F. Gerritsen, L. Bejenaru, M. Blüher, A. Campbell, G. Cavalleri, D. Comas, P. Froguel, E. Gilbert, S. M. Kerr, P. Kovacs, J. Krause, D. McGettigan, M. Merrigan, D. A. Merriwether, S. O'Reilly, M. B. Richards, O. Semino, M. Shamoon-Pour, G. Stefanescu, M. Stumvoll, A. Tönjes, A. Torroni, J. F. Wilson, L. Yengo, N. A. Hovhannisyan, N. Patterson, R. Pinhasi, D. Reich, Genomic insights into the origin of farming in the ancient Near East. *Nature* **536**, 419–424 (2016).

84. I. Lazaridis, N. Patterson, A. Mittnik, G. Renaud, S. Mallick, K. Kirsanow, P. H. Sudmant, J. G. Schraiber, S. Castellano, M. Lipson, B. Berger, C. Economou, R. Bollongino, Q. Fu, K. I. Bos, S. Nordenfelt, H. Li, C. de Filippo, K. Prüfer, S. Sawyer, C. Posth, W. Haak, F. Hallgren, E. Fornander, N. Rohland, D. Delsate, M. Francken, J.-M. Guinet, J. Wahl, G. Ayodo, H. A. Babiker, G. Bailliet, E. Balanovska, O. Balanovsky, R. Barrantes, G. Bedoya, H. Ben-Ami, J. Bene, F. Berrada, C. M. Bravi, F. Brisighelli, G. B. J. Busby, F. Cali, M. Churnosov, D. E. C. Cole, D. Corach, L. Damba, G. van Driem, S. Dryomov, J.-M. Dugoujon, S. A. Fedorova, I. Gallego Romero, M. Gubina, M. Hammer, B. M. Henn, T. Hervig, U. Hodoglugil, A. R. Jha, S. Karachanak-Yankova, R. Khusainova, E. Khusnutdinova, R. Kittles, T. Kivisild, W. Klitz, V. Kučinskas, A. Kushniarevich, L. Laredj, S. Litvinov, T. Loukidis, R. W. Mahley, B. Melegh, E. Metspalu, J. Molina, J. Mountain, K.

Näkkäläjärvi, D. Nesheva, T. Nyambo, L. Osipova, J. Parik, F. Platonov, O. Posukh, V. Romano, F. Rothhammer, I. Rudan, R. Ruizbakiev, H. Sahakyan, A. Sajantila, A. Salas, E. B. Starikovskaya, A. Tarekegn, D. Toncheva, S. Turdikulova, I. Uktveryte, O. Utevska, R. Vasquez, M. Villena, M. Voevoda, C. A. Winkler, L. Yepiskoposyan, P. Zalloua, T. Zemunik, A. Cooper, C. Capelli, M. G. Thomas, A. Ruiz-Linares, S. A. Tishkoff, L. Singh, K. Thangaraj, R. Villems, D. Comas, R. Sukernik, M. Metspalu, M. Meyer, E. E. Eichler, J. Burger, M. Slatkin, S. Pääbo, J. Kelso, D. Reich, J. Krause, Ancient human genomes suggest three ancestral populations for present-day Europeans. *Nature* **513**, 409–413 (2014).

85. W. Haak, I. Lazaridis, N. Patterson, N. Rohland, S. Mallick, B. Llamas, G. Brandt, S. Nordenfelt, E. Harney, K. Stewardson, Q. Fu, A. Mittnik, E. Bánffy, C. Economou, M. Francken, S. Friederich, R. G. Pena, F. Hallgren, V. Khartanovich, A. Khokhlov, M. Kunst, P. Kuznetsov, H. Meller, O. Mochalov, V. Moiseyev, N. Nicklisch, S. L. Pichler, R. Risch, M. A. Rojo Guerra, C. Roth, A. Szécsényi-Nagy, J. Wahl, M. Meyer, J. Krause, D. Brown, D. Anthony, A. Cooper, K. W. Alt, D. Reich, Massive migration from the steppe was a source for Indo-European languages in Europe. *Nature* **522**, 207–211 (2015).

86. M. E. Allentoft, M. Sikora, K.-G. Sjögren, S. Rasmussen, M. Rasmussen, J. Stenderup, P. B. Damgaard, H. Schroeder, T. Ahlström, L. Vinner, A.-S. Malaspinas, A. Margaryan, T. Higham, D. Chivall, N. Lynnerup, L. Harvig, J. Baron, P. Della Casa, P. Dąbrowski, P. R. Duffy, A. V. Ebel, A. Epimakhov, K. Frei, M. Furmanek, T. Gralak, A. Gromov, S. Gronkiewicz, G. Grupe, T. Hajdu, R. Jarysz, V. Khartanovich, A. Khokhlov, V. Kiss, J. Kolář, A. Kriiska, I. Lasak, C. Longhi, G. McGlynn, A. Merkevicius, I. Merkyte, M. Metspalu, R. Mkrtchyan, V. Moiseyev, L. Paja, G. Pálfi, D. Pokutta, Ł. Pospieszny, T. D. Price, L. Saag, M. Sablin, N. Shishlina, V. Smrčka, V. I. Soenov, V. Szeverényi, G. Tóth, S. V. Trifanova, L. Varul, M. Vicze, L. Yepiskoposyan, V. Zhitenev, L. Orlando, T. Sicheritz-Pontén, S. Brunak, R. Nielsen, K. Kristiansen, E. Willerslev, Population genomics of Bronze Age Eurasia. *Nature* **522**, 167–172 (2015).

87. C. Gamba, E. R. Jones, M. D. Teasdale, R. L. McLaughlin, G. Gonzalez-Fortes, V. Mattiangeli, L. Domboróczki, I. Kővári, I. Pap, A. Anders, Others, Genome flux and stasis in a five millennium transect of European prehistory. Nat Commun 5: 5257. [Preprint] (2014).

88. Z. Hofmanová, S. Kreutzer, G. Hellenthal, C. Sell, Y. Diekmann, D. Díez-Del-Molino, L. van Dorp, S. López, A. Kousathanas, V. Link, K. Kirsanow, L. M. Cassidy, R. Martiniano, M. Strobel, A. Scheu, K. Kotsakis, P. Halstead, S. Triantaphyllou, N. Kyparissi-Apostolika, D. Urem-Kotsou, C. Ziota, F. Adaktylou, S. Gopalan, D. M. Bobo, L. Winkelbach, J. Blöcher, M. Unterländer, C. Leuenberger, Ç. Çilingiroğlu, B. Horejs, F. Gerritsen, S. J. Shennan, D. G. Bradley, M. Currat, K. R. Veeramah, D. Wegmann, M. G. Thomas, C. Papageorgopoulou, J. Burger, Early farmers from across Europe directly descended from Neolithic Aegeans. *Proc. Natl. Acad. Sci. U. S. A.* **113**, 6886–6891 (2016).

89. I. Mathieson, S. Alpaslan-Roodenberg, C. Posth, A. Szécsényi-Nagy, N. Rohland, S. Mallick, I. Olalde, N. Broomandkhoshbacht, F. Candilio, O. Cheronet, D. Fernandes, M. Ferry, B. Gamarra, G. G. Fortes, W. Haak, E. Harney, E. Jones, D. Keating, B. Krause-Kyora, I. Kucukkalipci, M. Michel, A. Mittnik, K. Nägele, M. Novak, J. Oppenheimer, N. Patterson, S. Pfrengle, K. Sirak, K. Stewardson, S. Vai, S. Alexandrov, K.

W. Alt, R. Andreescu, D. Antonović, A. Ash, N. Atanassova, K. Bacvarov, M. B. Gusztáv, H. Bocherens, M. Bolus, A. Boroneanţ, Y. Boyadzhiev, A. Budnik, J. Burmaz, S. Chohadzhiev, N. J. Conard, R. Cottiaux, M. Čuka, C. Cupillard, D. G. Drucker, N. Elenski, M. Francken, B. Galabova, G. Ganetsovski, B. Gély, T. Hajdu, V. Handzhyiska, K. Harvati, T. Higham, S. Iliev, I. Janković, I. Karavanić, D. J. Kennett, D. Komšo, A. Kozak, D. Labuda, M. Lari, C. Lazar, M. Leppek, K. Leshtakov, D. L. Vetro, D. Los, I. Lozanov, M. Malina, F. Martini, K. McSweeney, H. Meller, M. Menđušić, P. Mirea, V. Moiseyev, V. Petrova, T. D. Price, A. Simalcsik, L. Sineo, M. Šlaus, V. Slavchev, P. Stanev, A. Starović, T. Szeniczey, S. Talamo, M. Teschler-Nicola, C. Thevenet, I. Valchev, F. Valentin, S. Vasilyev, F. Veljanovska, S. Venelinova, E. Veselovskaya, B. Viola, C. Virag, J. Zaninović, S. Zäuner, P. W. Stockhammer, G. Catalano, R. Krauß, D. Caramelli, G. Zariņa, B. Gaydarska, M. Lillie, A. G. Nikitin, I. Potekhina, A. Papathanasiou, D. Borić, C. Bonsall, J. Krause, R. Pinhasi, D. Reich, The genomic history of southeastern Europe. *Nature* **555**, 197–203 (2018).

90. I. Olalde, M. E. Allentoft, F. Sánchez-Quinto, G. Santpere, C. W. K. Chiang, M. DeGiorgio, J. Prado-Martinez, J. A. Rodríguez, S. Rasmussen, J. Quilez, O. Ramírez, U. M. Marigorta, M. Fernández-Callejo, M. E. Prada, J. M. V. Encinas, R. Nielsen, M. G. Netea, J. Novembre, R. A. Sturm, P. Sabeti, T. Marquès-Bonet, A. Navarro, E. Willerslev, C. Lalueza-Fox, Derived immune and ancestral pigmentation alleles in a 7,000-year-old Mesolithic European. *Nature* **507**, 225–228 (2014).

91. M. van de Loosdrecht, A. Bouzouggar, L. Humphrey, C. Posth, N. Barton, A. Aximu-Petri, B. Nickel, S. Nagel, E. H. Talbi, M. A. E. Hajraoui, S. Amzazi, J.-J. Hublin, S. Pääbo, S. Schiffels, M. Meyer, W. Haak, C. Jeong, J. Krause, Pleistocene North African genomes link Near Eastern and sub-Saharan African human populations. *Science* **360**, 548–552 (2018).

92. Q. Fu, C. Posth, M. Hajdinjak, M. Petr, S. Mallick, D. Fernandes, A. Furtwängler, W. Haak, M. Meyer, A. Mittnik, B. Nickel, A. Peltzer, N. Rohland, V. Slon, S. Talamo, I. Lazaridis, M. Lipson, I. Mathieson, S. Schiffels, P. Skoglund, A. P. Derevianko, N. Drozdov, V. Slavinsky, A. Tsybankov, R. G. Cremonesi, F. Mallegni, B. Gély, E. Vacca, M. R. G. Morales, L. G. Straus, C. Neugebauer-Maresch, M. Teschler-Nicola, S. Constantin, O. T. Moldovan, S. Benazzi, M. Peresani, D. Coppola, M. Lari, S. Ricci, A. Ronchitelli, F. Valentin, C. Thevenet, K. Wehrberger, D. Grigorescu, H. Rougier, I. Crevecoeur, D. Flas, P. Semal, M. A. Mannino, C. Cupillard, H. Bocherens, N. J. Conard, K. Harvati, V. Moiseyev, D. G. Drucker, J. Svoboda, M. P. Richards, D. Caramelli, R. Pinhasi, J. Kelso, N. Patterson, J. Krause, S. Pääbo, D. Reich, The genetic history of Ice Age Europe. *Nature* **534**, 200–205 (2016).

93. E. J. Pebesma, Multivariable geostatistics in S: the gstat package. *Comput. Geosci.* **30**, 683–691 (2004).

94. P. de B. Damgaard, N. Marchi, S. Rasmussen, M. Peyrot, G. Renaud, T. Korneliussen, J. V. Moreno-Mayar, M. W. Pedersen, A. Goldberg, E. Usmanova, N. Baimukhanov, V. Loman, L. Hedeager, A. G. Pedersen, K. Nielsen, G. Afanasiev, K. Akmatov, A. Aldashev, A. Alpaslan, G. Baimbetov, V. I. Bazaliiskii, A. Beisenov, B. Boldbaatar, B. Boldgiv, C. Dorzhu, S. Ellingvag, D. Erdenebaatar, R. Dajani, E. Dmitriev, V. Evdokimov, K. M. Frei, A. Gromov, A. Goryachev, H. Hakonarson, T. Hegay, Z. Khachatryan, R. Khaskhanov, E.

Kitov, A. Kolbina, T. Kubatbek, A. Kukushkin, I. Kukushkin, N. Lau, A. Margaryan, I. Merkyte, I. V. Mertz, V. K. Mertz, E. Mijiddorj, V. Moiyesev, G. Mukhtarova, B. Nurmukhanbetov, Z. Orozbekova, I. Panyushkina, K. Pieta, V. Smrčka, I. Shevnina, A. Logvin, K.-G. Sjögren, T. Štolcová, A. M. Taravella, K. Tashbaeva, A. Tkachev, T. Tulegenov, D. Voyakin, L. Yepiskoposyan, S. Undrakhbold, V. Varfolomeev, A. Weber, M. A. Wilson Sayres, N. Kradin, M. E. Allentoft, L. Orlando, R. Nielsen, M. Sikora, E. Heyer, K. Kristiansen, E. Willerslev, 137 ancient human genomes from across the Eurasian steppes. *Nature* **557**, 369–374 (2018).

95. P. Flegontov, N. E. Altınışık, P. Changmai, N. Rohland, S. Mallick, N. Adamski, D. A. Bolnick, N. Broomandkhoshbacht, F. Candilio, B. J. Culleton, O. Flegontova, T. M. Friesen, C. Jeong, T. K. Harper, D. Keating, D. J. Kennett, A. M. Kim, T. C. Lamnidis, A. M. Lawson, I. Olalde, J. Oppenheimer, B. A. Potter, J. Raff, R. A. Sattler, P. Skoglund, K. Stewardson, E. J. Vajda, S. Vasilyev, E. Veselovskaya, M. G. Hayes, D. H. O'Rourke, J. Krause, R. Pinhasi, D. Reich, S. Schiffels, Palaeo-Eskimo genetic ancestry and the peopling of Chukotka and North America. *Nature* **570**, 236–240 (2019).

96. G. A. Gnecchi-Ruscone, E. Khussainova, N. Kahbatkyzy, L. Musralina, M. A. Spyrou, R. A. Bianco, R. Radzeviciute, N. F. G. Martins, C. Freund, O. Iksan, A. Garshin, Z. Zhaniyazov, B. Bekmanov, E. Kitov, Z. Samashev, A. Beisenov, N. Berezina, Y. Berezin, A. Z. Bíró, S. Évinger, A. Bissembaev, G. Akhatov, A. Mamedov, A. Onggaruly, D. Voyakin, A. Chotbayev, Y. Kariyev, A. Buzhilova, L. Djansugurova, C. Jeong, J. Krause, Ancient genomic time transect from the Central Asian Steppe unravels the history of the Scythians. *Sci. Adv.* **7**, eabe4414 (2021).

97. G. A. Gnecchi-Ruscone, Z. Rácz, L. Samu, T. Szeniczey, N. Faragó, C. Knipper, R. Friedrich, D. Zlámalová, L. Traverso, S. Liccardo, S. Wabnitz, D. Popli, K. Wang, R. Radzeviciute, B. Gulyás, I. Koncz, C. Balogh, G. M. Lezsák, V. Mácsai, M. M. E. Bunbury, O. Spekker, P. le Roux, A. Szécsényi-Nagy, B. G. Mende, H. Colleran, T. Hajdu, P. Geary, W. Pohl, T. Vida, J. Krause, Z. Hofmanová, Network of large pedigrees reveals social practices of Avar communities. *Nature* **629**, 376–383 (2024).

98. É. Harney, A. Nayak, N. Patterson, P. Joglekar, V. Mushrif-Tripathy, S. Mallick, N. Rohland, J. Sedig, N. Adamski, R. Bernardos, N. Broomandkhoshbacht, B. J. Culleton, M. Ferry, T. K. Harper, M. Michel, J. Oppenheimer, K. Stewardson, Z. Zhang, Harashawaradhana, M. S. Bartwal, S. Kumar, S. C. Diyundi, P. Roberts, N. Boivin, D. J. Kennett, K. Thangaraj, D. Reich, N. Rai, Ancient DNA from the skeletons of Roopkund Lake reveals Mediterranean migrants in India. *Nat. Commun.* **10**, 3670 (2019).

99. C. Jeong, K. Wang, S. Wilkin, W. T. T. Taylor, B. K. Miller, J. H. Bemmann, R. Stahl, C. Chiovelli, F. Knolle, S. Ulziibayar, D. Khatanbaatar, D. Erdenebaatar, U. Erdenebat, A. Ochir, G. Ankhsanaa, C. Vanchigdash, B. Ochir, C. Munkhbayar, D. Tumen, A. Kovalev, N. Kradin, B. A. Bazarov, D. A. Miyagashev, P. B. Konovalov, E. Zhambaltarova, A. V. Miller, W. Haak, S. Schiffels, J. Krause, N. Boivin, M. Erdene, J. Hendy, C. Warinner, A dynamic 6,000-year genetic history of Eurasia's Eastern Steppe. *Cell* **183**, 890–904.e29 (2020).

100. J. H. Marcus, C. Posth, H. Ringbauer, L. Lai, R. Skeates, C. Sidore, J. Beckett, A. Furtwängler, A. Olivieri, C. W. K. Chiang, H. Al-Asadi, K. Dey, T. A. Joseph, C.-C. Liu, C.

Der Sarkissian, R. Radzevičiūtė, M. Michel, M. G. Gradoli, P. Marongiu, S. Rubino, V. Mazzarello, D. Rovina, A. La Fragola, R. M. Serra, P. Bandiera, R. Bianucci, E. Pompianu, C. Murgia, M. Guirguis, R. P. Orquin, N. Tuross, P. van Dommelen, W. Haak, D. Reich, D. Schlessinger, F. Cucca, J. Krause, J. Novembre, Genetic history from the Middle Neolithic to present on the Mediterranean island of Sardinia. *Nat. Commun.* **11**, 939 (2020).

101. Z. Maróti, E. Neparáczki, O. Schütz, K. Maár, G. I. B. Varga, B. Kovács, T. Kalmár, E. Nyerki, I. Nagy, D. Latinovics, B. Tihanyi, A. Marcsik, G. Pálfi, Z. Bernert, Z. Gallina, C. Horváth, S. Varga, L. Költő, I. Raskó, P. L. Nagy, C. Balogh, A. Zink, F. Maixner, A. Götherström, R. George, C. Szalontai, G. Szenthe, E. Gáll, A. P. Kiss, B. Gulyás, B. N. Kovacsóczy, S. S. Gál, P. Tomka, T. Török, The genetic origin of Huns, Avars, and conquering Hungarians. *Curr. Biol.* **32**, 2858–2870.e7 (2022).

102. N. Patterson, M. Isakov, T. Booth, L. Büster, C.-E. Fischer, I. Olalde, H. Ringbauer, A. Akbari, O. Cheronet, M. Bleasdale, N. Adamski, E. Altena, R. Bernardos, S. Brace, N. Broomandkhoshbacht, K. Callan, F. Candilio, B. Culleton, E. Curtis, L. Demetz, K. S. D. Carlson, C. J. Edwards, D. M. Fernandes, M. G. B. Foody, S. Freilich, H. Goodchild, A. Kearns, A. M. Lawson, I. Lazaridis, M. Mah, S. Mallick, K. Mandl, A. Micco, M. Michel, G. B. Morante, J. Oppenheimer, K. T. Özdoğan, L. Qiu, C. Schattke, K. Stewardson, J. N. Workman, F. Zalzala, Z. Zhang, B. Agustí, T. Allen, K. Almássy, L. Amkreutz, A. Ash, C. Baillif-Ducros, A. Barclay, L. Bartosiewicz, K. Baxter, Z. Bernert, J. Blažek, M. Bodružić, P. Boissinot, C. Bonsall, P. Bradley, M. Brittain, A. Brookes, F. Brown, L. Brown, R. Brunning, C. Budd, J. Burmaz, S. Canet, S. Carnicero-Cáceres, M. Čaušević-Bully, A. Chamberlain, S. Chauvin, S. Clough, N. Čondić, A. Coppa, O. Craig, M. Črešnar, V. Cummings, S. Czifra, A. Danielisová, R. Daniels, A. Davies, P. de Jersey, J. Deacon, C. Deminger, P. W. Ditchfield, M. Dizdar, M. Dobeš, M. Dobisíková, L. Domboróczki, G. Drinkall, A. Đukić, M. Ernée, C. Evans, J. Evans, M. Fernández-Götz, S. Filipović, A. Fitzpatrick, H. Fokkens, C. Fowler, A. Fox, Z. Gallina, M. Gamble, M. R. González Morales, B. González-Rabanal, A. Green, K. Gyenesei, D. Habermehl, T. Hajdu, D. Hamilton, J. Harris, C. Hayden, J. Hendriks, B. Hernu, G. Hey, M. Horňák, G. Ilon, E. Istvánovits, A. M. Jones, M. B. Kavur, K. Kazek, R. A. Kenyon, A. Khreisheh, V. Kiss, J. Kleijne, M. Knight, L. M. Kootker, P. F. Kovács, A. Kozubová, G. Kulcsár, V. Kulcsár, C. Le Pennec, M. Legge, M. Leivers, L. Loe, O. López-Costas, T. Lord, D. Los, J. Lyall, A. B. Marín-Arroyo, P. Mason, D. Matošević, A. Maxted, L. McIntyre, J. McKinley, K. McSweeney, B. Meijlink, B. G. Mende, M. Menđušić, M. Metlička, S. Meyer, K. Mihovilić, L. Milasinovic, S. Minnitt, J. Moore, G. Morley, G. Mullan, M. Musilová, B. Neil, R. Nicholls, M. Novak, M. Pala, M. Papworth, C. Paresys, R. Patten, D. Perkić, K. Pesti, A. Petit, K. Petriščáková, C. Pichon, C. Pickard, Z. Pilling, T. D. Price, S. Radović, R. Redfern, B. Resutík, D. T. Rhodes, M. B. Richards, A. Roberts, J. Roefstra, P. Sankot, A. Šefčáková, A. Sheridan, S. Skae, M. Šmolíková, K. Somogyi, Á. Somogyvári, M. Stephens, G. Szabó, A. Szécsényi-Nagy, T. Szeniczey, J. Tabor, K. Tankó, C. T. Maria, R. Terry, B. Teržan, M. Teschler-Nicola, J. F. Torres-Martínez, J. Trapp, R. Turle, F. Ujvári, M. van der Heiden, P. Veleminsky, B. Veselka, Z. Vytlačil, C. Waddington, P. Ware, P. Wilkinson, L. Wilson, R. Wiseman, E. Young, J. Zaninović, A. Žitňan, C. Lalueza-Fox, P. de Knijff, I. Barnes, P. Halkon, M. G. Thomas, D. J. Kennett, B. Cunliffe, M. Lillie, N. Rohland, R. Pinhasi, I. Armit, D. Reich, Large-scale migration into Britain during the Middle to Late Bronze Age. *Nature* **601**, 588–594 (2022).

103. M. Sikora, V. V. Pitulko, V. C. Sousa, M. E. Allentoft, L. Vinner, S. Rasmussen, A. Margaryan, P. de Barros Damgaard, C. de la Fuente, G. Renaud, M. A. Yang, Q. Fu, I. Dupanloup, K. Giampoudakis, D. Nogués-Bravo, C. Rahbek, G. Kroonen, M. Peyrot, H. McColl, S. V. Vasilyev, E. Veselovskaya, M. Gerasimova, E. Y. Pavlova, V. G. Chasnyk, P. A. Nikolskiy, A. V. Gromov, V. I. Khartanovich, V. Moiseyev, P. S. Grebenyuk, A. Y. Fedorchenko, A. I. Lebedintsev, S. B. Slobodin, B. A. Malyarchuk, R. Martiniano, M. Meldgaard, L. Arppe, J. U. Palo, T. Sundell, K. Mannermaa, M. Putkonen, V. Alexandersen, C. Primeau, N. Baimukhanov, R. S. Malhi, K.-G. Sjögren, K. Kristiansen, A. Wessman, A. Sajantila, M. M. Lahr, R. Durbin, R. Nielsen, D. J. Meltzer, L. Excoffier, E. Willerslev, The population history of northeastern Siberia since the Pleistocene. *Nature* **570**, 182–188 (2019).

104. Y. Tian, I. Koncz, S. Defant, C. Giostra, D. N. Vyas, A. Sołtysiak, L. Pejrani Baricco, R. Fetner, C. Posth, G. Brandt, E. Bedini, A. Modi, M. Lari, S. Vai, P. Francalacci, R. Fernandes, A. Steinhof, W. Pohl, D. Caramelli, J. Krause, A. Izdebski, P. J. Geary, K. R. Veeramah, The role of emerging elites in the formation and development of communities after the fall of the Roman Empire. *Proc. Natl. Acad. Sci. U. S. A.* **121**, e2317868121 (2024).

105. C.-C. Wang, H.-Y. Yeh, A. N. Popov, H.-Q. Zhang, H. Matsumura, K. Sirak, O. Cheronet, A. Kovalev, N. Rohland, A. M. Kim, S. Mallick, R. Bernardos, D. Tumen, J. Zhao, Y.-C. Liu, J.-Y. Liu, M. Mah, K. Wang, Z. Zhang, N. Adamski, N. Broomandkhoshbacht, K. Callan, F. Candilio, K. S. D. Carlson, B. J. Culleton, L. Eccles, S. Freilich, D. Keating, A. M. Lawson, K. Mandl, M. Michel, J. Oppenheimer, K. T. Özdoğan, K. Stewardson, S. Wen, S. Yan, F. Zalzala, R. Chuang, C.-J. Huang, H. Looh, C.-C. Shiung, Y. G. Nikitin, A. V. Tabarev, A. A. Tishkin, S. Lin, Z.-Y. Sun, X.-M. Wu, T.-L. Yang, X. Hu, L. Chen, H. Du, J. Bayarsaikhan, E. Mijiddorj, D. Erdenebaatar, T.-O. Iderkhangai, E. Myagmar, H. Kanzawa-Kiriyama, M. Nishino, K.-I. Shinoda, O. A. Shubina, J. Guo, W. Cai, Q. Deng, L. Kang, D. Li, D. Li, R. Lin, Nini, R. Shrestha, L.-X. Wang, L. Wei, G. Xie, H. Yao, M. Zhang, G. He, X. Yang, R. Hu, M. Robbeets, S. Schiffels, D. J. Kennett, L. Jin, H. Li, J. Krause, R. Pinhasi, D. Reich, Genomic insights into the formation of human populations in East Asia. *Nature* **591**, 413–419 (2021).

106. S. Rubinacci, D. M. Ribeiro, R. J. Hofmeister, O. Delaneau, Publisher Correction: Efficient phasing and imputation of low-coverage sequencing data using large reference panels. *Nat. Genet.* **53**, 412 (2021).

107. M. Bastian, S. Heymann, M. Jacomy, Gephi: An Open Source Software for Exploring and Manipulating Networks. *ICWSM* **3**, 361–362 (2009).

108. M. Jacomy, T. Venturini, S. Heymann, M. Bastian, ForceAtlas2, a continuous graph layout algorithm for handy network visualization designed for the Gephi software. *PLoS One* **9**, e98679 (2014).

109. J. Oksanen, F. G. Blanchet, M. Friendly, R. Kindt, P. Legendre, D. Mcglinn, Wagner, *Vegan: Community Ecology Package* (2020).

110. M. Scott, P. Le Roux, J. Sealy, R. Pickering, Lead and strontium isotopes as palaeodietary

indicators in the Western Cape of South Africa. *S. Afr. J. Sci.* **116** (2020).

111. C. Pin, A. Gannoun, A. Dupont, Rapid, simultaneous separation of Sr, Pb, and Nd by extraction chromatography prior to isotope ratios determination by TIMS and MC-ICP-MS. *J. Anal. At. Spectrom.* **29**, 1858–1870 (2014).

112. T. Waight, J. Baker, D. Peate, Sr isotope ratio measurements by double-focusing MC-ICPMS: techniques, observations and pitfalls. *Int. J. Mass Spectrom.* **221**, 229–244 (2002).

113. R. Longin, New method of collagen extraction for radiocarbon dating. *Nature* **230**, 241–242 (1971).

114. C. Knipper, S. L. Pichler, H. Rissanen, B. Stopp, M. Kühn, N. Spichtig, B. Röder, J. Schibler, G. Lassau, K. W. Alt, What is on the menu in a Celtic town? Iron Age diet reconstructed at Basel-Gasfabrik, Switzerland. *Archaeol. Anthropol. Sci.* **9**, 1307–1326 (2017).

115. B. Kromer, S. Lindauer, H.-A. Synal, L. Wacker, MAMS – A new AMS facility at the Curt-Engelhorn-Centre for Achaeometry, Mannheim, Germany. [Preprint] (2013). https://doi.org/10.1016/j.nimb.2012.01.015.

116. T. A. Brown, D. E. Nelson, J. S. Vogel, J. R. Southon, Improved Collagen Extraction by Modified Longin Method. *Radiocarbon* **30**, 171–177 (1988).

117. M. J. DeNiro, Postmortem preservation and alteration of in vivo bone collagen isotope ratios in relation to palaeodietary reconstruction. *Nature* **317**, 806–809 (1985).

118. P. J. Reimer, W. E. N. Austin, E. Bard, A. Bayliss, P. G. Blackwell, C. Bronk Ramsey, M. Butzin, H. Cheng, R. L. Edwards, M. Friedrich, P. M. Grootes, T. P. Guilderson, I. Hajdas, T. J. Heaton, A. G. Hogg, K. A. Hughen, B. Kromer, S. W. Manning, R. Muscheler, J. G. Palmer, C. Pearson, J. van der Plicht, R. W. Reimer, D. A. Richards, E. M. Scott, J. R. Southon, C. S. M. Turney, L. Wacker, F. Adolphi, U. Büntgen, M. Capano, S. M. Fahrni, A. Fogtmann-Schulz, R. Friedrich, P. Köhler, S. Kudsk, F. Miyake, J. Olsen, F. Reinig, M. Sakamoto, A. Sookdeo, S. Talamo, The IntCal20 Northern hemisphere radiocarbon age calibration curve (0–55 cal kBP). *Radiocarbon* **62**, 725–757 (2020).

119. C. B. Ramsey, Bayesian Analysis of Radiocarbon Dates. *Radiocarbon* **51**, 337–360 (2009).

120. C. Bronk Ramsey, Bayesian analysis of radiocarbon dates. *Radiocarbon* **51**, 337–360 (2009).

121. J. Olsen, J. Heinemeier, H. Lübke, F. Lüth, T. Terberger, Dietary habits and freshwater reservoir effects in bones from a Neolithic NE German cemetery. *Radiocarbon* **52**, 635–644 (2010).

122. B. Philippsen, The freshwater reservoir effect in radiocarbon dating. *Herit. Sci.* **1**, 24 (2013).

123. I. Pap, T. Hajdu, A. Anders, J. Dani, G. Kulcsár, L. Révész, B. Mende, E. Molnár, G. Pálfi, Antropológiai-régészeti együttműködés a biológiai antropológiai maradványok roncsolásos mintavételének szabályozására. *Anthropol. Kozl.* **58**, 75–80 (2017).

124. J. Haas, Á. Jámbor, "Quaternary Evolution" in *Geology of Hungary* (Springer Berlin Heidelberg, Berlin, Heidelberg, 2012), pp. 201–213.

125. D. Loczy, Ed., *Landscapes and Landforms of Hungary* (Springer International Publishing, Cham, Switzerland, ed. 2015, 2015)*World Geomorphological Landscapes*.

126. G. Csillag, K. Sebe, "Long-Term Geomorphological Evolution" in *World Geomorphological Landscapes* (Springer International Publishing, Cham, 2015), pp. 29–38.

127. G. Gábris, A. Nádor, Long-term fluvial archives in Hungary: response of the Danube and Tisza rivers to tectonic movements and climatic changes during the Quaternary: a review and new synthesis. *Quat. Sci. Rev.* **26**, 2758–2782 (2007).

128. Dövényi Z., Ed., *Magyarország kistájainak katasztere* (HUN-REN CSFK Geographical Institute | Library | Institutional publications, Budapest, 2010).

129. R. A. Bentley, T. D. Price, E. Stephan, Determining the "local" 87Sr/86Sr range for archaeological skeletons: a case study from Neolithic Europe. *J. Archaeol. Sci.* **31**, 365–375 (2004).

130. T. D. Price, J. H. Burton, R. A. Bentley, The characterization of biologically available strontium isotope ratios for the study of prehistoric migration. *Archaeometry* **44**, 117–135 (2002).

131. R. Alexander Bentley, Strontium Isotopes from the Earth to the Archaeological Skeleton: A Review. *Journal of Archaeological Method and Theory* **13**, 135–187 (2006).

132. C. A. Makarewicz, J. Sealy, Dietary reconstruction, mobility, and the analysis of ancient skeletal tissues: Expanding the prospects of stable isotope research in archaeology. *J. Archaeol. Sci.* **56**, 146–158 (2015).

133. A.-F. Maurer, S. J. G. Galer, C. Knipper, L. Beierlein, E. V. Nunn, D. Peters, T. Tütken, K. W. Alt, B. R. Schöne, Bioavailable 87Sr/86Sr in different environmental samples--effects of anthropogenic contamination and implications for isoscapes in past migration studies. *Sci. Total Environ.* **433**, 216–229 (2012).

134. M. L. C. Depaermentier, M. Kempf, E. Bánffy, K. W. Alt, Modelling a scale-based strontium isotope baseline for Hungary. *J. Archaeol. Sci.* **135**, 105489 (2021).

135. C. Knipper, Die Strontiumisotopenanalyse: Eine naturwissenschaftliche Methode zur Erfassung von Mobilität in der Ur- und Frühgeschichte. *jrgzm* **51**, 589–686 (2004).

136. J. I. Giblin, Strontium isotope analysis of Neolithic and Copper Age populations on the Great Hungarian Plain. *J. Archaeol. Sci.* **36**, 491–497 (2009).

137. S. J. AlQahtani, M. P. Hector, H. M. Liversidge, Brief communication: The London atlas of human tooth development and eruption. *Am. J. Phys. Anthropol.* **142**, 481–490 (2010).

138. J. H. Burton, T. D. Price, "Seeking the local$^{87}Sr/^{86}Sr$ ratio to determine geographic origins of humans" in *ACS Symposium Series* (American Chemical Society, Washington, DC, 2013)*ACS Symposium Series. American Chemical Society*, pp. 309–320.

139. S. Neil, J. Evans, J. Montgomery, C. Scarre, Isotopic evidence for landscape use and the role of causewayed enclosures during the earlier Neolithic in southern Britain. *Proc. Prehist. Soc.* **84**, 185–205 (2018).

140. M. A. Katzenberg, Stable isotope analysis: a tool for studying past diet, demography, and life history. *Biological anthropology of the human skeleton* **2**, 413–441 (2008).

141. J. A. Lee-Thorp, On isotopes and old bones. *Archaeometry* **50**, 925–950 (2008).

142. A. R. Ventresca Miller, C. A. Makarewicz, Intensification in pastoralist cereal use coincides with the expansion of trans-regional networks in the Eurasian Steppe. *Sci. Rep.* **9**, 8363 (2019).

143. L. Martin, E. Messager, G. Bedianashvili, N. Rusishvili, E. Lebedeva, C. Longford, R. Hovsepyan, L. Bitadze, M. Chkadua, N. Vanishvili, F. Le Mort, K. Kakhiani, M. Abramishvili, G. Gogochuri, B. Murvanidze, G. Giunashvili, V. Licheli, A. Salavert, G. Andre, E. Herrscher, The place of millet in food globalization during Late Prehistory as evidenced by new bioarchaeological data from the Caucasus. *Sci. Rep.* **11**, 13124 (2021).

144. R. E. M. Hedges, L. M. Reynard, Nitrogen isotopes and the trophic level of humans in archaeology. *J. Archaeol. Sci.* **34**, 1240–1251 (2007).

145. S. H. Ambrose, Effects of diet, climate and physiology on nitrogen isotope abundances in terrestrial foodwebs. *J. Archaeol. Sci.* **18**, 293–317 (1991).

146. G. J. van Klinken, Bone collagen quality indicators for palaeodietary and radiocarbon measurements. *J. Archaeol. Sci.* **26**, 687–695 (1999).

147. K. W. Alt, C. Knipper, D. Peters, W. Müller, A.-F. Maurer, I. Kollig, N. Nicklisch, C. Müller, S. Karimnia, G. Brandt, C. Roth, M. Rosner, B. Mende, B. R. Schöne, T. Vida, U. von Freeden, Lombards on the move – an integrative study of the migration period cemetery at szólád, Hungary. *PLoS One* **9**, e110793 (2014).

148. M. Raymond, F. Rousset, An exact test for population differentiation. *Evolution* **49**, 1280–1283 (1995).

149. B. Schloerke, D. Cook, J. Larmarange, F. Briatte, M. Marbach, E. Thoen, A. Elberg, J. Crowley, *GGally: Extension to 'ggplot2* (2025).

Acknowledgments:

Funding: This project has received funding from the European Research Council (ERC) under the European Union's Horizon 2020 Research and Innovation Programme (HistoGenes, grant 856453 ERC-2019-SyG); from the German Federal Ministry of Education and Research (BMBF) in the framework of Förderung durch das Bundesministerium für Bildung und Forschung (BMBF, grant number: 01 UA 0806B) and from Hungarian Scientific Research Fund (OTKA-NKFI; grant number: NN113157).

Author contributions:

Conceptualization: IK, PJG, KRV,
Formal analyses: YT, IK, NF, DNV, PF, PlR,
Sample preparation and laboratory work: BGM, RR, LT, GAG-R, RF, AS-N, CK, KWA, BS, DC, TS, TH, PT, IKP, PlR
Visualization:YT, IK, NF, SL
Supervision: ZH, WP, JK, TV, PJG, KRV
Writing - original draft: YT. IK. NF
Writing - review & editing: YT. IK. PJG. KRV

Competing interests: Authors declare that they have no competing interests.

Data and materials availability: Our newly generated sequence data from 314 individuals are available from the NCBI Sequence Read Archive (SRA) database under accession PRJNA1285465. We accessed the POPRES (Population Reference Sample) dataset collected and published by Nelson et al. (*31*) from dbGaP (accession phs000145.v4.p2). Radiocarbon dates and isotopic data with standardised metadata including quality criteria, as well as lab codes are provided in the Supplementary tables. No other materials were generated in this study.

Supplementary Materials

Supplementary Text

Figs. S1 to S30

Captions for Tables S1 to S8, S16- S18, S21-S22

Tables S9-S15, S19-S20, S23

References (*124-149*)

Fig. 1. **Geographic location and chronology of the sites included in this study**. The sites are marked by red and orange circles, the bars indicate their relative and absolute chronological positions (CE) with a degree of uncertainty. The number of genetic samples is shown in brackets.

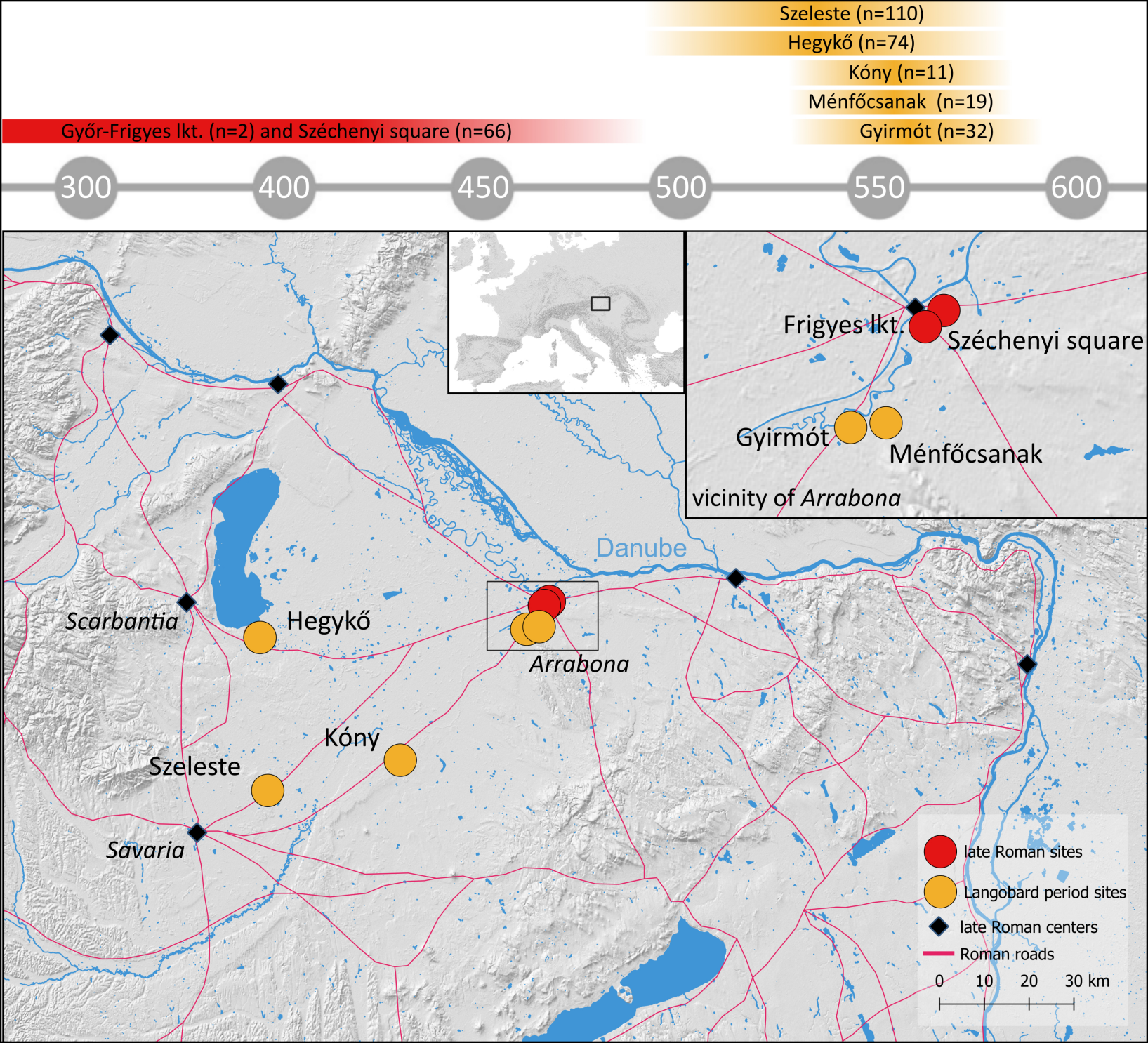
Fig. 2. **The genetic profiles of ancient individuals in this study**. A. PCA of 3rd-5th century and 6th century populations in the Little Hungarian Plain. Grey dots in the background represent reference data from POPRES. The Kernel Density Estimation of PC1 is displayed above. B.

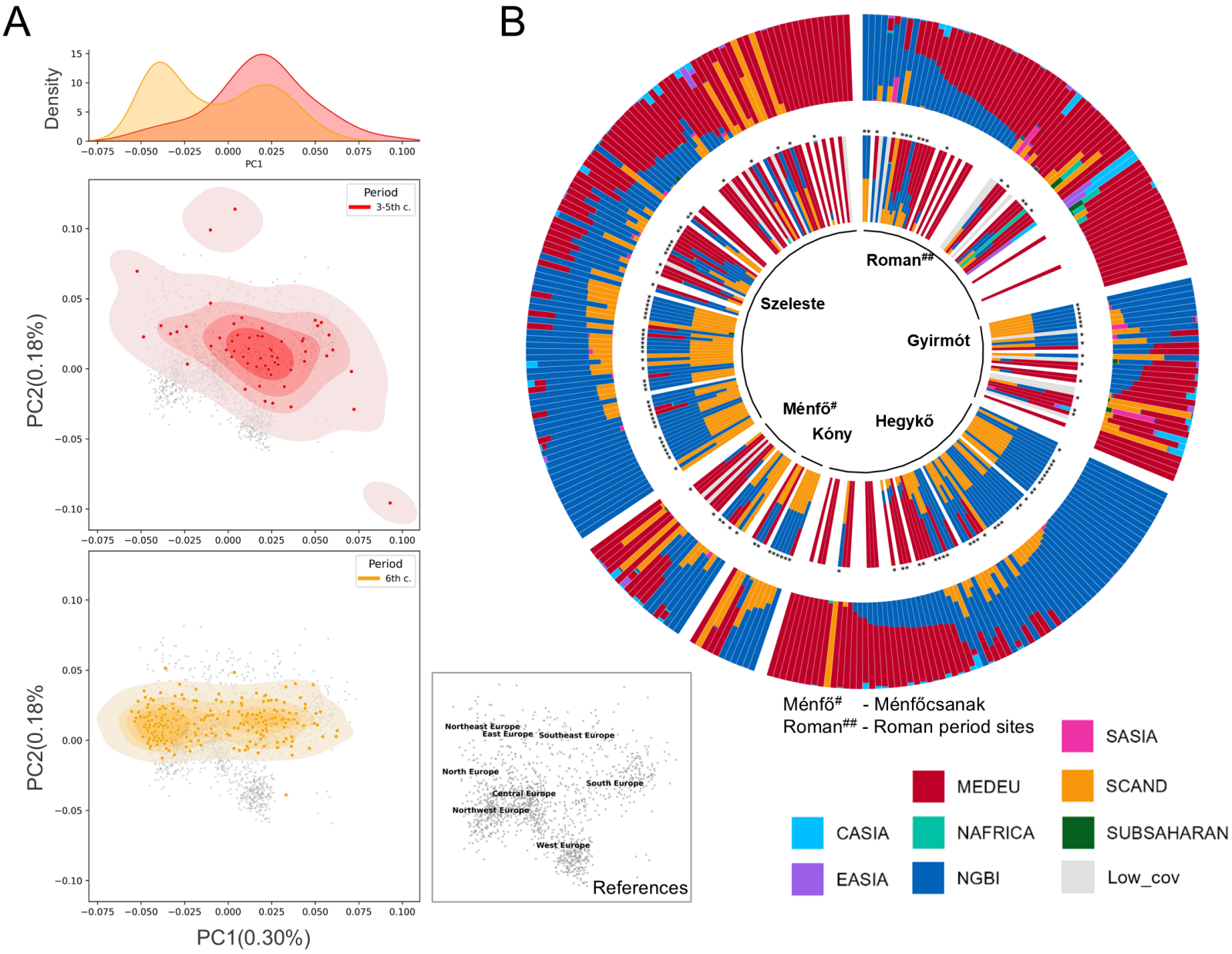
FastNGSadmix results are shown in the outer circle, while qpAdm results are displayed in the inner circle. FastNGSadmix includes all individuals in its plot, whereas qpAdm only displays individuals that could be successfully modeled (p>0.01) (Table S5). Asterisks denote individuals for whom qpAdm results represent an average across multiple functional models (see Table S5-S6). Reference (source) groups for both analyses are shown as legend.

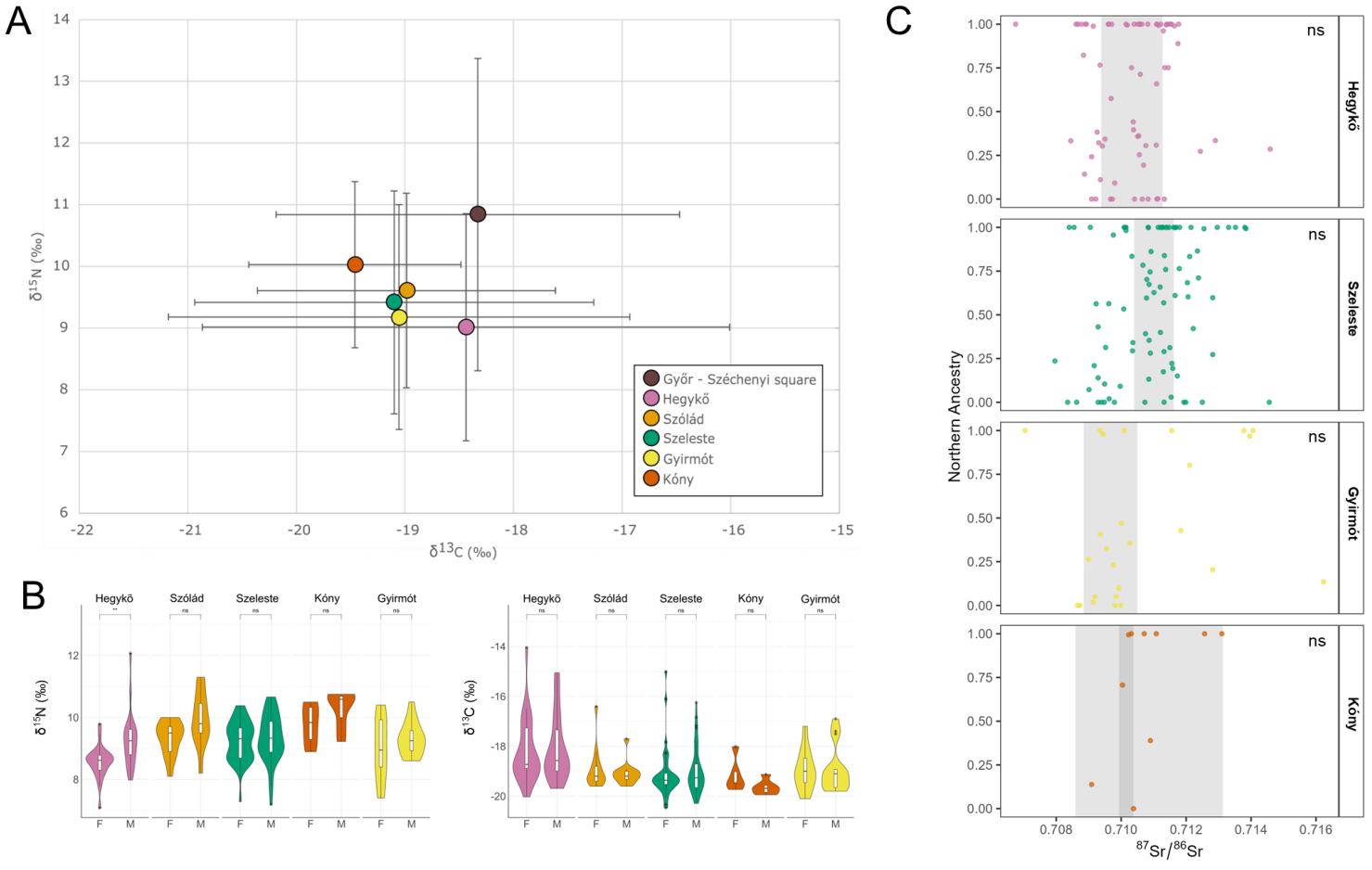
Fig. 3. Shifts in genetic ancestry and connection patterns between populations from the Roman and post-Roman periods. (A) Spatially interpolated visualization of qpWave modeling results for the Roman (left) and post-Roman (right) periods. Color intensity indicates the proportion of LHP individuals from each period that can be explained by ancestry from a given geographic region. (B) Heatmap summary of qpWave results. Colors represent the proportion of Roman (left) and post-Roman (right) individuals successfully modeled using each source population. (C) Network of Identity-by-Descent (IBD) sharing (>=12cM) among post-Langobard migration sites, including published data from Collegno and Szólád. Nodes represent individuals, with size proportional to the number of connections (degree). Edges represent the level of haplotype sharing, with line width proportional to normalized pi-hat values (range: 0–0.5). (D) Comparison of site-level connectivity between the pre-Langobard (top) and post-Langobard (bottom) migration periods. Edge width reflects the normalized strength of IBD connections between sites.

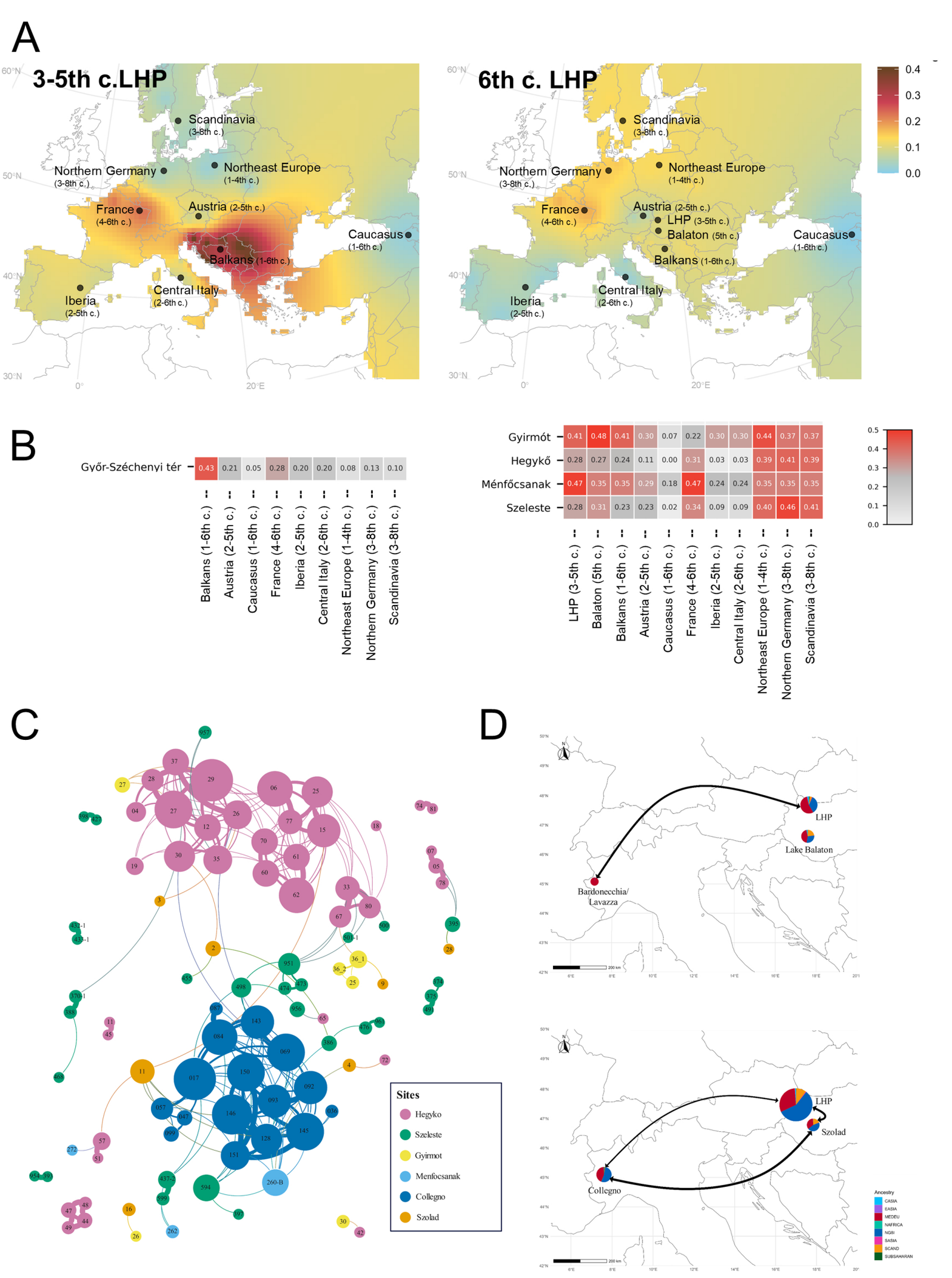
Fig. 4. Isotope results from the sites in this study. A. Scatter plot of $\delta^{13}C$ and $\delta^{15}N$ for all sites, with means and ±2 standard deviations indicated by whiskers. B. $\delta^{13}C$ and $\delta^{15}N$ datasets broken down into values by sex for the 6th century CE sites, using combined violin and box plots. Whiskers extend from the box to the largest and smallest data points within 1.5 times the interquartile range; values beyond this range are shown as outliers, marked with circles and stars. C. Plots of strontium isotope ratios compared to ratios of Northern European genetic ancestry (NGBI plus SCAND) for four post-Roman period sites. The grey shaded areas indicate the local ranges defined by the double standard deviation (DSD) of infans1 individuals (in case of Kóny additionally the DSD of all human results is also marked due to the low number of infans1 individuals). “ns” indicates non-significant association between Northern European ancestry and isotope value.

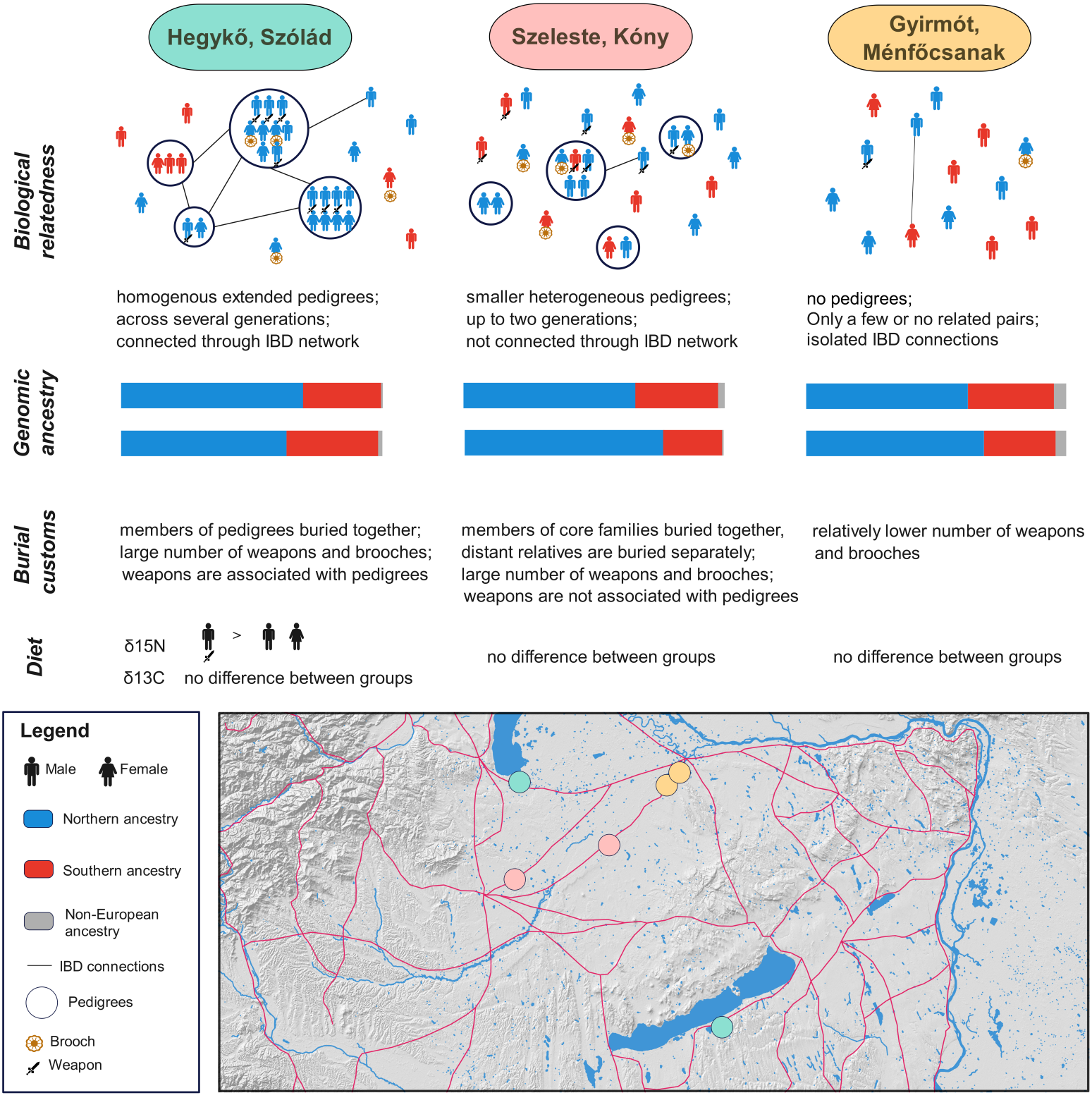
Fig. 5. Schematic synthesis illustrating the social and genetic organizational patterns of 6th-century LHP communities. The model summarizes findings for three site patterns (columns) across four data categories (rows). (*i*) Biological Relatedness: These panels provide a schematic representation of social structures; human icons and pedigrees are illustrative symbols based on observed trends and do not represent specific individuals or actual reconstructed genealogies. Icons are colored by their predominant genetic ancestry (Northern or Southern European) to reflect the general composition of the sites; this coloring does not imply 100% ancestry from a single source. Actual pedigrees with individual-level data are provided in Figure S29 (*ii*) Genomic Ancestry: Horizontal bars represent a quantitative site-wide summary, displaying the mean ancestry proportions for all sampled individuals at each site derived from fastNGSadmix analysis. Detailed individual-level results are available in Figure 2 and Tables S4–S6. (*iii*) Burial Customs: A summary of archaeological trends (e.g., weapon/brooch associations, see Supplementary Table S1) (*iv*) Diet: A summary of stable isotope results from Fig. 4. Inset Map: Displays geographic locations of the sites with markers color-coded to match the three site groupings


Szeleste (n=110)
Hegykő (n=74)
Kóny (n=11)
Ménfőcsanak (n=19)
Győr-Frigyes lkt. (n=2) and Széchenyi square (n=66)
Gyirmót (n=32)
300
400
450
500
550
600
Frigyes lkt.
Széchenyi square
Gyirmót
Ménfőcsanak
vicinity of Arrabona
Danube
Scarbantia
Hegykő
Arrabona
Kóny
Szeleste
Savaria
late Roman sites
Langobard period sites
late Roman centers
Roman roads
0
10
20
30 km


A
B
Density
PC1
Period
3-5th c.
6th c.
PC2(0.18%)
PC1(0.30%)
Northeast Europe
East Europe
Southeast Europe
North Europe
South Europe
Central Europe
Northwest Europe
West Europe
References
Roman##
Szeleste
Gyirmót
Ménfő#
Kóny
Hegykő
Ménfő# - Ménfőcsanak
Roman## - Roman period sites
SASIA
MEDEU
SCAND
CASIA
NAFRICA
SUBSAHARAN
EASIA
NGBI
Low_cov


A
B
C
δ15N (‰)
δ13C (‰)
Győr - Széchenyi square
Hegykő
Szólád
Szeleste
Gyirmót
Kóny
Hegykő
Szólád
Szeleste
Kóny
Gyirmót
δ15N (‰)
δ13C (‰)
F
M
Northern Ancestry
87Sr/86Sr
ns


A
3-5th c.LHP
Scandinavia
(3-8th c.)
Northern Germany
(3-8th c.)
Northeast Europe
(1-4th c.)
France
(4-6th c.)
Austria (2-5th c.)
Caucasus
(1-6th c.)
Balkans (1-6th c.)
Central Italy
(2-6th c.)
Iberia
(2-5th c.)
6th c. LHP
Scandinavia
(3-8th c.)
Northern Germany
(3-8th c.)
Northeast Europe
(1-4th c.)
France
(4-6th c.)
Austria (2-5th c.)
LHP (3-5th c.)
Balaton (5th c.)
Caucasus
(1-6th c.)
Balkans (1-6th c.)
Central Italy
(2-6th c.)
Iberia
(2-5th c.)
60°N
50°N
40°N
30°N
0°
20°E
0.4
0.3
0.2
0.1
0.0
B
Győr-Széchenyi tér
0.43 0.21 0.05 0.28 0.20 0.20 0.08 0.13 0.10
Balkans (1-6th c.)
Austria (2-5th c.)
Caucasus (1-6th c.)
France (4-6th c.)
Iberia (2-5th c.)
Central Italy (2-6th c.)
Northeast Europe (1-4th c.)
Northern Germany (3-8th c.)
Scandinavia (3-8th c.)
Gyirmót 0.41 0.48 0.41 0.30 0.07 0.22 0.30 0.30 0.44 0.37 0.37
Hegykő 0.28 0.27 0.24 0.11 0.00 0.31 0.03 0.03 0.39 0.41 0.39
Ménfőcsanak 0.47 0.35 0.35 0.29 0.18 0.47 0.24 0.24 0.35 0.35 0.35
Szeleste 0.28 0.31 0.23 0.23 0.02 0.34 0.09 0.09 0.40 0.46 0.41
LHP (3-5th c.)
Balaton (5th c.)
Balkans (1-6th c.)
Austria (2-5th c.)
Caucasus (1-6th c.)
France (4-6th c.)
Iberia (2-5th c.)
Central Italy (2-6th c.)
Northeast Europe (1-4th c.)
Northern Germany (3-8th c.)
Scandinavia (3-8th c.)
0.5
0.4
0.3
0.2
0.1
0.0
C
Sites
Hegyko
Szeleste
Gyirmot
Menfocsanak
Collegno
Szolad
D
LHP
Lake Balaton
Bardonecchia/
Lavazza
LHP
Szolad
Collegno
200 km
Ancestry
CASIA
EASIA
MEDEU
NAFRICA
NGIBI
SASIA
SCAND
SUBSAHARAN


Hegykő, Szólád
Szeleste, Kóny
Gyirmót, Ménfőcsanak
Biological relatedness
homogenous extended pedigrees;
across several generations;
connected through IBD network
smaller heterogeneous pedigrees;
up to two generations;
not connected through IBD network
no pedigrees;
Only a few or no related pairs;
isolated IBD connections
Genomic ancestry
Burial customs
members of pedigrees buried together;
large number of weapons and brooches;
weapons are associated with pedigrees
members of core families buried together,
distant relatives are buried separately;
large number of weapons and brooches;
weapons are not associated with pedigrees
relatively lower number of weapons
and brooches
Diet
δ15N
>
δ13C
no difference between groups
no difference between groups
no difference between groups
Legend
Male
Female
Northern ancestry
Southern ancestry
Non-European ancestry
IBD connections
Pedigrees
Brooch
Weapon

Science
AAAS

Supplementary Materials for

Unveiling the complexity of post-Roman polity formation in Pannonia using ancient DNA

Authors: Yijie Tian[1,#], István Koncz[2,#,*], Norbert Faragó[2], Corina Knipper[3], Ronny Friedrich[3], Deven N. Vyas[1], Levente Samu[2], Olga Spekker[4], Tamás Szeniczey[5], Tamás Hajdu[5,6], Balázs Gusztáv Mende[7], Péter Tomka[8], Ildikó Katalin Pap[9], Dávid Czigány[8], Rita Radzeviciute[10], Luca Traverso[10], Guido Alberto Gnecchi-Ruscone[10,11,12], Paolo Francalacci[13], Bernd Schöne[14], Gábor Tóth[15], Anna Szécsényi-Nagy[7,16], Petrus le Roux[17], Kurt W. Alt[14,18], Zuzana Hofmanová[10,19], Walter Pohl[20], Johannes Krause[10], Tivadar Vida[2,7], Patrick J. Geary[21,*] and Krishna R. Veeramah[1,*]

Corresponding authors. Email: krishna.veeramah@stonybrook.edu, geary@ias.edu and koncz.istvan@btk.elte.hu

The PDF file includes:

Provenance
Supplementary Text
Figs. S1 to S30
Captions for Tables S1 to S8, S16- S18, S21-S22
Tables S9-S15, S19-S20, S23

Other Supplementary Materials for this manuscript include the following:

Tables S1 to S8, S16- S18, S21-S22

Provenance

The archaeological material of the investigated sites are stored and available for viewing in the following institutions: Rómer Flóris Művészeti és Történeti Múzeum in Győr (Gyirmót, Győr-Széchenyi square, Győr-Frigyes lkt., Ménfőcsanak), Sopron Museum in Sopron (Hegykő), Hungarian National Museum in Budapest (Hegykő grave 18), and in Savaria Megyei Hatókörű Városi Múzeum in Szombathely (Szeleste). The osteological material is stored in the Rómer Flóris Művészeti és Történeti Múzeum in Győr (Gyirmót, Győr-Széchenyi square, Győr-Frigyes lkt., Ménfőcsanak), Hungarian natural History Museum in Budapest (Hegykő), and in Savaria Megyei Hatókörű Városi Múzeum in Szombathely (Szeleste). These institutions are named partners of the HistoGenes project and cooperate with it through formal collaboration agreements.

All samples used for aDNA analyses were collected in the framework of the HistoGenes project, ERC SynGrant grant 856453 ERC-2019-SyG between 2020-2022 from the maintained collections of the aforementioned institutions by Balázs Gusztáv Mende and István Koncz in close collaboration with colleagues of the local museums who are also authors on the study. Sample preparation was done in the ELTE RCH Institute of Archaeogenomics, Budapest, while the analyses were done at the facilities of the MPI Leipzig/Jena and Stony Brook University - all partner institutes of the project.

Isotope sampling was done in the framework of various projects. Hegykő and Gyirmót was sampled in the framework of BMBF project grant number: 01 UA 0806B by Corina Knipper in 2012; Szeleste in the framework of OTKA-NKFI project grant number: NN113157 by Corina Knipper and István Koncz in 2016; Kóny in the framework of the HistoGenes project, ERC SynGrant grant 856453 ERC-2019-SyG by Balázs Gusztáv Mende and István Koncz in 2022.

Prior to sampling, the materials from the sites were subjected to a condition assessment and revision. In all cases, samples were collected in the presence of an osteologist in order to minimize potential mixing. Sampling followed the national protocol recommended for destructive sampling for biological anthropological remains (*123*) as well as inhouse rules of the hosting institutions to minimize the invasive nature of the sampling and preserve the osteological material. The dating of the sampled sites is based on archaeological chronology; however, in every case this has also been verified through radiocarbon analyses, see Table S1 below for more detail on each individual site.

Supplementary Text

S1. Description of sites

S1.1. Gyirmót, Győr–Moson–Sopron County, Hungary

mid 6th century CE

37 graves, 37 individuals, 36 aDNA samples

The site was excavated in 1994 as part of the rescue excavations between 1990 and 2012 connected to the building of the main road 83. The site is located on an elevated ridge near the Roman road in the vicinity of the Roman town Arrabona (today's Győr). By the 6th century, Arrabona lost its urban character and its military and administrative role, it is even questionable to what extent was it inhabited during this period, so the small site at Gyirmót probably represents a smaller, rural community that settled along the Roman road connecting Arrabona and Scarbantia. The cemetery is completely excavated. Most of the unearthed graves showed signs of contemporary disturbance: the traces of secondary openings were clearly observable in the soil, skeletons were generally out of position, only parts remained in situ. Due to the disturbance, the archaeological material is also fragmentary. Male burials generally did not contain many grave goods, just belt elements (mostly buckles), iron knives and contents of a pouch, such as tweezers, fire strikers, etc. Among females, more richly furnished burials with bow brooches, S-shaped brooches and various types of disc brooches were observed. The archaeological dating of the site is based on the small finds, mostly female jewellery, especially the earlier mentioned brooches that are characteristic finds of the mid 6th century. The cemetery is one of those sites in the region, similarly to Ménfőcsanak and Kóny, that were established a few decades after the initial settlement of the Langobards in the region in the mid-6th century.

The site is unpublished, but an extensive report is available written by the excavator, Péter Tomka. The archaeological and skeletal material is currently stored in the Rómer Flóris Művészeti és Történeti Múzeum in Győr.

Tomka, Péter: Langobardenforschung in Nordwestungarn. In Pohl, W. & Erhart, P. (Hrsg.): *Die Langobarden. Herrschaft und Identität. Ergebnisse eines vom 2. bis 4. November 2001 in Wien abgehaltenen internationalen Symposiums.* Vienna: Verlag der Österreichischen Akademie der Wissenschaften 2005, 247–264.

Tomka, Péter: Kulturwechsel der spätantiken Bevölkerung eines Auxiliarcastells: Fallbeispiel Arrabona. In Friesinger, H. & Stuppner, A. (Hrsg.): *Zentrum und Peripherie – Gesellschaftliche Phänomene in der Frühgeschichte*. Vienna: Verlag der Österreichischen Akademie der Wissenschaften 2004, 389–409.

S1.2. Győr - Frigyes laktanya (GYR), Győr–Moson–Sopron County, Hungary

3rd-4th century CE

3 individuals, 3 aDNA samples

Three Roman period burials dating to the second half of the 3rd to 4th centuries CE were excavated at the Győr-Frigyes laktanya site in western Hungary in 2009. The site probably belonged to a smaller, rural settlement near Arrabona, situated along the trade route connecting Arrabona and Savaria, two important Roman period centres in the Little Hungarian Plain. Arrabona, established on the site of an earlier Celtic settlement, was one of the most significant auxiliary forts along the Danube Limes. The individuals – an adult male and two adult females – were buried in simple pit graves without any notable grave goods. Osteological analysis revealed severe and distinctive lesions on one of the individuals and identified it as the result of bone tuberculosis.

The site is archaeologically unpublished; the osteological information was published by Tamás Hajdu et al. 2012. The archaeological and skeletal material is currently stored in the Rómer Flóris Művészeti és Történeti Múzeum in Győr.

Hajdu, Tamás *et al.:* Bone tuberculosis in Roman Period Pannonia (western Hungary). *Mem. Inst. Oswaldo Cruz* 107 (2012) 1048–1053.

S1.3. Győr - Széchenyi square (GYS), Győr–Moson–Sopron County, Hungary

4th-5th century CE

at least 80 graves, at least 80 individuals, 66 aDNA samples

In the area of present-day Győr, the eastern cemetery of the vicus (civilian settlement) presumably belonging to the Roman period auxiliary camp of Arrabona has been uncovered. The site has been known since 1949, and burials have been found in several stages since then—about 80 in total, of which 66 have been fully excavated over the past decades. The auxiliary camp of Arrabona and its associated civilian settlement were an important centre in the region during the Roman period. Although the vicus was gradually abandoned during the 4th century—likely due to the turbulent nature of the period—the civilian population probably moved into the better-protected military camp, which likely remained in use until the early 5th century.

The cemetery's dating is based on its relation to the so-called ‘dark earth’ (*schwarze Schicht*, *sötét réteg*), a dark stratum observed across Europe that separates Roman and medieval layers. A significant portion of the burials were dug into this ‘dark earth’, which is dated by coins from the early 5th century. Several instances of stratigraphic superposition were observed in the cemetery (partly why not all skeletons could be tied to a clear archaeological context), suggesting long-term use of the burial site.

Graves are generally very poorly furnished; the most common artefacts are simple iron buckles and double-sided combs. Only the late antique basket-shaped earring from grave 31 provides any substantial dating evidence. Stones and Roman bricks found in some of the graves reflect late Roman burial practices, but the presence of artificial cranial deformation in several cases clearly indicates usage during the mid-5th century, during the Hunnic period.

The site is unpublished, but extensive reports are available written by the excavators, Péter Tomka and Szilvia Bíró. The archaeological and skeletal material is currently stored in the Rómer Flóris Művészeti és Történeti Múzeum in Győr.

Tomka, Péter: Kulturwechsel der spätantiken Bevölkerung eines Auxiliarcastells: Fallbeispiel Arrabona. In Friesinger, H. & Stuppner, A. (Hrsg.): Zentrum und Peripherie – Gesellschaftliche Phänomene in der Frühgeschichte. Vienna: Verlag der österreichischen Akademie der Wissenschaften 2004, 389–409.

Bíró, Szilvia & Tomka, Péter: A Győr, Széchenyi téri fekete réteg rejtélyei. In Csóka úrtól Gáspár atyáig. Ünnepi kötet Csóka Gáspár OSB 75. Születésnapjára. Győr: Szent Mór Bencés Perjelség 2013, 521-538.

Bíró, Szilvia & Tomka, Péter: Über die mysteriöse ‘schwarze Schicht’ und das sog. ‘hunnenzeitliche Gräberfeld’ von Győr-Széchenyi Platz. In: *Na hranicích impéria = Extra fines imperii: Jaroslavu Tejralovi k 80. Narozeninám*. Brno: Masarykova univerzita – Archeologický ústav AV ČR, Brno 2017, 53–72.

S1.4. Hegykő - Mező utca (HMU), Győr–Moson–Sopron County, Hungary

late 5th- mid 6th century CE

81 graves, 81 individuals, 74 aDNA samples

The cemetery at Hegykő is perhaps the most extensively researched site from the Langobard-period Pannonia. The site has been known since 1955, and excavations were carried out in several phases between 1959 and 1962. The cemetery is located near the southern shore of Lake Fertő (*Neusiedlersee*), approximately 18 km from the Roman town of Scarbantia (modern-day Sopron). The cemetery, which contains 81 graves, escaped the typical disturbance of graves—a fundamental problem of this period—making it particularly suitable for the study of chronological, cultural, and social questions. Burial customs at Hegykő differ from those observed in "classical Langobard" cemeteries: the graves are simple pit graves, considered shallow for the period, and do not feature the wooden structures interpreted elsewhere as "houses of the dead." Food offerings are found in very few cases, but there is a relatively high number of objects decorated with crosses, primarily belt buckles, which archaeological research interpreted as symbols of Christianity. Due to its distinctive characteristics, the cemetery gave its name to the so-called ‘Hegykő Group’, and was described as a community where surviving late antique groups, pre-Langobard Germanic peoples (Heruli, Suebi, etc.), and Langobards lived together. However, both this type of ethnic interpretation and the defining characteristics of the ‘Hegykő Group’ have come under criticism in recent research.

From a chronological standpoint, the site is of exceptional importance. In Transdanubia, one of the long-standing questions of archaeological research concerns the relationship between 5th- and 6th-century sites and the chronological gap between them. The polyhedral earrings with garnet inlays found in graves 3 and 23 at Hegykő are primarily known from 5th-century contexts, suggesting that, like the cemetery at Szeleste, Hegykő is one of the sites that likely began around the end of the 5th century and might represent the connection between the two horizons. This

early foundation may explain the differences in burial customs observed in a community whose roots may go back to the 5th century. Based on women's jewelry, particularly the brooches, it can be assumed that the cemetery was abandoned sometime in the second half of the 6th century.

The cemetery is divided into two spatially separate grave groups, which show no demographic or socio-cultural differences. Research has primarily interpreted them as family units. Among both male and female graves, there are exceptionally rich burials. In grave 18, the remains of a woman buried in the so-called "four-brooch" dress (*Vierfibeltracht)* were found—two rosette disc fibulae fastened her outer garment, while a pair of bow fibulae were found near the pelvis. Her clothing was also adorned with an ornamented belt pendant ending in a silver-mounted decorative key and faceted pendant, and she was buried with a footed glass vessel that has parallels in northern Italy. Grave 34 at Hegykő is one of the richest male burials from the period in Pannonia. The young deceased was buried with an axe, a scale (with Roman coins used as weights), an ornate comb, and a copper bowl (so called *Perlrandbecken*) likely originating from the Mediterranean. The cemetery's finds indicate complex cultural and trade connections. In addition to the Mediterranean links mentioned in connection with the two richly furnished burials, disc and bow brooches found at the site suggest primarily Western European, Merovingian connections. Interestingly, the S-shaped brooches that are among the most common in the region are entirely absent from this site. The high number of imported items may suggest that the community played some role in the trade along the Danube, which could also explain the cemetery's overall wealth.

The site is published posthumously by the excavator István Bóna. The osteological material was first analysed and published by István Kiszely and later reevaluated by Irene Barbiera and Olga Spekker. The archaeological material is currently stored in the Sopron Museum in Sopron with the exception of grave 18 which is exhibited in the Hungarian National Museum, Budapest. The osteological material is stored in the Hungarian Natural History Museum, Budapest.

Barbiera, Irene: *Changing Lands in Changing Memories. Migration and identity during the Lombard Invasions*. Firenze 2005.

Bóna István: Das langobardenzeitliche Gräberfeld von Hegykő, Komitat Győr-Sopron. In Anreiter, P.–Bartosiewicz, L.–Jerem, E.–Meid, W. (Eds.): *Man and the animal World. Studies in Archaeozoology, Archaeology, Anthropology and Palaeolinguistics in memoriam Sándor Bökönyi.* Budapest 1998.

Bóna István – B. Horváth Jolán: Hegykő-Mező utca. In Bóna, I. & B. Horváth, J.: Langobardische Gräberfelder in West-Ungarn. Monumenta Germanorum Archaeologica Hungariae vol. 6. Budapest 2009, 31-57.

Horváth Eszter: Gemstone and glass inlaid fine metalwork from the Carpathian Basin: the Hunnic and Early Merovingian Periods. *Dissertationes Archaeologicae* 3(1) (2013) 275–302.

Kiszely István: *The Anthropology of Lombards*. BAR International Series 1979.

Koncz, István: A hegykői 6. századi temető időrendje és kapcsolatrendszere. (The chronology and cultural contacts of the 6th century cemetery at Hegykő) *Archaeologiai Értesítő* 139 (2014) 71–98.

Tomka, Péter: Problémák a Hegykő-csoport körül (The Hegykő problem). In Kovács, László & Révész, László & Bollók, Á. & Gergely, K. & Kolozsi, B. & Pető, Zs. & Szenthe, G. (eds): *Népek és kultúrák a Kárpát-medencében: Tanulmányok Mesterházy Károly tiszteletére*. Budapest: Magyar Nemzeti Múzeum 2016, 185-190.

S1.5. Kóny – Markotai út (KMU), Győr–Moson–Sopron County, Hungary

mid 6th century CE

20 (22?) graves, 20 individuals, 11 aDNA samples

During the rescue excavations preceding the construction of a motorway, 22 graves – two of them did not contain any human remains – dated to the 6th century came to light in 2014. The site is located close to the Roman road connecting Arrabona (today's Győr) and Scarbantia (today's Sopron) about ca. 25 kms east from the former. The cemetery is completely excavated, two of the graves were destroyed before the excavation by modern construction. All graves show the signs of contemporaneous disturbance: the traces of secondary openings were clearly observable in the soil, skeletons were generally out of position, only parts remained in situ. Due to the disturbance, the archaeological material is fragmentary. Archaeological dating of the site is based on a well-preserved pot with stamped-in decoration, shield-on-tongue belt buckles (*Schilddornschnallen*), single-sided combs and other small finds, all characteristic of the middle third of the 6th century, so the site belongs to the same horizon with the nearby Gyirmót and Ménfőcsanak cemeteries. Both the archaeological material, as well as the small number of burials suggest a short occupation of use.

The site is unpublished. The archaeological and skeletal material is currently stored in the Rómer Flóris Művészeti és Történeti Múzeum in Győr.

S1.6. Ménfőcsanak (MFC), Győr–Moson–Sopron County, Hungary

mid 6th century CE

25 inhumations and 3 cremations, 28 individuals, 19 aDNA samples

The Ménfőcsanak site, similarly to Gyirmót that is only ca. 1 km apart, was excavated between 1995 and 1997 as part of the rescue excavations between 1990 and 2012 connected to the building of the main road 83. The cemetery is located on an elevated ridge near the Roman road in the vicinity of the Roman town Arrabona (today's Győr). The graves were heavily disturbed, and the area was also flooded sometime after the 6th century resulting in very bad preservation of both the archaeological and osteological material. Among the grave goods placed in the burials, primarily simple, everyday items (buckles, iron knife, tweezers, beads, spindle whorl) have survived, while the more valuable items, in the case of both men and women, fell victim to disturbance. Ménfőcsanak is one of the few cemeteries – together with Kajdacs and Tamási –

described as biritual in 6th-century Pannonia. While cremation burials do appear together at these sites, their dating and thus their exact connection to the inhumation burials is dubious and requires further analysis. Similarly to Gyirmót and Kóny, the Ménfőcsanak cemetery was probably used by a rural community for a short period of time in the middle of the 6th century.

The site is published by the excavator Andrea Vaday. The osteological material was analysed and published by Balázs Gusztáv Mende. The archaeological and skeletal material is currently stored in the Rómer Flóris Művészeti és Történeti Múzeum in Győr.

Vaday, Andrea: The Langobard cemetery at Ménfőcsanak. *Antaeus* 33 (2015) 163–242.

Mende, Balázs Gusztáv: Brief overview of the migration period population from Ménfőcsanak. *Antaeus* 33 (2015) 243-248.

S1.7. Szeleste (SZL), Vas County, Hungary

late 5th- mid 6th century CE

112 graves, 112 individuals, 110 aDNA samples

With 112 graves the cemetery at Szeleste, excavated in 2013, is the largest known cemetery from the first half of the 6th century in Transdanubia (present-day Western Hungary). The site is located about 20 km west of the Roman-era town of Savaria (today's Szombathely). Although by the 6th century Savaria likely lost its urban character and administrative role, as a provincial centre and due to the nearby Amber Road, it was an important regional hub during the Roman period.

In Transdanubia, researchers have long been intrigued by the chronological gap between sites associated with Germanic groups—such as the Heruli, Rugii, Suebi, and Goths—dating to the second half of the 5th century, and the newly founded cemeteries of the 6th century. The latest cemeteries belonging to the earlier group—such as those at Soponya and Balatonszemes—can be dated at most to the last decades of the 5th century. In contrast, regarding the 6th-century cemeteries (with the exception of the cemetery at Hegykő), the possibility of an origin in the 5th century has not yet been raised. This results in a shorter hiatus in Northern Transdanubia, and a longer, possibly generational gap in Southern Transdanubia, where researchers date the foundation of 6th-century cemeteries to the middle third of the century.

In Northern Transdanubia, alongside the previously mentioned Hegykő, the Szeleste cemetery may hold the key to solving this chronological gap. From the northern part of the cemetery, six individuals with artificially deformed skulls were recovered. The practice of artificial cranial deformation was widespread in the Carpathian Basin during the 5th century, but despite being well-known in neighbouring regions such as Lower Austria, it is not known from 6th-century sites in the area. Other features suggestive of a 5th-century origin include the presence of three graves lined with Roman bricks and *tegulae*, a practice not known from other 6th-century Transdanubian sites. These have parallels in 5th-century cemeteries (e.g., Mözs), and their origin can be traced to Late Roman cemeteries, such as those in nearby Savaria. However, in most cases, both the 5th-century and Szeleste examples lack the structural regularity of Late Roman

brick graves. The existence of brick-lined graves and cranial deformation provides only indirect evidence for the cemetery's 5th-century beginnings. Based on the recovered finds, the cemetery clearly remained in use at least until the middle third of the 6th century.

The most important datable grave goods in the cemetery are the fibulae. These include well-known types from the period: pairs of S-shaped fibulae of the Schwechat-Pallersdorf type, single-zoned disc brooch or pairs of rosette disc fibulae. The S-fibula type is known from 11 sites in the Carpathian Basin, making it the most common small fibula type of the era. The disc fibulae have good parallels in the Hegykő and Szentendre cemeteries, and the rosette form was widespread in both Western Europe and Transdanubia. A much rarer type is represented by a pair of bow brooches with bird-head ends (so called *Vogelkopffibel*), with the closest parallels in the eastern Carpathian Basin, specifically in the Szolnok-Szanda cemetery. This fibula type was widespread in present-day France and Germany, with the geographically closest and most accurate parallels found in present-day Czechia. Overall, based on both bow brooches and small fibula types, the site forms a transitional link between Lower Austrian and Transdanubian sites and shows clear cultural connections toward Western Europe, the Mediterranean, and Scandinavia.

The site is unpublished. The archaeological and skeletal material is currently stored in the Savaria Megyei Hatókörű Városi Múzeum in Szombathely.

Pap, Ildikó Katalin: Savaria keleti temetője és a szelestei germán temető épített és tegulás sírjai (Savaria's eastern cemetery and the built and tegula tombs of the Szeleste Langobard cemetery). *Savaria* 38 (2016) 91–105.

Tóth, Gábor & Pap, Ildikó Katalin: Germán temető a Nyugat-Dunántúlon. In Nagy, M. & Poráčová, J. (eds): *Trendek és eredmények a biológiai kutatás és oktatás terén*. Komarno: János Selye University 2016, 22–27.

S2. Sr, C and N isotope analysis

S2.1. The geological and pedological setting of Northwestern Transdanubia and the Little Hungarian Plain

In the present-day territory of Hungary, Quaternary geological development has produced thick strata in large areas, which can be classified into two main facies: hilly and flatland areas (*124*). The region under study is one of these, with Quaternary formations predominating in the North Transdanubian region and the Little Hungarian Plain. The hilly areas, and in general most of the Transdanubian region, are characterised by loess deposits of varying thickness during the Pleistocene, which are dissected by rivers and other watercourses and the gravel-sand sediments deposited by them (*124–126*). In western and northern Transdanubia, these loess layers are deposited at approximately 0-50 m thickness and represent mostly the younger Pleistocene (*124*, *127*). Their subsoil is covered by river sand and gravel layers of older Pleistocene age. Of our sites, only Szeleste is located in such a micro-region, namely the Gyöngyös Plain.

The flatland areas comprise most of Hungary's territory and can be further classified into three facies: the Great Plain, the Győr Basin and the Dráva Basin. The Quaternary sequence is much thicker in these areas, with a maximum of 450 m in the Győr basin (*124*, *126*, *127*). The Danube and the Rába deposited most of the alluvium, creating extensive and thick alluvial fans during the Pleistocene and Holocene. Special mention should be made of the depressions and basins around Lake Fertő and Hanság, where a layer of lacustrine, marshy, peaty sediment was formed up to a thickness of about 20 m(*124*). Among our sites, Hegykő is located in this area, while Kóny and Gyirmót are situated on the alluvial cone of the Rába, on the Csorna plain.

The geological and soil characteristics of the micro-regions comprising each site can be broadly characterised within this framework, but it is also worth considering them separately.

Fertő-Basin (Hegykő)

It is a small micro-region, bordered by the Hanság to the east, the Ikva Plain to the south, and the Fertő Hills and the Sopron Basin to the west (*128*). A considerable part of its surface is still swampy and covered with water; the other part is a low floodplain. Before the regulation of Lake Fertő, almost the entire area was covered with water at high water levels. The soil is peaty in the marshy parts and covered with floodplain silt, boggy clay and meadow clay in the areas protected from water. Underneath are thick layers of Pleistocene sand and gravel.

Csorna-Plain (Kóny, Gyirmót)

The area is bordered by the Pápa-Devecser Plain to the south and east, the Kapuvár Plain to the west and the Hanság and Moson Plain to the north (*128*). The vast majority of its surface is high and low floodplain, and the formation of the area itself can be linked to the alluvial fan of the River Rába. The soils are typically river silt, marshy and meadow clay, peat and sand. Underlying layers of sand and gravel of Pleistocene age are 50-100 m thick.

Gyöngyös-Plain (Szeleste)

It is a relatively large micro-region, bordered by the Rába alluvial plain in the south and east, the Vas mountain and the Kőszeg foothills in the west, and the Répce plain in the north (*128*). The surface of the area is relatively flat, with only a slight slope to the southeast, mainly covered by glacial loam and loess. Towards the south, the glacial strata are mixed with late Pleistocene gravel layers, accompanied by solifluction and cryoturbation. These gravel layers, deposited mainly by the rivers Gyöngyös, Répce and Rába, played a decisive role in the formation of the present form of the landscape.

S2.2. Bioavailable Sr and its relationship with the environment

Research of $^{87}Sr/^{86}Sr$ connected to mobility studies is based on the fact that ^{87}Sr is a radiogenic isotope and partly formed in the parent rock with the decay of the radioactive isotope ^{87}Rb (4.88-1010 years half-life), and then is transported by further weathering processes to the soil and groundwater, and then through plants to the whole food chain (*129*, *130*). In general, the older the rock, the more the ratio of ^{87}Sr to ^{86}Sr may shift in favour of the former and it does not undergo significant fractionation in the food chain, so in theory for any region we should obtain a typical $^{87}Sr/^{86}Sr$ ratio, which is consistent with the local geological context (*131*). The reality is different, even the determination of the value of the parent rock is problematic since it matters which minerals were measured in the given piece of rock (*131*). Moreover, weathering processes

are also highly dependent on many factors, so typically the bioavailable Sr value for a given region, when examined, does not fully overlap with that measured in the parent rock (*130*, *132*). Thus, traditionally, one of the most obvious solutions for determining the local baseline, in addition to contemporaneous human and faunal measurements, is to examine a recurrent environmental sample (*133*).

In our study region, very few measurements have been made on archaeological material based on the literature, but fortunately, such data are available from the site of Kóny 85 Enese (Table S15), which is very close to our sites (*134*). Unfortunately, the sample set is not very numerous, only one human bone, three dentin samples from animal teeth of the same age and four shells of the same age were measured. The literature indeed suggests that these are the most suitable proxies for determining locally detectable bioavailable strontium when it is not possible to take environmental samples (*130*, *131*, *135*). The reported data have a rather wide range, from 0.71095 to 0.70975, with an average of 0,7099.

There is no other information available for Kisalföld, nor for the wider North-Western Transdanubian region. Another lesson from the micro-regional baselines experimentally established for Hungary, supported by a variety of geographic, hydrological and geological factors, is that the relationship between bioavailable strontium and the environment is far from clear (*134*). With all this in mind, the averaged values of 0.708-0.710 (*129*) for Central European loess soils and 0.7096 (*136*) for the Danube can be taken into account only as an indication.

S2.3. Defining possible local $^{87}Sr/^{86}Sr$ baselines on human datasets

The available $^{87}Sr/^{86}Sr$ dataset allowed us to employ and compare various approaches to define possible 'local' ranges for the investigated sites. Important to note, isotope sampling was done for these sites in the framework of various projects (Hegykő and Gyirmót was sampled in the framework of BMBF project grant number: 01 UA 0806B; Szeleste in the framework of OTKA-NKFI project grant number: NN113157; Kóny in the framework of the HistoGenes project, ERC SynGrant grant 856453 ERC-2019-SyG) with different sampling strategies, not all approaches were possible at all sites. In all cases teeth from all individuals were measured, but in Hegykő and Szeleste it was complemented with measurements from bone as well as faunal measurements (teeth); in Szeleste faunal measurements were available; while Kóny only has a dataset from human teeth (Table S1 and S16).

As a baseline, possible 'local' ranges were generally defined based on the Sr values of infans1 (children below the age of 6 years) individuals. Using results from nonadult individuals as indicators of 'local' range is a generally accepted method and is based on the notion that Sr that was stored in the teeth a few months or years prior to death of the respective individuals and that the short time span between the incorporation of the strontium and the premature death of the individuals, increase the statistical probability of the trace element for being of local origin (*137*, *138*). Results of published large datasets also show that nonadults tend to show less variable Sr results compared to those of adult individuals (*51*, *139*).

These defined "local" ranges were subsequently compared with the available faunal samples (exclusively teeth; no bones were analysed) as well as with human bone samples. Human bone

was included as an indicator because it not just undergoes continuous remodeling throughout an individual's lifetime, it is also susceptible to diagenetic alteration, i.e. it incorporates available strontium from the soil (Table S16). One limiting factor is that the biologically available strontium in the cemetery does not necessarily correspond to the strontium ratio of the settlement area or the areas involved in agriculture. We found that the suggested 'local' ranges by the faunal samples and human bone samples overlap with the ranges based on the infans1 results (these generally, further indicating that the infans1 results are reliable proxies.

S2.4. $^{87}Sr/^{86}Sr$ isotopic data at Kóny

From the Kóny site, we have a total of 14 measurements from 14 individuals, taken from their tooth enamel (Table S15, Fig. S2). The lowest value, 0.70909, is from a Maturus male buried in grave 445, while the highest value, 0.7131, was measured from the teeth of a male buried in grave 558. The mean of the samples is 0.71086, and the median is 0.71055. The sex ratio is relatively even, with 6 males and 5 females, in addition to two children (graves 442 and 552) and one juvenile-aged individual of indeterminate sex buried in grave 553. In the lack of extensive child datasets or bone or faunal measurements, we could only rely on the 2SD values of the whole population. There are no outliers between the values, and the data set can be considered homogeneous. There is also no significant difference between the values for men and women; both their median (women 0.71055, men 0.71099) and their mean (women 0.71103, men 0.71074) are considered similar. As the data series were found to be normally distributed by the Shapiro-Wilk test, their means are comparable by analysis of variance. The result of the ANOVA performed is p=0.9683; df=1;8; F=0.001685, i.e. there is no significant difference between the means of men and women. The difference is only in the two gender ranges, with men's values covering a slightly larger interval than women's values. At the same time, the Kolmogorov-Smirnov test run shows that there is no significant difference between their distributions (D=0.333; p=0.847).

The age distribution, apart from the under-representation of children and young adults, is quite heterogeneous, and therefore, for such a small sample size, only 1-3 individuals are included in each category. In addition, the categories with 2-3 values show very wide intervals, with individual measurements falling far apart so that they reflect the range of the population as a whole. Such categories are Adultus I, Adultus II-Maturus I, Maturus I, Maturus II-Senile. Unfortunately, the data set representing the ages does not lend itself to serious statistical comparisons, but a visual inspection of the values does not reveal any outliers.

A moderate correlation was observed for within-cemetery genetic relatedness and heavy isotopic data. The strontium values of the adult male 1 buried in grave 447 and his direct descendant, the infant child 1 found in grave 442, were found to be very similar, with a difference of only 0.00008 between the two. The other first-degree relationship showed a slightly larger difference (0.0015) between the adult male of grave 444 and the mature female of grave 449.

S2.5. 87Sr/86Sr isotopic data at Gyirmót

From the Gyirmót site, we have a total of 40 strontium measurements from 27 individuals (Fig. S3). In two cases, three measurements were taken from one individual (graves 25 and 31), which, in addition to two teeth, also represent a sample from a long bone. Four individuals also have long bone data, but only one tooth was measured (graves 11, 14, 21 and 32). A further five

individuals had two teeth sampled, these being graves 15, 17, 20, 27 and 35. The smallest value in the whole data set belongs to the male juvenile-age deceased in grave 15 (0.70704), while the largest value belongs to the male juvenile-age deceased buried in grave 30 (0.71623). This is the only outlier in the whole data set. The mean of the series is 0.71045, while the median is 0.70984. In the case of Gyirmót, we also have a few sub-adult measurements, so to define the local baseline, we relied on measurements from bones and their 2SD data, which interestingly matched the data for men quite well.

The distribution of men and women is even, with nine in the former group and eleven in the latter, plus three children (20, 12, 36) and four individuals of unspecified gender (5). An interesting pattern has emerged in the breakdown of men and women, with men forming a relatively homogeneous group and, apart from outliers (15 and 30), falling into a narrower band. Women, on the other hand, show a broader range of values, with at least four distinct groups. Samples from children, bones and unidentifiable individuals all show similarities with men, so in this respect, women reflect a unique pattern. However, despite the lack of visual discrimination, an interesting result is obtained when the above groups are statistically tested, using exclusively the results coming from teeth, as, despite the former assumption, there is no significant difference between the medians (Mann-Whitney: $H=5.011$; $p=0.286$). Due to the lack of a normal distribution, the means cannot be compared, but the distributions can, and their analysis yields a surprising result, as there is no difference between males and females in this respect (Kolmogorov-Smirnov: $D=0.4125$; $p=0.1051$). Another interesting addition is that the values for males, individuals of indeterminate sex, coincided very well with the results from the bone samples, together allowing the definition of a very marked and well-defined local baseline.

Also, when examining the age distribution, only samples from teeth were included to ensure that other biasing effects did not affect the results. The largest groups were Adultus I and Adultus II, with 8 individuals in the former and 7 in the latter. The distribution of the samples was not at all similar, however, with the former group occupying a very narrow zone on the scale (between 0.70866 and 0.7127) and the latter a relatively wide zone (between 0.70919 and 0.71378). The other age groups were broadly similar, falling into one of these two distributions, but with no more than 2-4 individuals. The Adultus-Senilis group was similar to Adultus I, and Adultus I-II, Juvenis, Maturus I, and Infans I-II were similar to Adultus II.

It is also worth mentioning individuals with double or even triple measurements. The first molar (36) of the Infans I-II individual buried in grave 20 showed a significant difference from the value measured in the second molar (37), and the second value falls in the middle of the zone defined as the local baseline. This suggests that in later life he may have lived only in the narrower neighbourhood and been reared elsewhere in his younger childhood. Another possibility is that we see the mother's ratio reflected in this measurement. Among the females, there were three double measurements, the first being grave 31, with both teeth (16 and 18 molars) within the local zone but at the two extreme ends of the zone. The woman buried in grave 27 reflects a different situation. In her earlier years, this individual may also have spent more time away from this region before living and being buried here.

Unfortunately, it is difficult to reconcile the strontium isotope results with the genetic results, as apart from a third-degree linkage, no first-degree links and hence pedigrees within the community could be reconstructed. Moreover, of the Infans I child and the Juvenis buried in

grave 36, only the former yielded results, so we cannot comment on the relationship between the two from an isotopic perspective

S2.6. 87Sr/86Sr isotopic data at Szeleste

From the site of Szeleste, we have a total of 96 Sr measurements, of which 90 were taken on human teeth and 6 from archaeological animal bones (Fig. S4). Only one tooth from each human skeleton was measured, except for the individual Infans I from grave 550, whose teeth 16 and 75 were also measured, but the difference between the two measurements was negligible (0.71121 and 0.71116). The mean of the whole data set is 0.71098, the median is 0.71117, the minimum value is 0.70796 (Adultus male from grave 534), and the maximum is 0.71456 (Maturus female from grave 434). The whole data set covers a wide range, and the standard deviation is small (0.001285), yet its distribution is homogeneous and continuous, with perhaps the only measurement from grave 434 being minimally different from the others. In the case of Szeleste, we could rely not only on the abundance of children but also on faunal data to define the local baseline. The 2SD boundaries for the children defined a narrower middle range, while the 2SD boundaries for the animals outlined a wider range.

The sex distribution is evenly balanced, with the same number of adult males for every 34 adult females, 16 measurements of 15 Infans I individuals and 6 Infans II children, and a separate group of six animal data to compare directly with these groups. The sub-groups are not characterised by outlier values either; the only one that stands out in a negative sense from the Infans I group is the measurement of the child buried in grave 953, who is too remote from the other individuals in the group. Excluding this measurement from the analysis, the Infans I group already followed a normal distribution, so there was no obstacle to performing the ANOVA. However, as Levene's test for homogeneity of variances ($p=0.0001575$) was not satisfied, a Welch F test was used ($F=0.3658$; $df=18.89$; $p=0.8299$), which indicated that there was no significant difference between the group means. Pairwise Tukey's tests were performed to look for additional possible between-group differences, but were unsuccessful, with significant agreement found in all subgroup pairwise comparisons.

When comparing the different age groups, we found a diverse mix of groups. The group with the largest number of items is represented by Maturus individuals, with 34. Second in line is the Adultus group, with 24 individuals, while third place goes to the Infans I group, with the 16 children already mentioned. The Infans II group is made up of three subgroups, and in addition to the three children classified as Infans II, it also includes two Infans I-II and one Infans II-Juvenile. Other categories include Juvenis (4), Adultus-Maturus (3) and Maturus-Senilis (3). No outlier was found in any group except the Infans I category mentioned above, so it was considered worthwhile to compare the Adultus and Maturus categories statistically, as there was a noticeable difference in the medians and distributions in the plot. However, although Maturus individuals appeared to have a higher Sr rate, the tests did not confirm our hypothesis. The F-test showed that the variances of the two groups did not differ significantly ($F=1.1929$; $p=0.667$), and the t-test confirmed that their means did not differ significantly ($t=1.6955$; $p=0.09554$), thus indicating that there is no difference between the two groups.

In the case of Szeleste, genetic testing has revealed a first-degree relationship in several cases, although in most cases, no extensive relationships have been identified. For the most part, only

nuclear families have been reconstructed, so that the correlation between the Sr rate and genetic relatedness can only be investigated partially. One of the largest family trees includes the head of the family buried in grave 962, his two sons (graves 473 and 479), and their niece (474) from an unknown sibling. Unfortunately, of these individuals, measurements are only from the two brothers, but the results confirm their close descent, with a difference of only 0.00009 between the two measurements. Moreover, both of them are located within the local range defined by Infans I, in the upper half of it. A similar situation was observed for graves 451 and 595, where the two were also brothers, and their measurements were also very close to each other, with a difference of only 0.00003. These two measurements were, albeit slightly, outside the locally defined zone, but still within the wider local range defined by the animals. Another nuclear family is formed by the individuals buried in graves 552, 954 and 393, of which only the father (552) and mother (954) have Sr measurements. The difference between the two results is 0.00058, which is still not a large difference in the overall range of the dataset, and both individuals are outside the narrower local range defined by Infans. The last kinship relationship worth examining in terms of Sr isotope was between the males of grave 427 (father) and grave 398 (son). Again, the difference between the two measurements is relatively small, 0.00029, but while technically the father is outside the local range of Infans I, the son is located inside.

S2.7. $^{87}Sr/^{86}Sr$ isotopic data at Hegykő

At Hegykő, we have a total of 88 strontium isotope measurements from 69 individuals (Fig. S5). Of the individuals with multiple samples, we also have data from 9 cases of bone inorganic material, so apart from children, we have more solid data on the local baseline. These individuals represent roughly equal proportions of children (graves 5, 74), females (graves 21, 28, 53, 54) and males (graves 20, 42, 69). For the majority of these individuals, we have data from only one tooth in addition to bone, but for the female in grave 21, we have three measurements altogether from the left femur and two from different teeth. In total, we have ten individuals in our data set for whom we have mobility data from two different teeth. In addition to 2SD data from Infans I children, 2SD data from Infans II individuals were also used to define local baselines, but the narrowest zone was still the 2SD data from measurements of the inorganic bone material.

The maximum value of the whole data set is 0.71459 (10th grave Maturus male), while the minimum is 0.70675 (65th grave Maturus female), both of them can be considered outliers, but the other measurements rather form a homogeneous array. The mean is 0.71039, the median is 0.71046, and the standard deviation is 0.00112. If only the sampled teeth are considered, the ratio of males to females seems balanced, with 23 males for every 26 females, but the proportion of children is markedly high, with a total of 30 infants I (n=10) and II (n=20). The individual categories do not show a normal distribution, so they were compared with each other using Kruskall-Wallis and paired Mann-Whitney tests. The result of the former test showed no significant differences between males, females, Infans I, Infans II and bone-derived values ($H=7.687$; $p=0.1037$), whereas the latter showed moderate differences between the Infans II category and the other groups, which disappeared after sequential Bonferroni correction.

In terms of ages, the picture is very varied, with many anthropological age categories represented, but in fact, most categories only include one or two individuals. Four of them can be highlighted and statistically compared: the Adult I-II category, where we have 12 measurements, the Infans II group, where we have 20 measurements, the Infans I group, where we have 10 results, and the Maturus I-II category, with 7 results. In the statistical comparison, the outcome

was similar to the one mentioned above, with a significant difference between the age categories based on the Kruskal-Wallis test (H=7.879; p=0.04854), and the Mann-Whitney paired tests also showed that the main reason for this was due to the elements of the Infans II group, with significantly higher strontium ratios than the other three groups. In synchrony with the above, these differences disappeared again by applying the sequential Bonferroni correction. The values for the other age categories, with one or two exceptions, are scattered within the very wide Adultus I-II range, so there is no age pattern or trend reflected in the Sr values.

Thanks to the numerous pedigrees, we also have the opportunity to compare genetic and isotopic data in more detail. At the same time, one of the pedigrees, in which we find many nuclear families linked by many third-degree relationships, represented only a few sampled individuals, all of whom were associated with the Infans II age. In the case of graves 27 and 29, there are two female siblings, and there was not even a large difference (0.0004) between their values, but they are separated by the local baseline defined by the 2SD of the Infans I values. The 8-9 year old girl buried in grave 27 can thus still be considered local, while her sister buried in grave 29 has a value outside the narrow local zone. The other elements of the same pedigree, the individuals buried in graves 31, 35 and 40, are only loosely related, but it is remarkable how close their values are to each other compared to the two sisters mentioned above, so that they all occupy a narrow range of values outside the local boundary. Unfortunately, we also have only sporadic data on another extensive pedigree: in addition to the grandmother buried in grave 61, we have also measured the grandchildren buried in graves 60 and 75, who are also cousins. The values of all three of them were within the aforementioned range, a little above the locality threshold.

The children buried in graves 5 and 16 were part of a small nuclear family as siblings, and we have double measurements of both of them. The bone measurement of the former child represented the centre of the narrow local zone defined by the bones, but the sample from tooth 46 was already in the positive band outside the local zone outlined above. Both values from grave 16 were located in the same band, also, around the upper border of the local baseline. The siblings buried in graves 8 and 9 also represented a fragment of an elementary family, but their Sr isotope values were within the narrow local range defined by the human bones, in relative proximity to each other. In relation to parent-child relationships, four family tree fragments also carry information, so we have important data on this as well. The difference between the Maturus age male found in tomb 11 and his son found in tomb 45 is 0.00064, which means that the father is still within the narrow local range, while the son is outside the local range of Infans I. The distance between the strontium values of the mother in tomb 41 and the son in tomb 24 is larger, 0.0009, yet both are within the local range of Infans I. The mother-son pair of graves 81 and 74 is a more interesting case, although their Sr values are very close, they both fall outside the Infans I local range, but in a more negative direction. The last parent-child pair is the pair of graves 51 and 57, with Sr values of 0.00113, i.e. the largest difference. The child is on the border of the narrow local range defined by the bones, but the mother is far beyond the local range of the Infans I's, in the more positive range.

Among the double-measured individuals, the largest difference was found for the woman buried in grave 65, with her tooth 16 value of 0.70675, while her tooth 38 value was 0.71057. This means that she was probably later in the area of the future cemetery, since her tooth 38 is located in the local band defined by the bones, while her earlier years were spent at a considerable distance, since her tooth 16 can be interpreted as an outlier for the whole community. The second largest distance between two teeth from the same individual was from Juvenis associated with

grave 34, interestingly, the situation here was similar to the previous one. The 36th tooth suggests that he was not raised locally, but may have spent his later life in the local area, at least as tooth 18 suggests. The value of the individual tooth of Maturus II buried in grave 28 was also very far from the local values, suggesting that he was not locally raised, but the sample from his bone confirmed the narrower local range. A similar situation is shown by individuals 74, 5, 21, 53, all of whom had tooth values in a range outside the narrow local range, but had their bone values in a very narrow local range.

S2.8. Comparative $\delta^{13}C$ and $\delta^{15}N$ data at Győr, Szeleste, Gyirmót, Hegykő and Kóny

$\delta^{13}C$ and $\delta^{15}N$ isotopic ratios are commonly used in archaeology to study ancient diets. Thanks to the fractionation of these isotopes, an insight can be acquired about the basic photosynthetic pathway of the food web of the ancient organism, and its position in it (*140*, *141*). Millet (Panicum miliaceum), domesticated in East Asia in the mid-6th millennium, had already become an intensively cultivated plant in Europe by the beginning of the 1st millennium, but its C_4 photosynthetic way differs from that of C_3 photosynthetic way of temperate cereals (*142*, *143*) In this sense, $\delta^{13}C$ is a good indicator of the different crop diets, with a more positive value (>-18‰) reflecting a higher rate of direct or indirect millet intake. Generally, marine-derived diets have the same directional effect; however, freshwater diets can be reflected in variable $\delta^{13}C$ values, sometimes resulting in more negative values (<-21‰) than herbivores. $\delta^{15}N$ is a predictor of the position of the former organism in the food web; generally speaking, an increase of +2 - 6‰ per trophic level can be expected (*132*, *141*, *144*).

When analysing the diet data, we first wanted to know whether the aggregated 6th century data, i.e. the population data of Szeleste (n=105), Hegykő (n=75), Gyirmót (n=35) and Kóny (n=19), together show any deviation from the late Roman data of Győr (n=60). Only measurements that met the commonly used collagen quality criteria in the literature (*145*, *146*) were considered. First, comparing $\delta^{13}C$ values, we were immediately confronted with the lack of a normal distribution of the data series, so we used the Mann-Whitney test. The result was a significant difference ($U=3811$; $p<0.0001$), i.e. overall, we find significantly higher $\delta^{13}C$ values in the late antique period than in the 6th century (Fig. S6), which is most likely due to the different rates of millet consumption. It is worth noting, however, that we have a large number of outliers in the 6th century, which are in a range that suggests even more pronounced millet consumption than the values for Győr.

There is also a characteristic difference in $\delta^{15}N$ values (Fig. S7), but we did not find as many outliers as for δ13C values, i.e. our data set turned out to be much more homogeneous. Due to the lack of a normal distribution, we again resorted to the Mann-Whitney test ($U=2148$; $p<0.0001$), and the result confirmed our expectations, with significantly higher protein intakes among individuals from the Győr site.

We looked for further reasons for the significant difference by using site-by-site disaggregation, and first looked at the $\delta^{13}C$ values (Table S9, Fig. S8). Mainly outliers are found in the populations of Hegykő and Szeleste, and these are in a more positive range than the Győr values, yet the median values of Gyirmót and Kóny, which show fewer such outliers, seem to fall much further away from the Győr median. In the absence of a normal distribution, we used paired Mann-Whitney tests and sequential Bonferroni correction, and the results confirmed our observations. The difference between Győr and Hegykő is no longer significant, and the

difference between Szeleste and Kóny is negligible. Gyirmót is also related to Kóny and Szeleste, but in all other combinations, there is a significant difference between the sites.

$\delta^{15}N$ values were subjected to a similar analysis, and here the picture is somewhat consistent, with all sites except Kóny in a much more negative range (Table S10, Fig. S9). It is noteworthy that in this case, too, Hegykő has a more significant amount of outliers, but here there is a clear difference between the average values for Győr and Hegykő. Together with Gyirmott and Szeleste, they are clearly in a different band. The Mann-Whitney paired tests carried out show clear evidence of similarity between Szeleste and Gyirmót, and after the sequential Bonferroni correction, the difference between Hegykő and Gyirmót is no longer significant. However, the combination of all other sites and their differences remained significant, and Győr and Kóny are no exception.

Further breaking down our dataset into adult males and females without sub-adults (Table S11, Fig. S10), but this time sticking only to the 6th century sites, we sought to answer the question of whether the different behaviour of Hegykő and Kóny is sex-specific. In addition, at this level, we felt justified in including the reported data from Szólád (n=25), since many similarities can be found between Szólád and Hegykő (*147*). Apparently, there is no difference in the case of Hegykő concerning $\delta^{13}C$, with the quartiles shown in the boxplots occupying very similar bands, while in the case of Kóny, some divergence is noticeable. Only a moderate number of outliers are observed, with most cases coming from the group of women and men found in Szeleste; in this respect, Szólád shows even more unique cases for both sexes. The data isolated at each site show no gender differentiation, with perhaps only Kóny showing some variation between males and females.

In the statistical analysis, most of the categories showed a non-normal distribution, so again, paired Mann-Whitney tests were used. The results faithfully reflect the observations on the boxplot, with the Hegykő site different from all other sites. However, after performing a sequential Bonferroni correction, most of these significant differences disappear, remaining only for the female data associated with Szeleste. A similar phenomenon is observed for the male data associated with Kóny, where we see differences for several other sites, but after the correction, a significant difference remains for the female data from Hegykő.

The breakdown of $\delta^{15}N$ values by sex revealed exciting differences (Table S12, Fig. S11). The differences between the sexes at individual sites seem to be much more marked in this respect, with Hegykő and Szólád in particular being good examples. In the case of Hegykő, the significant number of outliers with high values seems to be largely associated with men, so it is not surprising that they disappear in the male-female breakdown. Surprisingly, the distribution of each category followed a normal distribution in the vast majority of cases, and in the remaining two cases was just below the significance threshold, so instead of a Mann-Whitney test we tried ANOVA, which revealed a significant difference (df=181 [9,172]; F=5,338; p<0,0001) with equal variance (Levene's test: p=0,1246).

Thanks to the pairwise Tukey's tests, it is also clear that the results of the women associated with Hegykő cause the greatest fluctuation in the data set, with all categories except those associated with Gyirmót differing significantly or very close to the significance level.

One more aspect we were curious about was the result of comparing dietary data across sites, and this concerned the dietary habits of men buried with weapons. For this purpose, we collected

separately the armed men of Szólád (n=11), Hegykő (n=11) and Szeleste (n=18) and compared them with the non-armed adult population of the same sites. In terms of $\delta^{13}C$ data, the separateness of the individuals buried without weapons from Hegykő is immediately striking, as well as the extremely wide range of their data (Table S13, Fig. S12). The difference from the individuals with weapons from the same sites is remarkable, but not observed in Szólád and Szeleste, where the diet is more consistent. In the absence of normal distributions, Mann-Whitney pairwise tests were performed and our suspicion was confirmed: the difference in the non-armed individuals in the Hegykő is significant, and it is significant for almost all other subgroups.

There is also much greater fluctuation in $\delta^{15}N$ values within sites, and apparently higher protein intakes were associated with the armed male group (Table S14, Fig. S13). In this respect, the population of Hegykő seems to be in the lead, and this phenomenon is moderately observed for Szeleste. A positive result was obtained when testing for a normal distribution, so there was no obstacle to running the ANOVA. The key lesson is that the individuals buried without weapons in Hegykő are significantly different from almost all other categories and sites, including the individuals buried with weapons at Hegykő. The other interesting phenomenon is that no significant difference is found among armed males from any site. The third important observation is that in Seleste this differentiation does not reach a significant level between the individuals buried with and without weapons.

S3. IBD analysis

We firstly conducted both country level and site level analysis to understand the IBD sharing the patterns between LHP individuals and contemporaneous populations. In total, we collected 861 individuals from 38 countries and 165 sites, shown in Table S3, which summarizes the IBD connections between reference populations and the 3rd–5th c. LHP individuals (Columns E–H) as well as the 6th LHP individuals (Columns I–L). For each period, we report four metrics:

1. The number of individuals at each site sharing IBD segments >=12cM with the LHP individuals.
2. The total number of IBD connections the site shares with the LHP individuals.
3. The total number of possible IBD connections (calculated as: Site size* LHP sample size (n), where n=31 for the 3-5th c. and n=130 for the 6th c.).
4. The ratio of observed to possible connections (shown as a percentage).

We firstly examined IBD connections between Roman-period individuals from the LHP and other populations (columns E-H). In total, we identified 220 IBD-sharing pairs. Notably, two individuals—Gy-Szt_29 and Gy-Szt_32—accounted for a disproportionately large number of these connections. Gy-Szt_29 shared IBD segments with 49 individuals from diverse regions including Germany, the Netherlands, Kazakhstan, Ireland, Romania, Hungary, Denmark, Sweden, and Mongolia. Gy-Szt_32 exhibited shared IBD with 125 individuals spanning a remarkably wide geographic range, including Germany, Kyrgyzstan, Italy, Kazakhstan, the Netherlands, Hungary, Turkey, Croatia, India, Taiwan, Spain, Russia, Ireland, Kenya, Romania, Mongolia, Denmark, Sweden, Norway, and even Botswana. Several of these shared segments

exceeded 55 cM in length. Despite passing quality filters, the extraordinary number and extent of connections suggest these two individuals may be problematic, and we treated them with caution in subsequent analyses.

After excluding Gy-Szt_29 and Gy-Szt_32, we identified 44 IBD-sharing pairs involving 27 individuals outside the LHP. However, none of the connections has IBD segments longer than 20cM.

When looking at the site level, we found a low connection rate (0.16%) between the 3rd–5th century LHP individuals and reference populations (27 individuals and 44 connections). The site with the highest ratio was Groningen (3.87%), Netherlands, where 5 individuals shared 12 IBD connections with individuals from Győr-Széchenyi square. Additionally, Oland, Sweden (2.05%) was the only other site with a ratio exceeding 1.5% (excluding all the other sites with only 1 connection).

We then examined IBD connections between post-Roman individuals from the Little Hungarian Plain (LHP) and those from other populations. In total, we identified 240 pairs of IBD segments longer than 12 cM shared between post-Roman LHP individuals and individuals from other regions. These involved in total 116 individuals outside of the LHP (Table S18 Column I-L).

However, when focusing on IBD segments longer than 20 cM, only 23 pairs of related remained, involving 19 individuals from outside the LHP. Notably, two individuals from Hegykő (Hegykő_47 and Hegykő_49, a parent-offspring pair) shared an approximately 20 cM segment with an individual from West Heslerton, UK (I11587). Another individual from Hegykő (Hegykő_36) shared ~20 cM with an individual from Dover Buckland, UK (BUK009), while Hegykő_35 shared ~25 cM with an individual from Lower Saxony, Germany (DRU016). Hegykő_11 also shared ~20 cM with an individual from Tian Shan, Kazakhstan.

In Szeleste, two individuals (Szeleste_498 and Szeleste_370-2) shared ~40 cM with the same individual from Haven, Germany (HVN004). Additionally, we found five connections between Szeleste individuals and those from Dover Buckland, UK: Szeleste_468 with BUK041, Szeleste_370-1 with BUK049, Szeleste_388 with BUK049, Szeleste_486 with BUK038, and Szeleste_437-1 with BUK053. Notably, Szeleste_370-1 and Szeleste_388 form another parent-offspring pair. Two Szeleste individuals also showed IBD sharing with individuals from Croatia: Szeleste_598-B with I26859 and Szeleste_534 with I26749. Szeleste_498 also shared segments with three individuals from Collegno, Italy (COL_069, COL_017, and COL_143), all from the same pedigree. Szeleste_437-2 shared ~30 cM with COL_017. Furthermore, Szeleste_380 had IBD connections with two individuals from Rákóczifalva, Hungary (RKF207 and RKF237) and one from Szólád, Hungary (Sz_28).

Additionally, Gyirmót_26 shared IBD segments with two individuals from Szólád, Hungary (AV1 and AV2).

Despite these findings, the longest IBD segment identified between LHP individuals and those from other populations was only 44 cM, and the highest sum of IBD sharing is 121cM, which only suggests ~6th degree relatedness.

For the site level analysis, the connection rate was slightly higher at 0.21%. The highest site-specific ratio was found in Groningen, Netherlands (4.08%), involving 7 individuals sharing 53 connections with the LHP. We also identified two sites in Germany with ratios above 1.5%: Hannover-Anderten 1.83% and Häven 1.54%. In total, 21 sites shared more than one connection with the LHP individuals.

Although the overall connection ratios are low for both periods, the site-level analysis reveals distinct patterns. We observed an increase in connectivity with northern populations in the 6th c. period. For instance, while none of the 23 sites from the UK connected with 3rd–5th century individuals, 12 connected with 6th-century sites. Similarly, among 12 German sites, only 2 connected with the 3rd–5th century group, while 6 connected with the 6th-century group. This pattern was also observed in Denmark.

To facilitate a regional-level comparison of LHP individuals across the two periods, we defined a Northern European population by aggregating the country-level data of 303 individuals from eight countries (Denmark, Estonia, Germany, Ireland, the Netherlands, Norway, Sweden, and the UK), as detailed in Table S18.

Regarding uniparental markers, we observed that Roman period individuals with IBD connections to other populations (n=17) included 8 males. These males primarily belonged to Y-haplogroups R1a, R1b, G2, and J2 ($H_{Y_Roman} = 0.86$). In the post-Roman period, 97 individuals exhibited IBD connections. Among the males in this group (n=47), the observed Y-haplogroups included E, G2a, I1, I2, N, R1a, and R1b ($H_{Y_postRoman} = 0.81$). These results suggest that IBD connections are not enriched for several specific Y-haplotypes.

We observed similarly high diversity at mtDNA level, identifying nine main haplogroups among Roman period individuals with IBD connections, including H1, H2, HV, J1, K1, T1, T2, U1, and W ($H_{mtDNA_Roman} = 0.90$). In the post-Roman period, we observed 24 distinct haplogroups among individuals with IBD connections ($H_{mtDNA_postRoman} = 0.91$). The most frequent lineages in this group were H2 (n=23), H1 (n=15), and U5 (n=10). The results also suggest the mtDNA has high diversity and is not enriched for several specific haplotypes.

S4. Uniparental marker analysis

We also performed a joint analysis to assess uniparental marker diversity across different groups of samples. We firstly quantified the diversity of both mtDNA and Y haplogroups for all individuals in the LHP using major clade definitions (main branches for non-recombining portion of the Y-chromosome (NRY); 2-character resolution for mtDNA). We found that the haplogroup diversity (the probability that two random individuals from this population have different haplogroups) was similarly high for both the NRY (HY = 0.85) and mtDNA (HmtDNA = 0.86).

We analyzed differentiation in mtDNA and Y-chromosome haplotypes between sites using pairwise Fisher's exact tests with contingency tables extended for multiple haplotypes (R

function fisher.test) (this is statistically equivalent to the Exact Test of Population Differentiation integrated into the Arlequin software package (*148*)) This analysis was performed on two datasets: the first included all available data, while the second excluded related individuals up to the fourth degree. To control for the increased probability of Type I errors (false positives) inherent in multiple statistical comparisons, we applied a False Discovery Rate (FDR) correction to the resulting p-values.

In the complete dataset (Table S19), the only significant difference observed after this adjustment was in Y-haplotype frequencies between the Roman period sites and Hegykő. However, in the dataset excluding relatives (Table S20), no significant differences were found. Collectively, these results suggest a lack of significant haplotype differentiation across the studied sites.

We then compared individuals within pedigrees to those outside of pedigrees at the two largest sites, Hegykő and Szeleste. This analysis revealed consistently high levels of haplotype diversity (0.80–0.90) across all categories, indicating no meaningful differentiation at the uniparental level. In Hegyko, mtDNA diversity was 0.89 overall (0.87 in pedigree vs. 0.88 non-pedigree), and Y-chromosome diversity was 0.85 overall (0.80 in pedigree vs. 0.86 non-pedigree). Similarly, Szeleste displayed stable high diversity, with mtDNA values of 0.80 overall (0.83 in pedigree vs. 0.80 non-pedigree) and Y-chromosome values of 0.82 overall (0.86 in pedigree vs. 0.80 non-pedigree)

S5. Pedigree construction

For pedigree reconstruction, we focused on biological relatives up to the third degree by adapting the procedure described in previous literature. The process began with the identification of all first degree relatives within each site, such as parent offspring pairs and siblings. Using these first degree connections as a foundation, we sequentially integrated second and third degree relationships to expand the small pedigrees into more complex structures. Relatedness estimates were primarily derived from lcMLkin output values, specifically pi-hat as well as Z0ag, Z1ag, and Z2ag coefficients. We then cross referenced these findings with results generated by KIN. Throughout the construction process, we prioritized the lcMLkin data while utilizing KIN as a secondary reference and incorporating uniparental markers to further refine the pedigree structures.

We compared the initial degree of relatedness inferred by KIN with the results generated by lcMLkin (Dataset S9, column “lcMLkin_compare”). Among the 213 related pairs (up to third degree) identified by KIN, 96 had fewer than 10,000 shared SNPs and were therefore excluded from the lcMLkin analysis. Of the remaining 117 pairs, 107 (91%) showed consistent results between KIN and lcMLkin. An additional five pairs matched the second-best guess from KIN, and two were consistent with KIN’s second-best guess within the same degree category. For the three remaining pairs, two were classified as third-degree relatives by KIN but as unrelated according to lcMLkin results. The last pair was identified as unrelated by KIN but as second-degree by lcMLkin.

To refine pedigree construction, we incorporated additional data to resolve the directionality of isolated parent-offspring pairs. First, we utilized Osteological Age information (Table S1, column E); in pairs consisting of an adult and a sub-adult, the adult was assigned to the parental generation.

Second, we examined uniparental markers to resolve ambiguities, particularly between adult pairs. Mitochondrial DNA (mtDNA) provided decisive resolution for male-female pairs: discordant mtDNA haplotypes excluded the possibility of a maternal relationship (mother-son), thereby identifying the pair as father and daughter. By integrating these lines of evidence, we successfully resolved the directionality of several relationships.

Győr Széchenyi tér and Frigyes laktanya

We first focused on first degree relative pairs, including all parent offspring pairs and siblings. At Győr Széchenyi tér, this identified three parent offspring pairs: Gy_Szt_31 and Gy_Szt_33, Gy_Szt_10 and Gy_Szt_08, and Gy_Szt_17 and Gy_Szt_12. There is no age information for the site, so we only integrated uniparental markers to help resolve the directionality of isolated parent-offspring pairs. Notably, Gy_Szt_10 and Gy_Szt_08 possess different mtDNA haplotypes; this discordance excludes a maternal relationship, confirming them as a father-daughter pair. Conversely, Gy_Szt_17 and Gy_Szt_12 share the same mtDNA haplotype, a finding consistent with a mother-son relationship.

lcMLkin initially suggested that Gy_Szt_29 and Gy_Szt_30 were second degree relatives. However, this may have been a false signal because the method is highly dependent on external allele frequencies. Given that most individuals in this study are of European ancestry, we initially used CEU_TSI allele frequencies. This specific pair exhibits predominantly Central and East Asian ancestry, which caused them to appear more related under a European reference. After reapplying the analysis using EAS_SAS allele frequencies, the pair was identified as unrelated (pi-hat = 0). This was further confirmed by KIN analysis; consequently, they were excluded from the pedigree figures.

In the Roman period site of Győr Frigyes laktanya, no related individuals were identified.

In Hegykő, we identified 24 parent offspring pairs: Hegyko_28 and Hegyko_27, Hegyko_28 and Hegyko_29, Hegyko_26 and Hegyko_34, Hegyko_26 and Hegyko_40, Hegyko_26 and Hegyko_37, Hegyko_49 and Hegyko_44, Hegyko_49 and Hegyko_47, Hegyko_48 and Hegyko_44, Hegyko_48 and Hegyko_47, Hegyko_77 and Hegyko_6, Hegyko_61 and Hegyko_62, Hegyko_62 and Hegyko_75, Hegyko_65 and Hegyko_75, Hegyko_67 and Hegyko_33, Hegyko_33 and Hegyko_55, Hegyko_33 and Hegyko_80, Hegyko_78 and Hegyko_16, Hegyko_78 and Hegyko_05, Hegyko_07 and Hegyko_05, Hegyko_07 and Hegyko_16, Hegyko_11 and Hegyko_45, Hegyko_41 and Hegyko_24, Hegyko_81 and Hegyko_74, Hegyko_51 and Hegyko_57.

We also identified 16 sibling pairs: Hegyko_27 and Hegyko_28, Hegyko_31 and Hegyko_46, Hegyko_34 and Hegyko_40, Hegyko_34 and Hegyko_37, Hegyko_40 and Hegyko_37, Hegyko_44 and Hegyko_47, Hegyko_77 and Hegyko_25, Hegyko_77 and Hegyko_15,

Hegyko_25 and Hegyko_15, Hegyko_73 and Hegyko_60, Hegyko_73 and Hegyko_70, Hegyko_60 and Hegyko_70, Hegyko_08 and Hegyko_09, Hegyko_19 and Hegyko_23, Hegyko_16 and Hegyko_05, Hegyko_55 and Hegyko_80.

Based on these connections, we generated small nuclear pedigrees. These included a father and three sons (Hegyko_26, Hegyko_34, Hegyko_40, and Hegyko_37), a parents and two daughters pedigree (Hegyko_49, Hegyko_48, Hegyko_44, and Hegyko_47), a parents and two sons pedigree (Hegyko_78, Hegyko_07, Hegyko_16, and Hegyko_05), and a mother and two daughters pedigree (Hegyko_28, Hegyko_27, and Hegyko_29).

By integrating second degree relatedness, we identified further extensions: Hegyko_67 is the father of Hegyko_33 and the grandfather of Hegyko_55 and Hegyko_80; Hegyko_06 is the daughter of Hegyko_77 and the niece of Hegyko_25 and Hegyko_15; and Hegyko_61 is the father of Hegyko_62 and the grandfather of Hegyko_75. We also linked the siblings Hegyko_31 and Hegyko_46 to the pedigree of Hegyko_26, as both siblings are second degree related to him. We then incorporated third degree relatedness pairs to further expand these pedigrees.

By incorporating osteological age, we were able to resolve the relationships between Hegyko_11/Hegyko_45, Hegyko_24/Hegyko_11, Hegyko_81/Hegyko_74, Hegyko_51/Hegyko_57 pairs.

Szeleste
In Szeleste, we identified 14 parent offspring pairs: Szeleste_962 and Szeleste_473, Szeleste_962 and Szeleste_479, Szeleste_554 and Szeleste_502, Szeleste_968 and Szeleste_502, Szeleste_388 and Szeleste_389 (Szeleste_370_1), Szeleste_427 and Szeleste_398, Szeleste_566 and Szeleste_577, Szeleste_395 and Szeleste_477, Szeleste_437_2 and Szeleste_599, Szeleste_511 and Szeleste_550, Szeleste_491 and Szeleste_375, Szeleste_491 and Szeleste_373, Szeleste_552 and Szeleste_393, Szeleste_954 and Szeleste_393

We also identified three sibling pairs: Szeleste_473 and Szeleste_479, Szeleste_451 and Szeleste_595, and Szeleste_375 and Szeleste_373. Based on these first degree relations, we constructed small pedigrees, including two parents and a daughter (Szeleste_552, Szeleste_954, and Szeleste_393) as well as Szeleste_554, Szeleste_968, and Szeleste_502. We also identified a father and two siblings (Szeleste_962, Szeleste_473, and Szeleste_479) and a father and two sons (Szeleste_491, Szeleste_375, and Szeleste_373). The integration of second and third degree relatedness further expanded these groups.

By incorporating osteological age, we were able to resolve the relationships between Szeleste _389(370-1)/Szeleste_388, Szeleste_577/Szeleste_566, Szeleste_477/Szeleste_395, Szeleste_437-2/Szeleste_599, and Szeleste_551/Szeleste_550 pairs.

Gyirmót, Kóny and Ménfőcsanak
In Gyirmót, we identified only one pair of third degree related individuals: Gyirmot_36_1 and Gyirmot_36_2. In Kóny, we identified two parent offspring pairs: Kony_442 and Kony_447, and Kony_449 and Kony_444. Since Kony_447 is an adult and Kony_442 is an infant, we put Kony_447 in the early generation. Kony_449 and Kony_444 are both adults, but they share the

same mtDNA haplotype, we consider them a mother and son pair. No relatedness within three degrees was identified in Ménfőcsanak.

Supplementary Figures

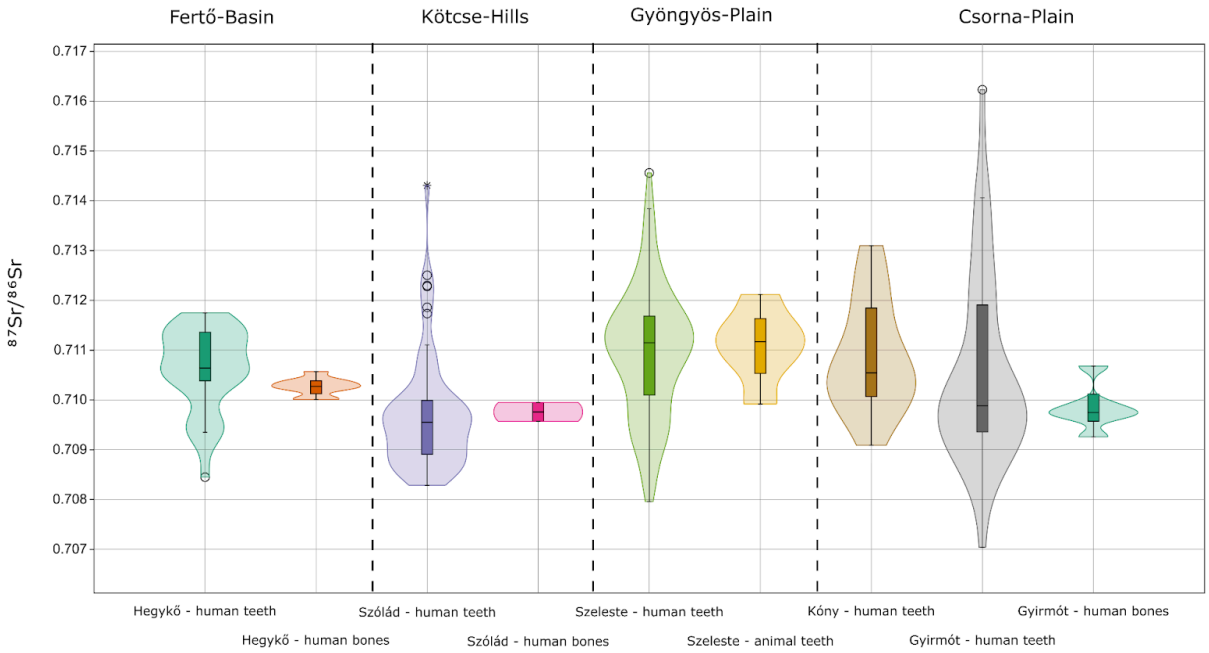


Fig. S1. $^{87}Sr/^{86}Sr$ results of the investigated 6th-century sites with comparative material used to test for 'local' baselines grouped according to microregion within the LHP

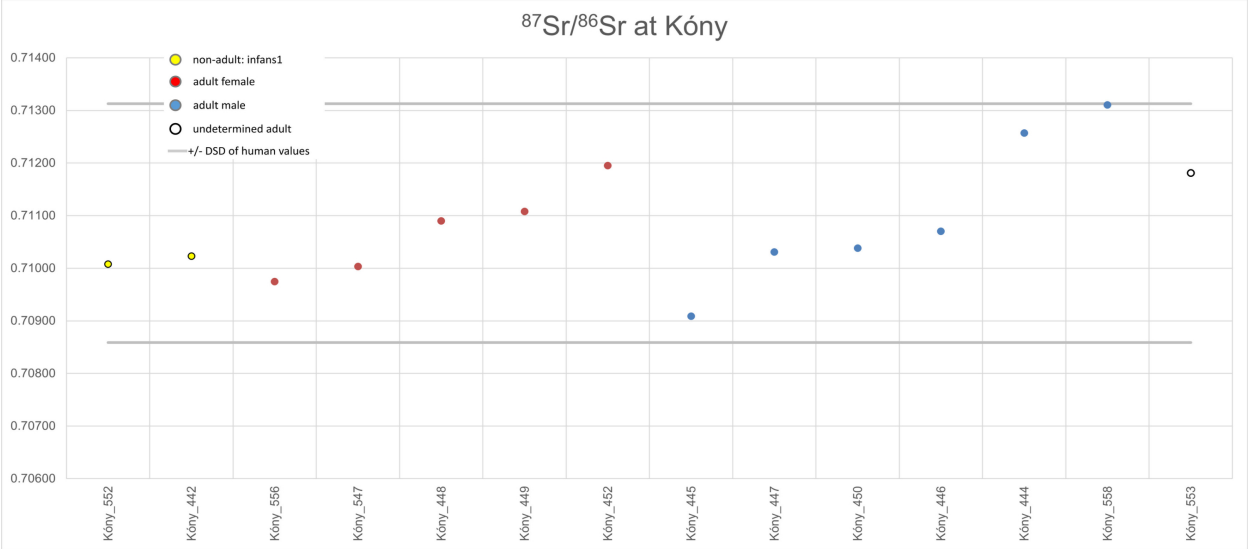


Fig. S2. $^{87}Sr/^{86}Sr$ isotopic data at Kóny. Nonadult values are marked with yellow, adult females with red, adult males with blue, while an unidentifiable adult individual with white (all measurements from teeth). The lines represent the double standard deviation (DSD) range of all human values.

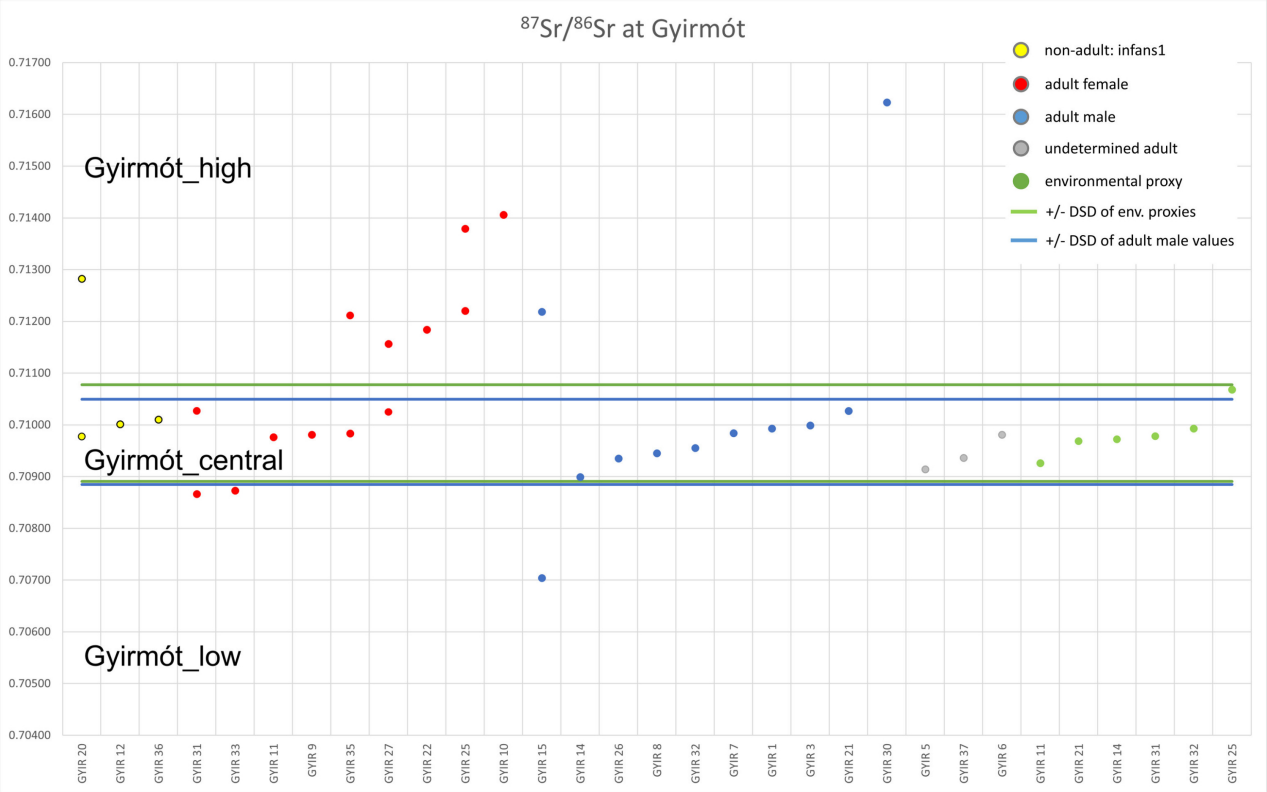


Fig. S3. $^{87}Sr/^{86}Sr$ isotopic data at Gyirmót. Nonadult values are marked with yellow, adult females with red, adult males with blue (all measurements from teeth). Values from human bone samples are marked with green. Blue lines represent a presumed 'local' $^{87}Sr/^{86}Sr$ range based on the double standard deviation (DSD) of adult male individuals (due to the low number of nonadults), while green lines represent the DSD of human bone samples.

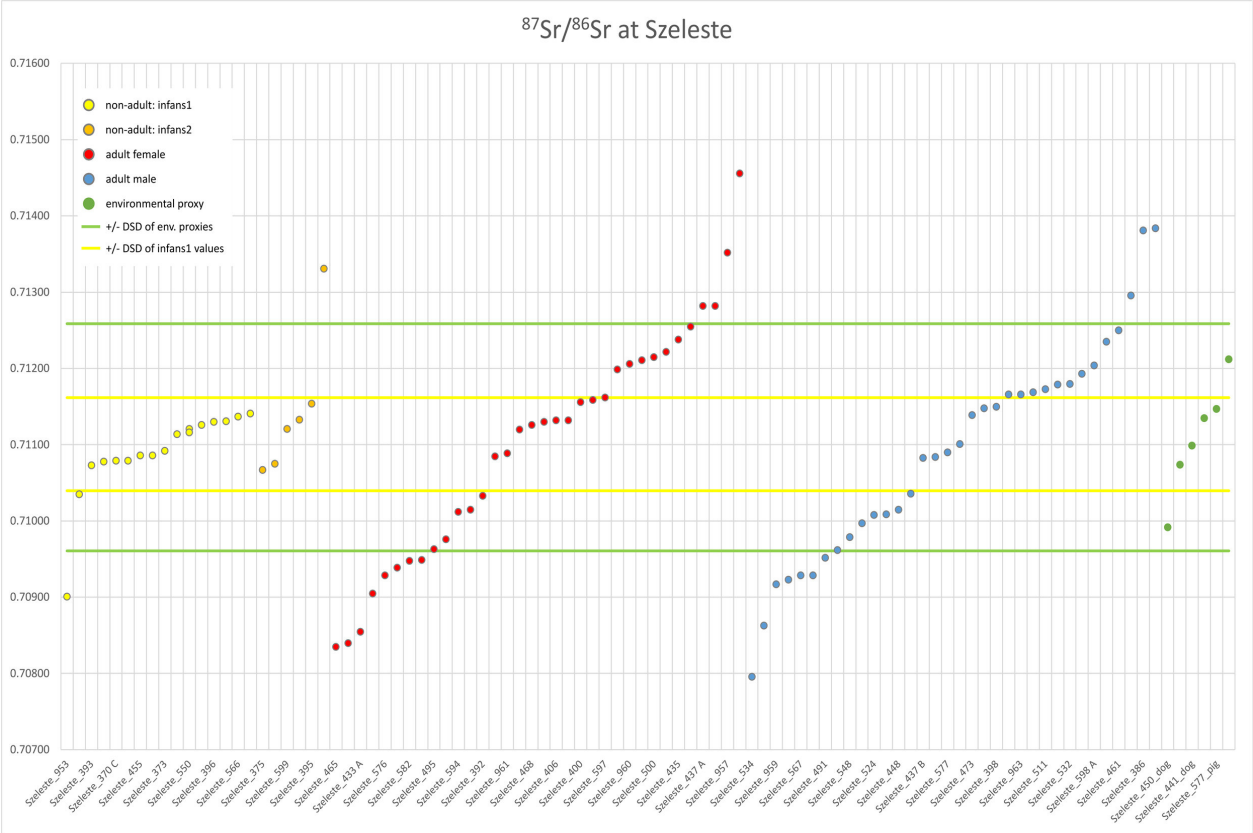


Fig. S4. $^{87}Sr/^{86}Sr$ isotopic data at Szeleste. Infans 1 individuals are marked with yellow, infans 2 individuals with orange, adult females with red, adult males with blue (all measurements from teeth). Faunal samples are marked with green. Yellow lines represent a presumed 'local' $^{87}Sr/^{86}Sr$ range based on the double standard deviation (DSD) of infans1 individuals, while green lines represent the DSD of all faunal samples.

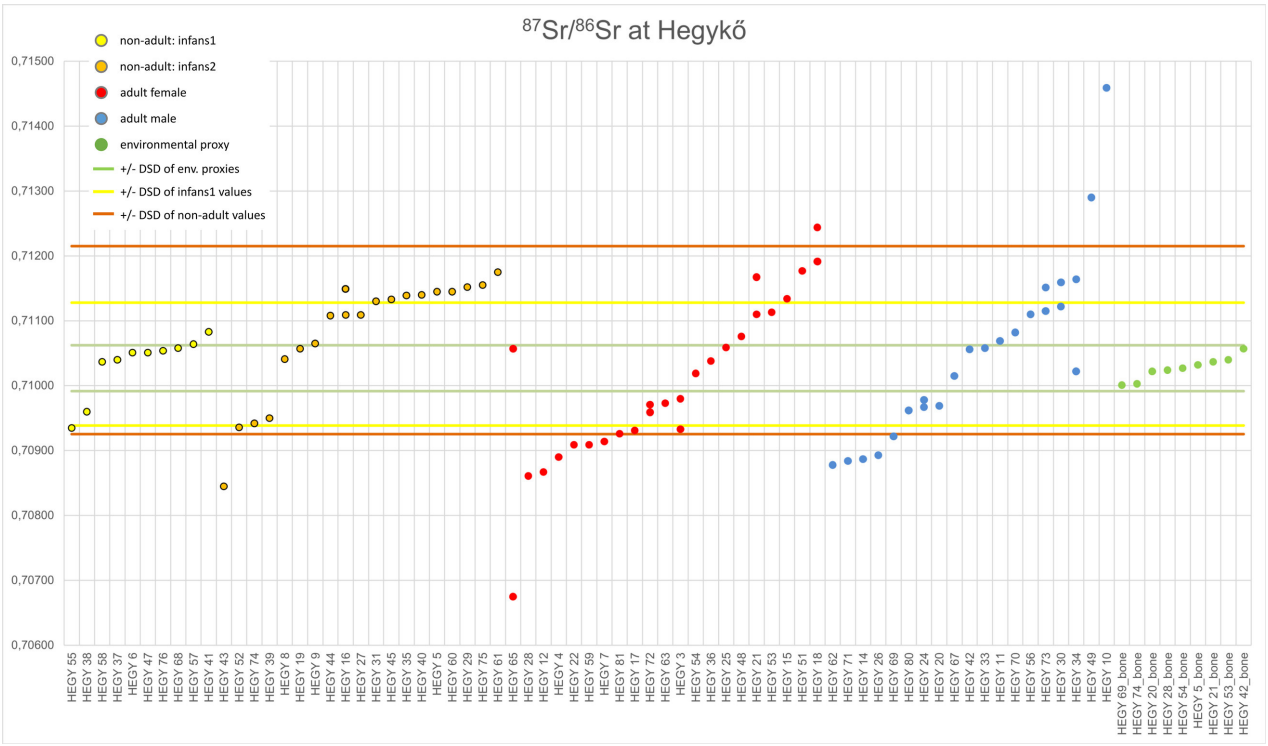


Fig S5. $^{87}Sr/^{86}Sr$ isotopic data at Hegykő. Infans 1 individuals are marked with yellow, infans 2 individuals with orange, adult females with red, adult males with blue (all measurements from teeth). Values from human bone samples are marked with green. Yellow lines represent a presumed 'local' $^{87}Sr/^{86}Sr$ range based on the double standard deviation (DSD) of infans1 individuals, orange lines represent the DSD range of all nonadult individuals, while green lines represent the DSD of human bone samples.

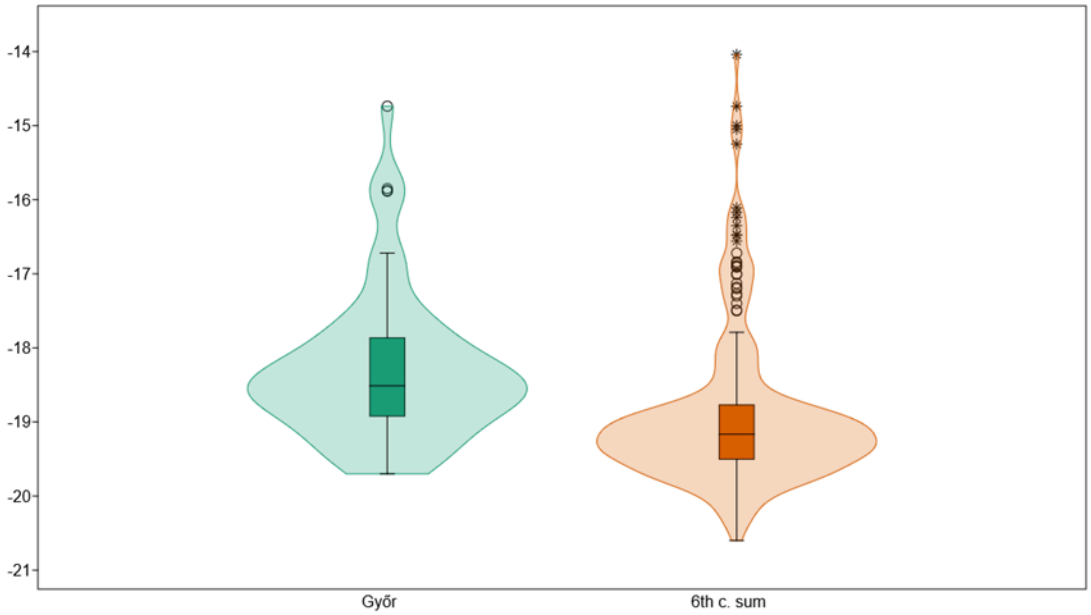


Fig. S6. Comparison of $\delta^{13}C$ values between 4-5th century site and 6th century sites

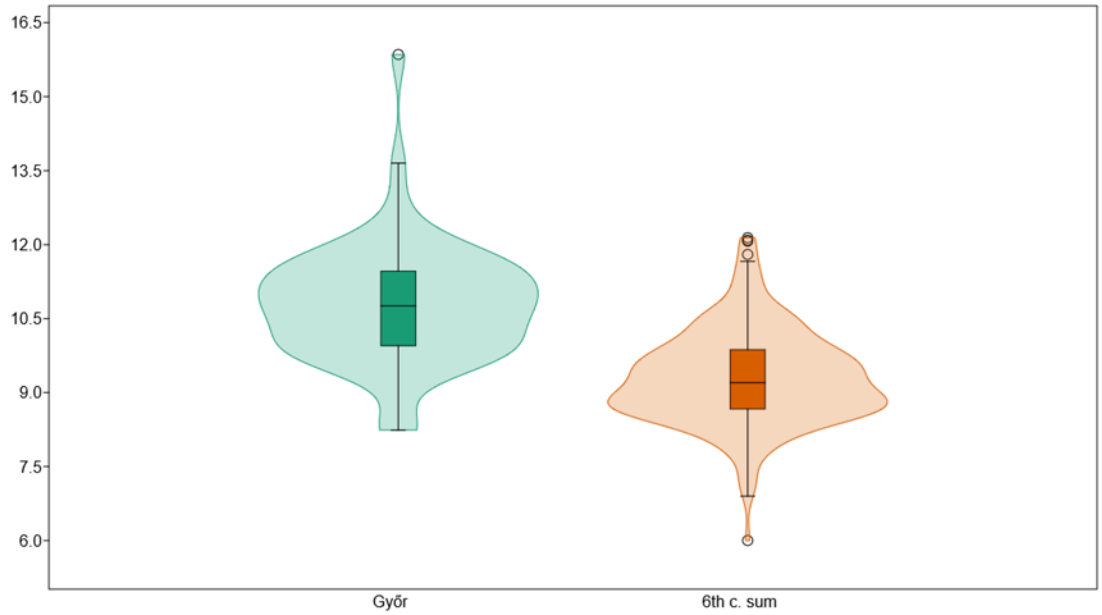


Fig. S7. Comparison of $\delta^{15}N$ values between 4-5th century site and 6th century sites

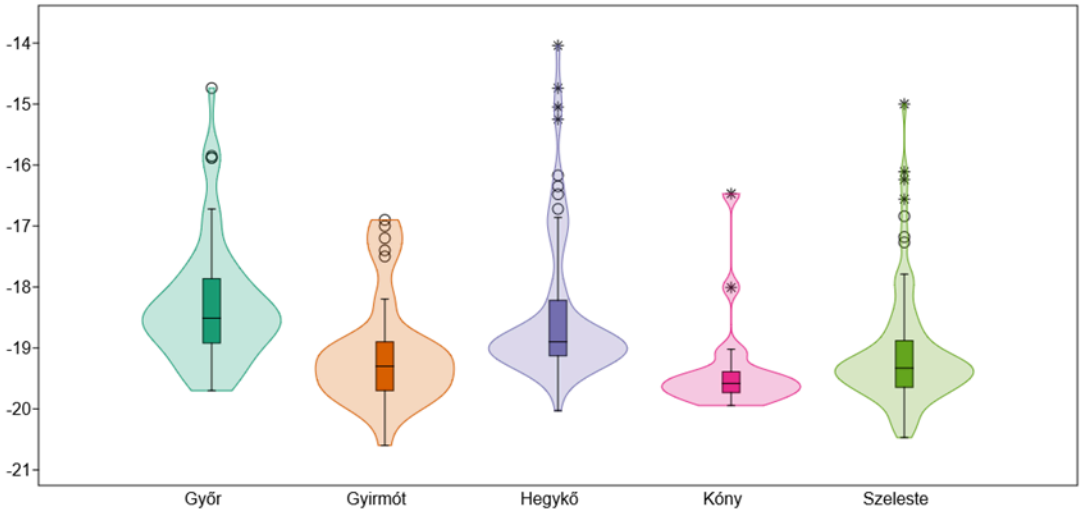


Fig. S8. Comparison of $\delta^{13}C$ values across five sites

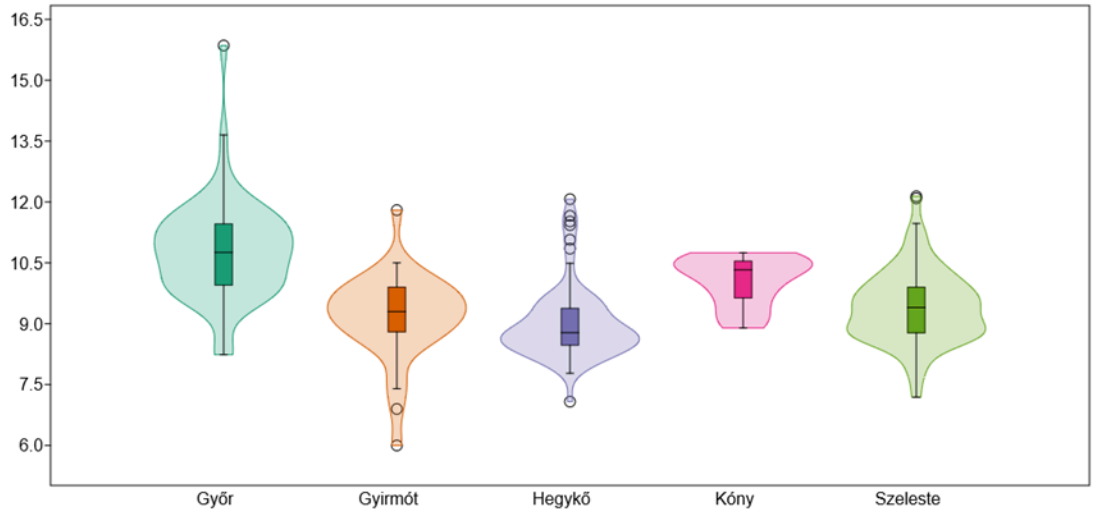


Fig. S9. Comparison of $\delta^{15}N$ values across five sites

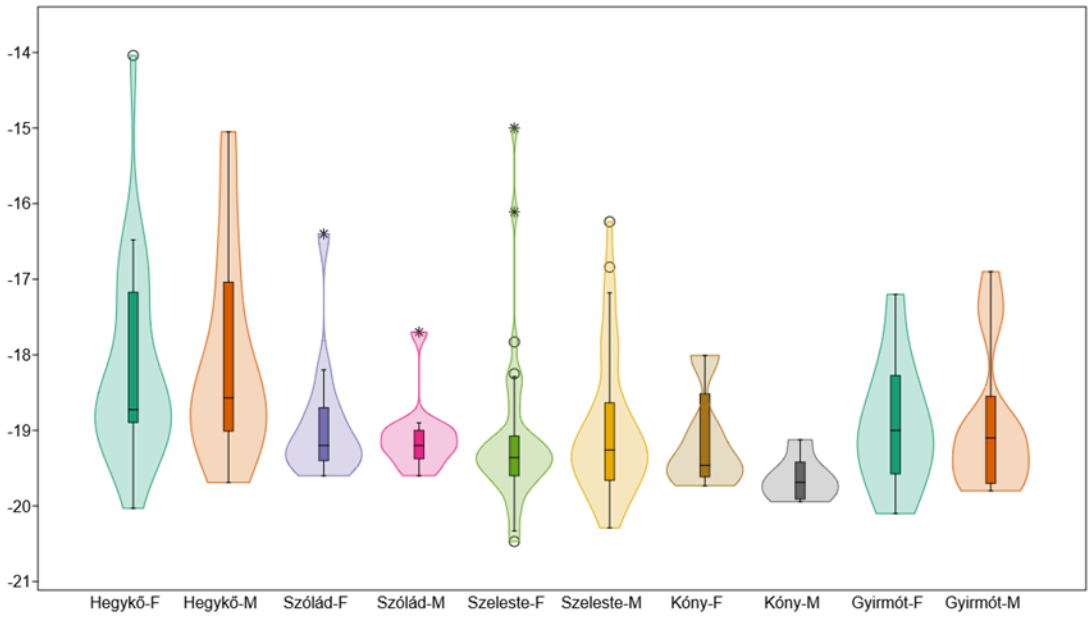


Fig. S10. Comparison of $\delta^{13}C$ values across five sites, focusing on adult males and females

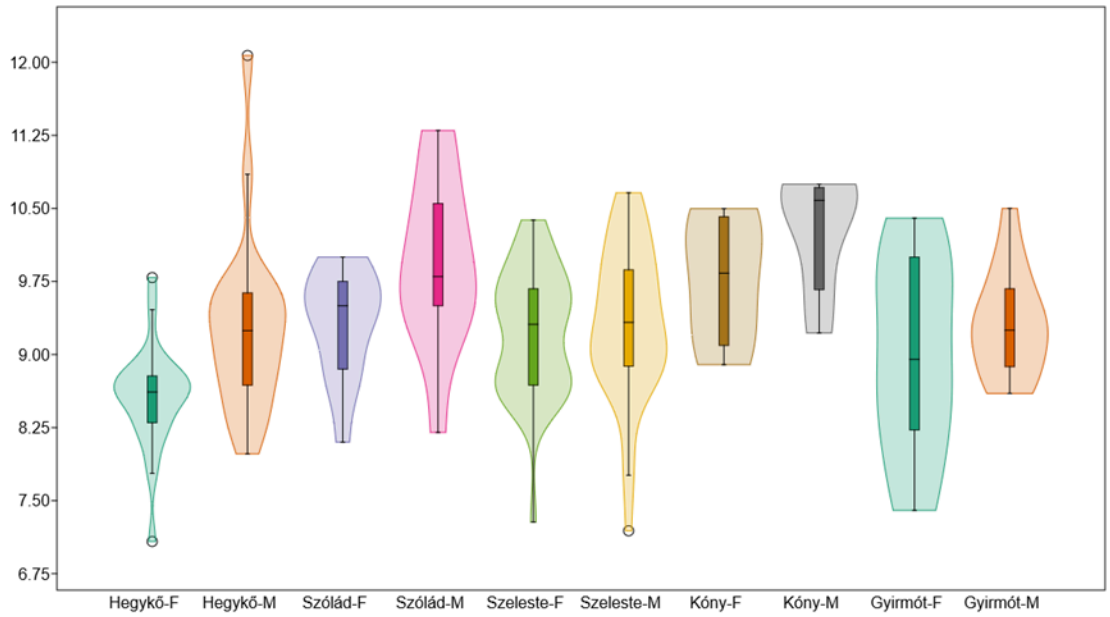


Fig. S11. Comparison of $\delta^{15}N$ values across five sites, focusing on adult males and females

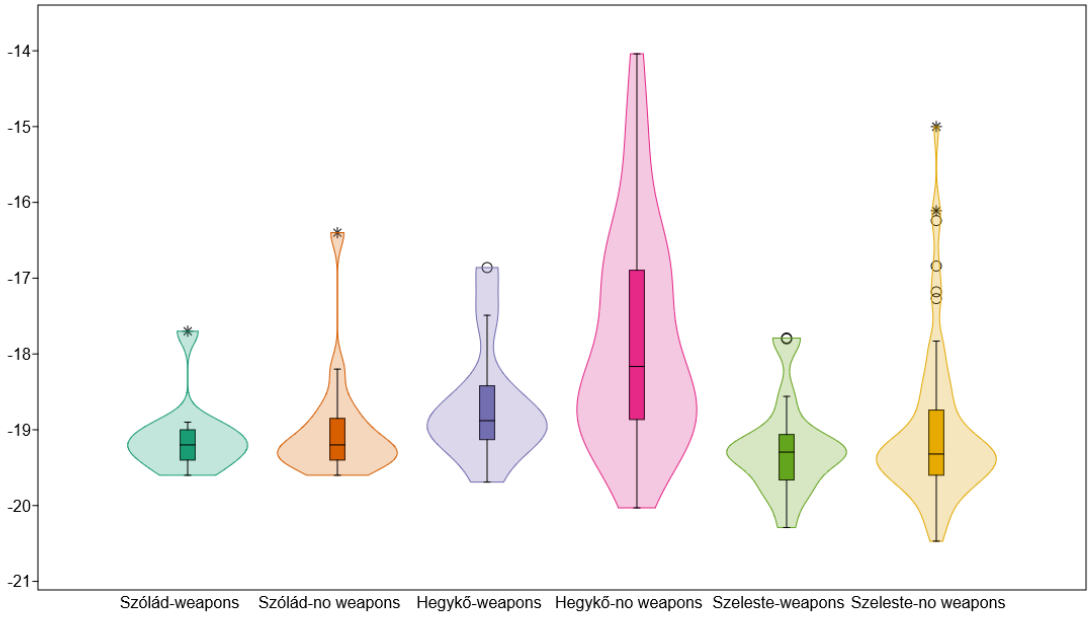


Fig. S12. Comparison of $\delta^{13}C$ values across three sites, focusing on males with weapons and other adults without weapons.

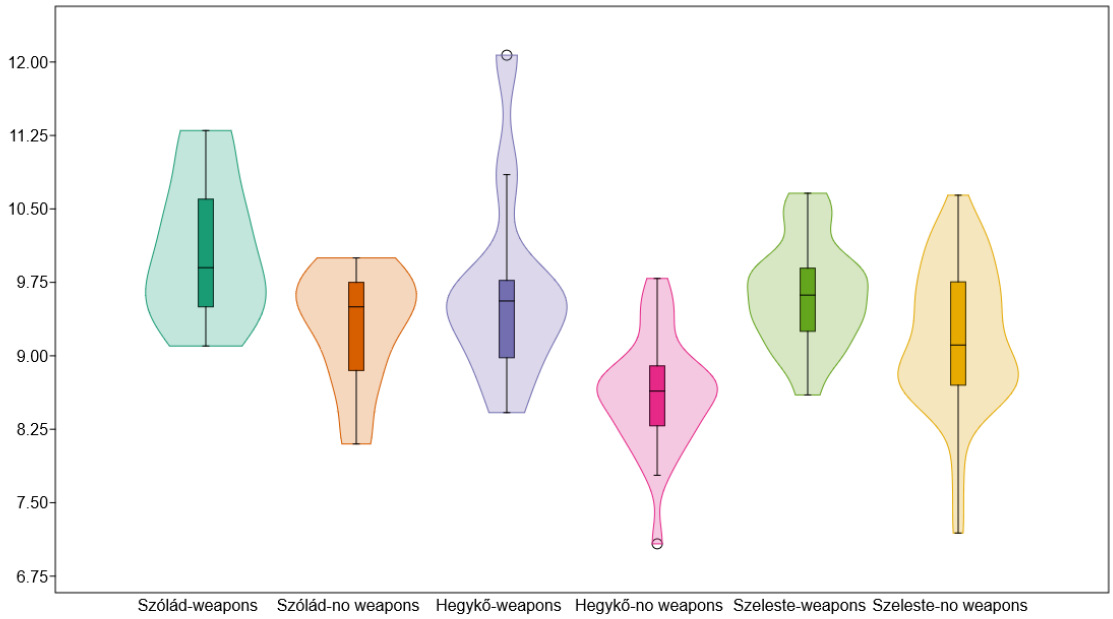


Fig. S13. Comparison of $\delta^{15}N$ values across three sites, focusing on males with weapons and other adults without weapons.

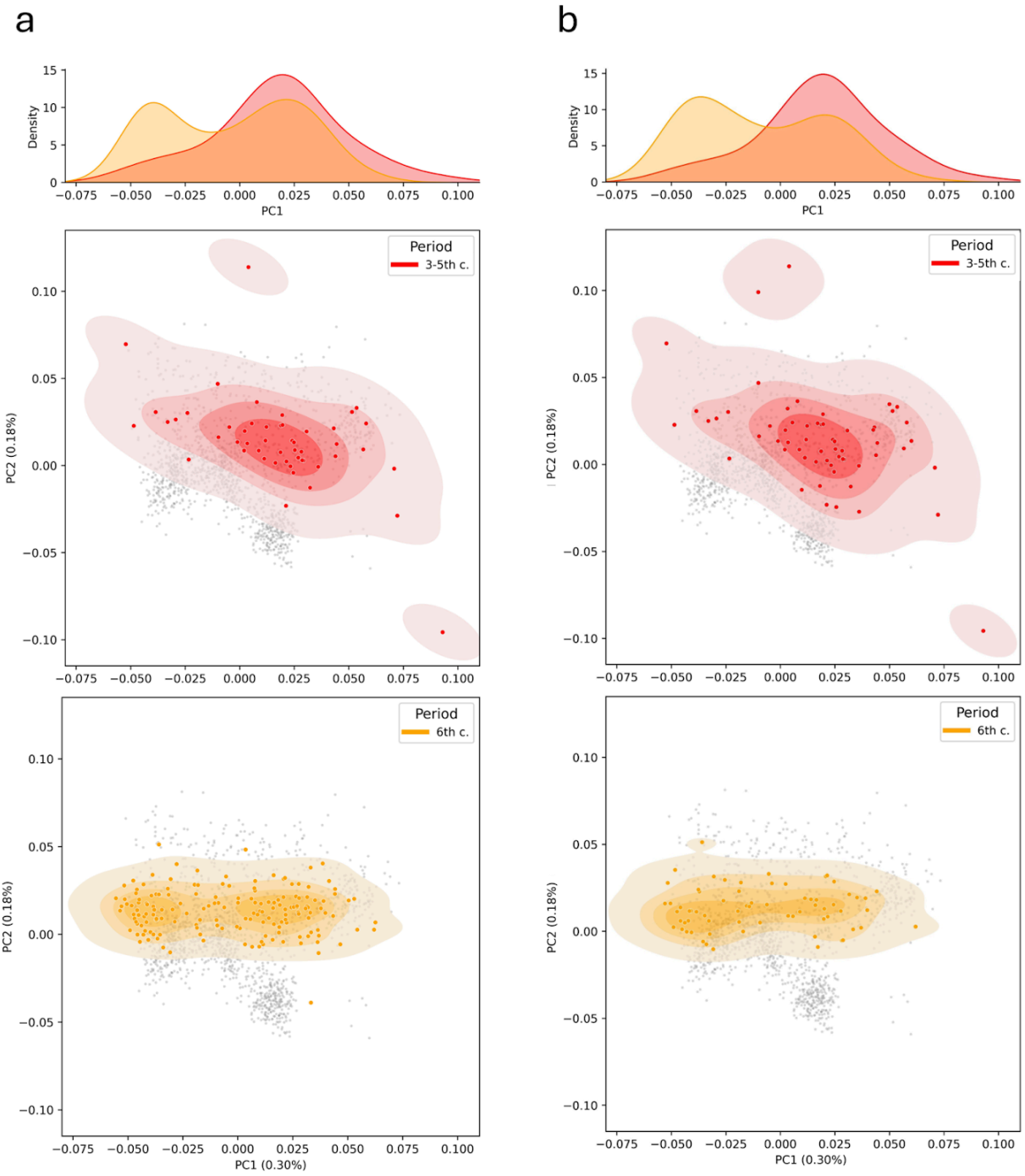


Fig. S14. a. PCA results removing all the relatives up to 3rd degree for both the 3-5th c, and 6th c. sites. b.PCA results for 3-5th c. sites (n=68) and a downsampled version of the 6th c. sites (n = 68).

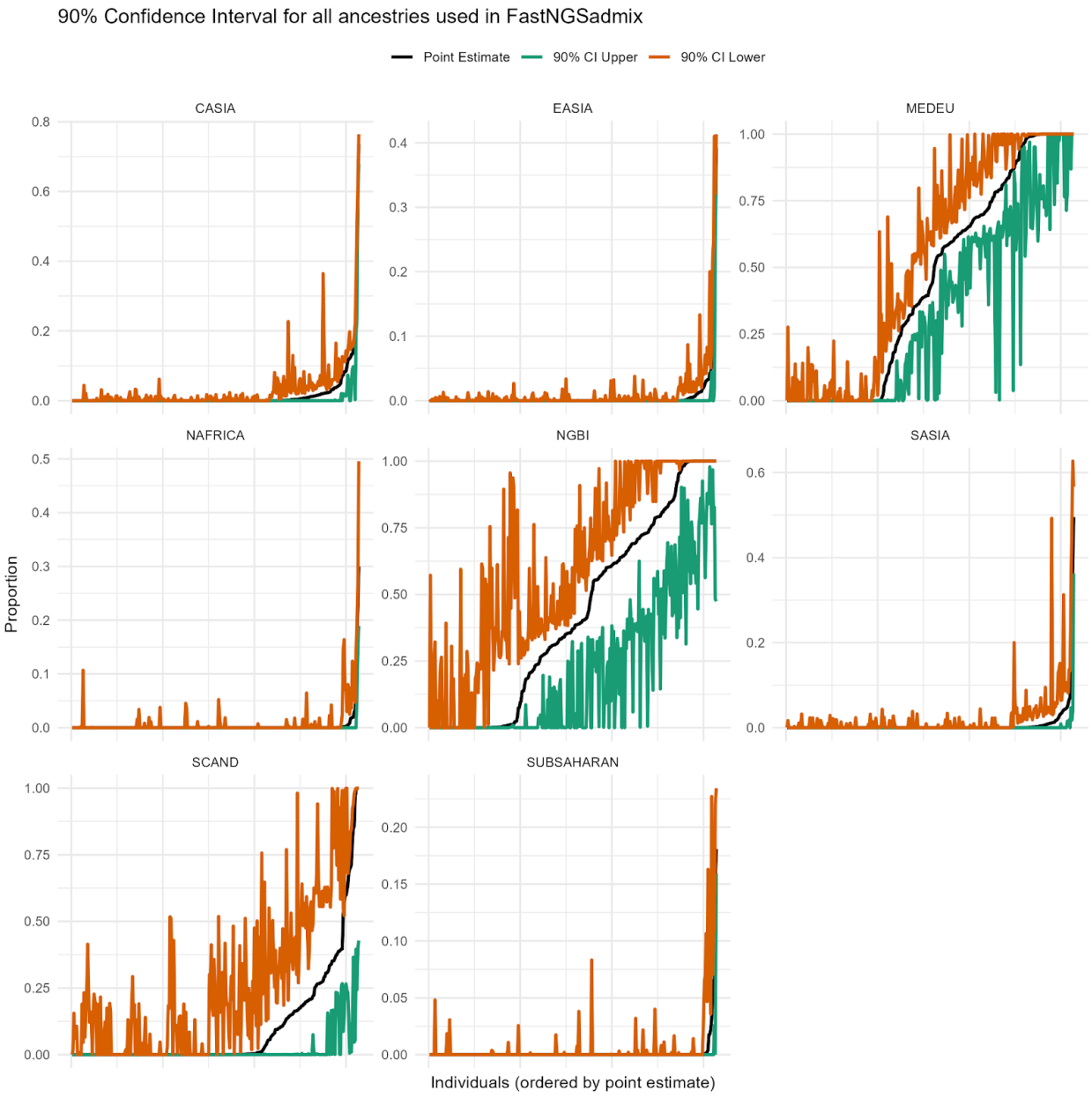


Fig. S15. Bootstrap results for all ancestries, including point estimates and 90% confidence intervals

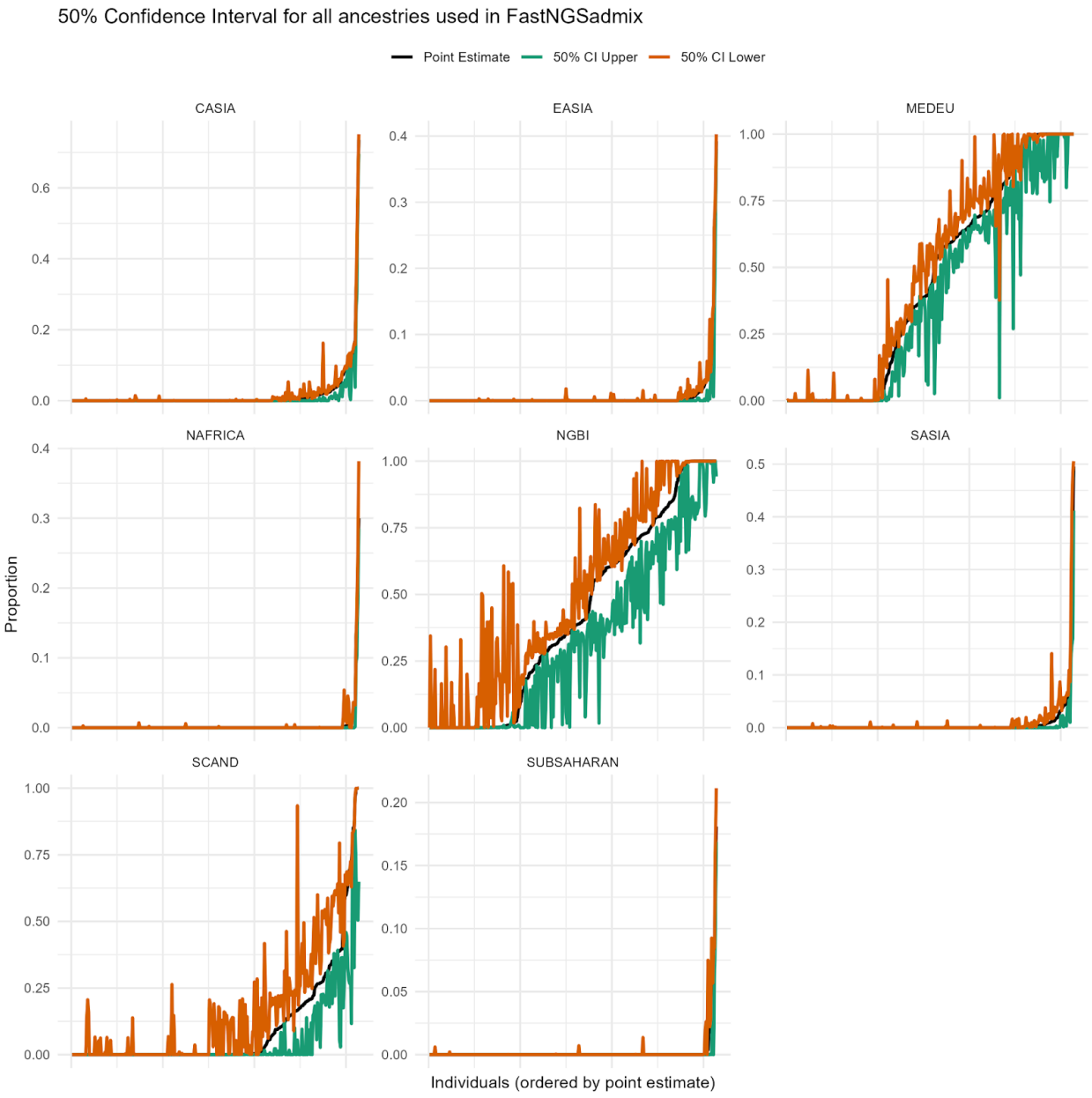


Fig. S16. Bootstrap results for all ancestries, including point estimates and 50% confidence intervals

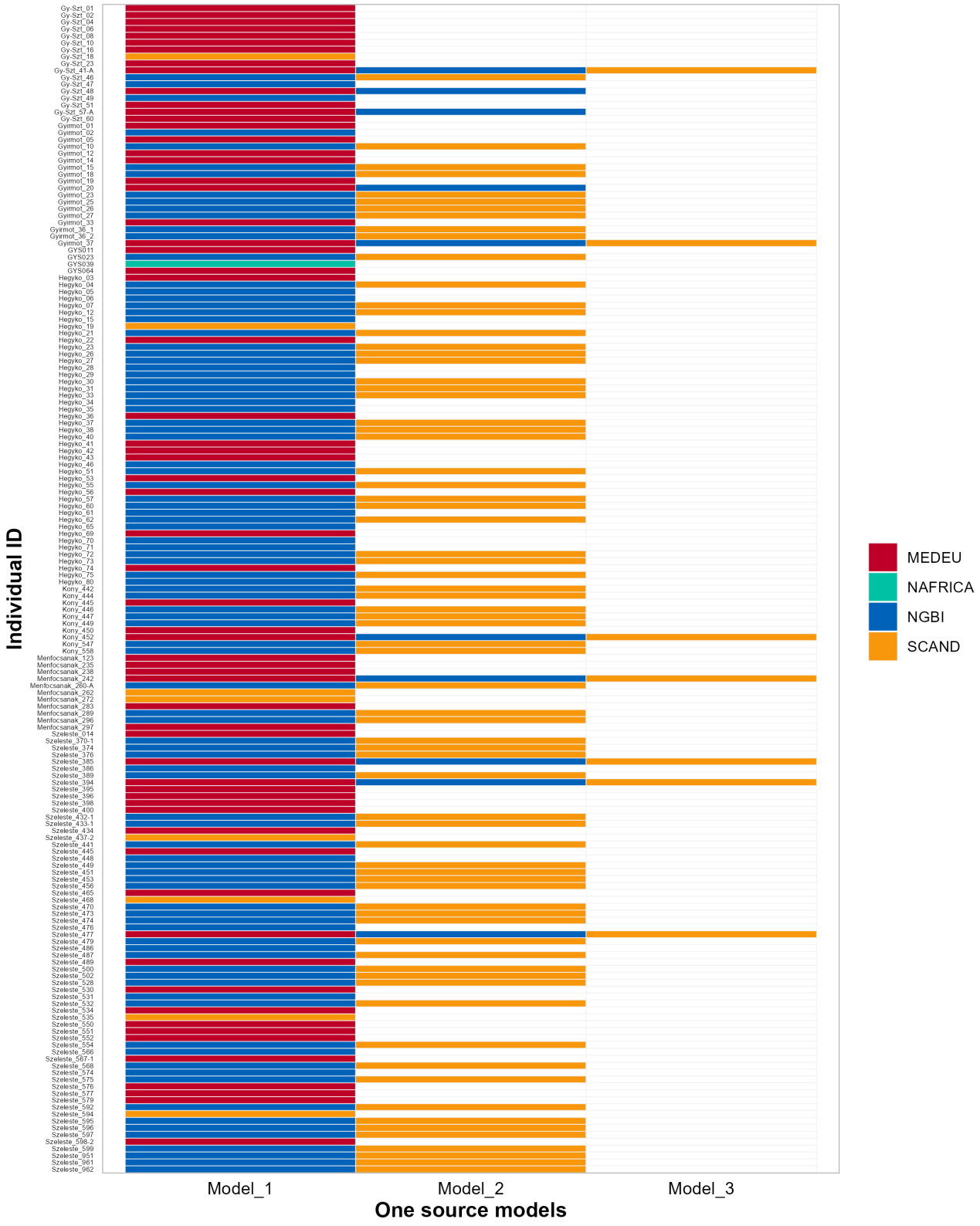


Fig. S17. Successful one source qpAdm models. Each row represents a unique individual ID, displaying all valid models.

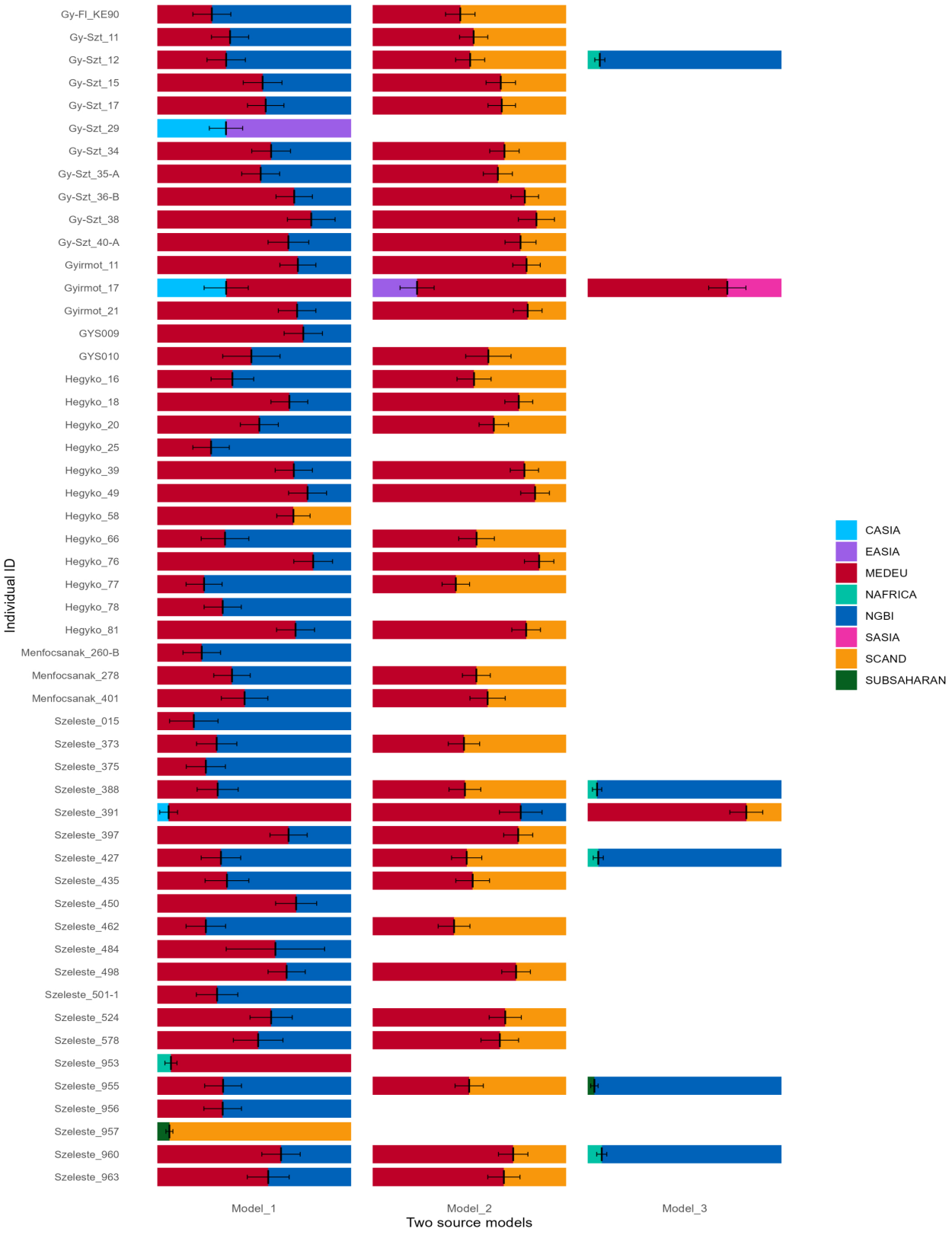


Fig. S18. Successful two source qpAdm models. Each row represents a unique individual ID, displaying all valid models. Error bars indicate standard error.

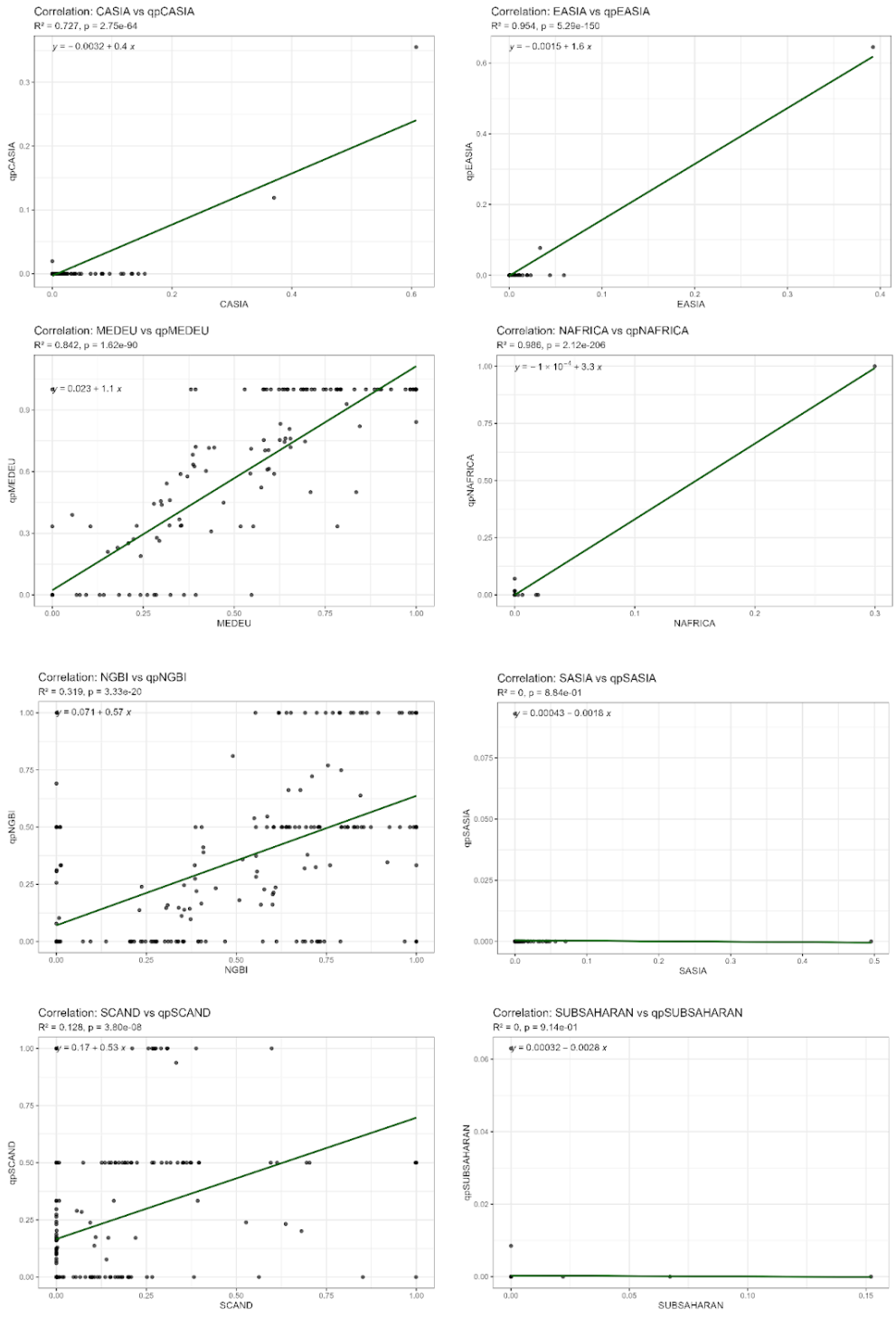


Fig. S19. Correlation and linear regression analyses between fastNGSadmix and qpAdm results (starting with 'qp') for eight penecontemporaneous reference populations. Analyses included all individuals with data from both methods and a coverage greater than 0.01x.

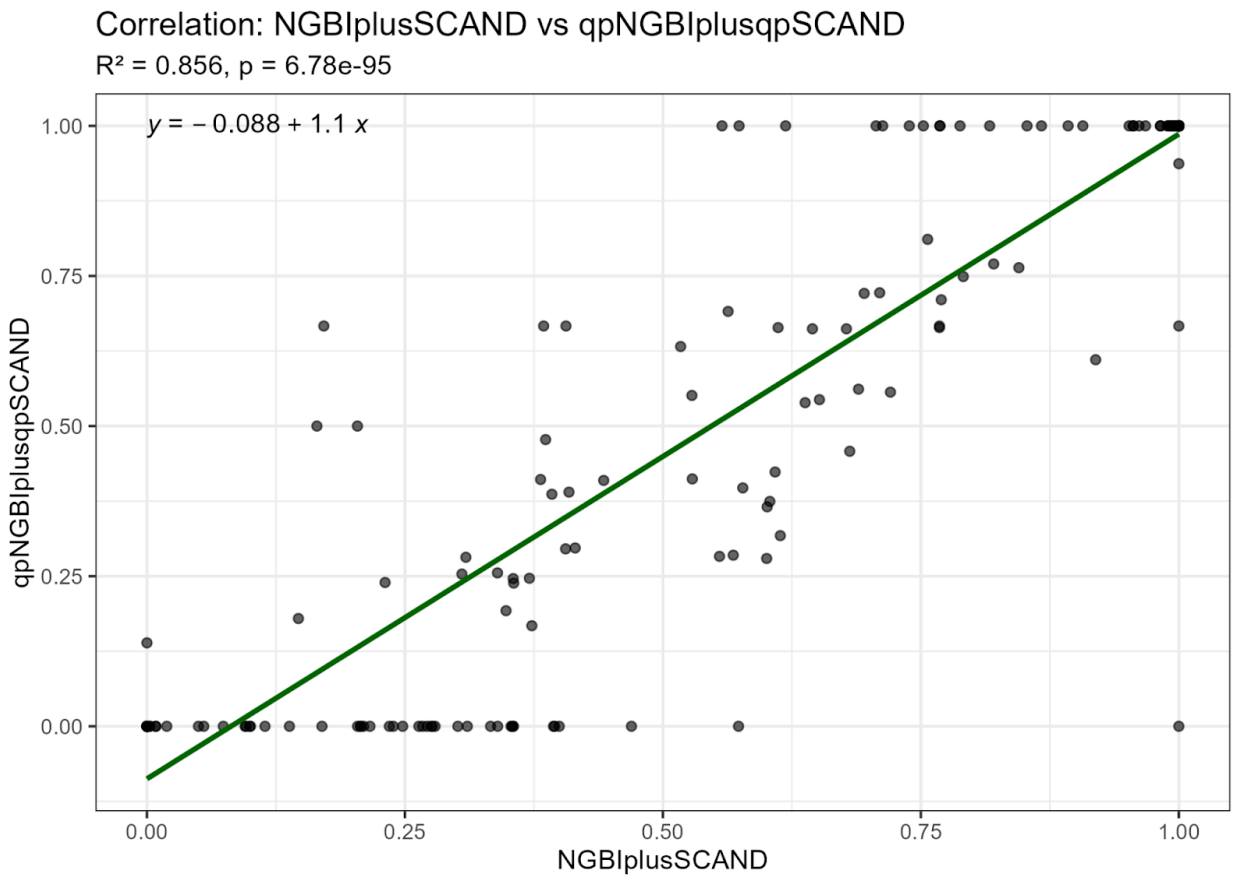


Fig. S20. Correlation and linear regression analyses between fastNGSadmix and qpAdm results (starting with 'qp') for northern components (NGBI plus SCAND).

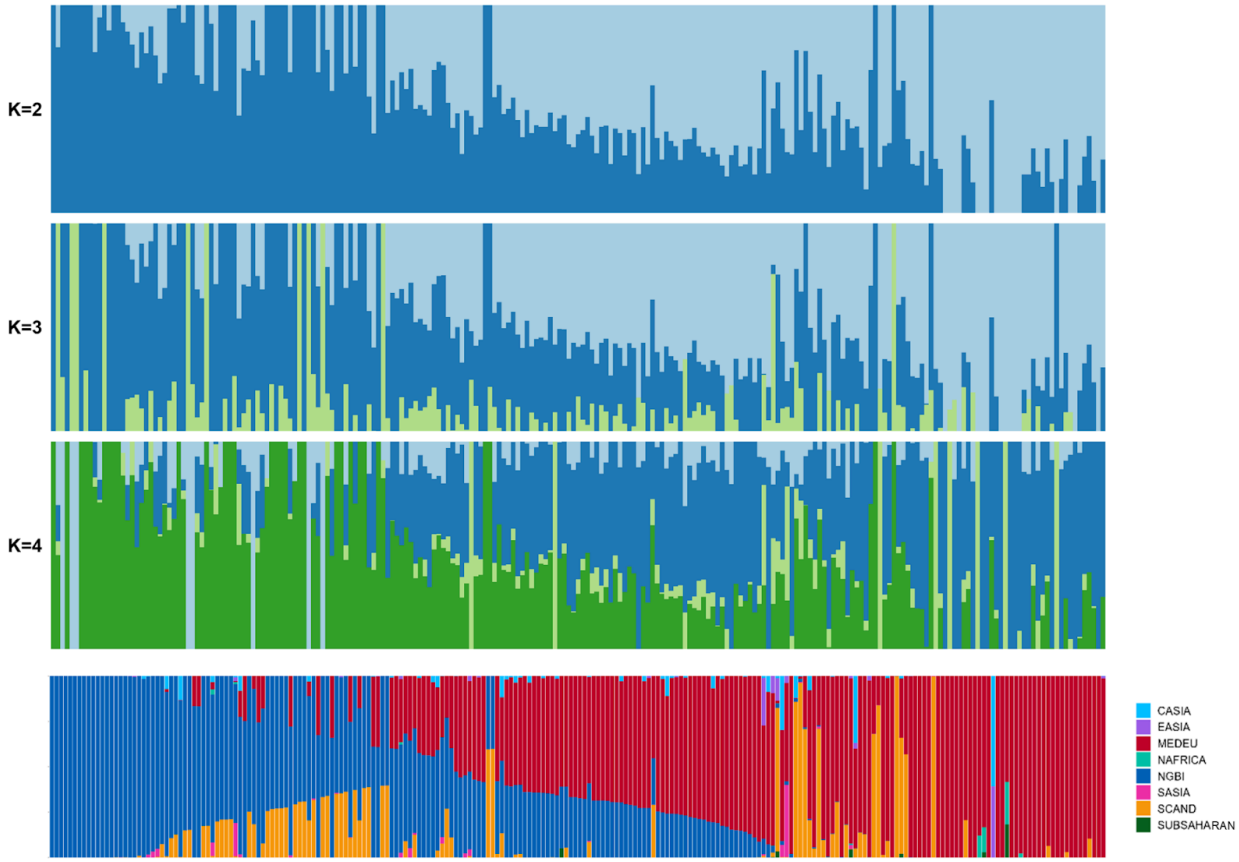


Fig. S21. Comparison of unsupervised (NGSadmix) and supervised (fastNGSadmix) population structure. Each vertical bar represents a single individual. The dataset was filtered to exclude related individuals..

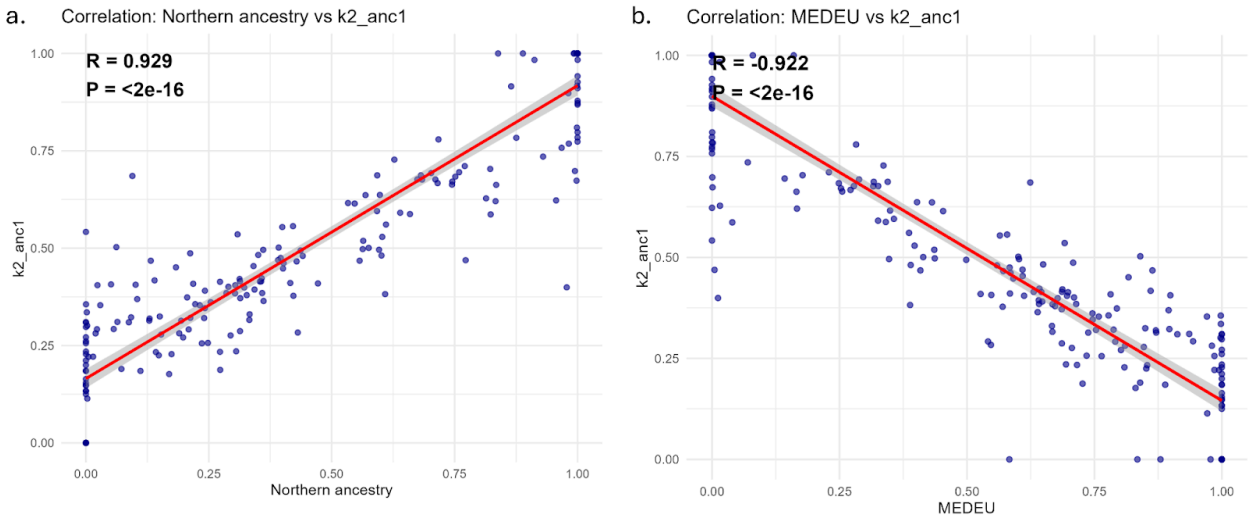


Fig. S22. Correlation between unsupervised ancestry components (NGSadmix, K=2) and supervised ancestry estimates (fastNGSadmix).
(a) Correlation between the first unsupervised component and Northern European ancestry proportions (defined as the sum of NGBI and SCAND).
(b) Correlation between the second unsupervised component and the MEDEU reference, representing Southern European ancestry.

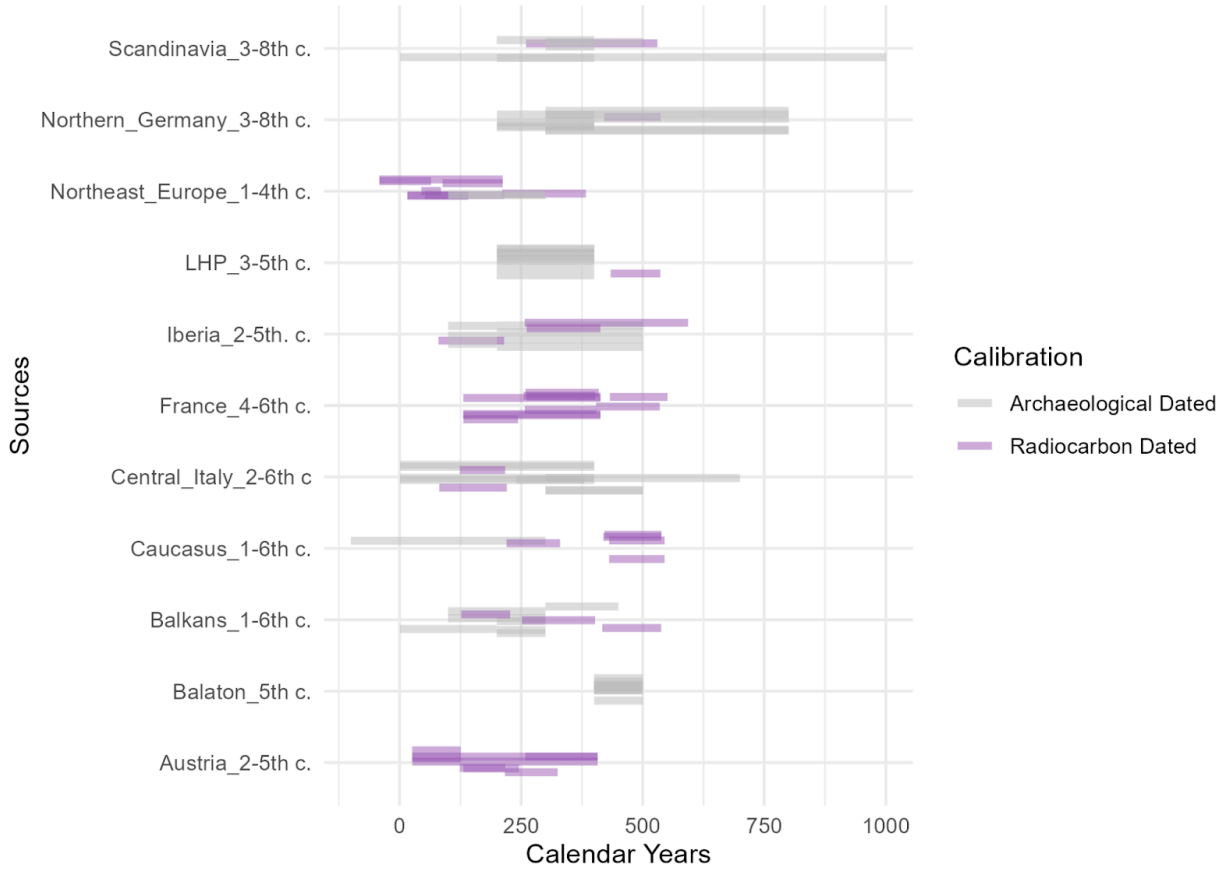


Fig. S23. Dating ranges of source individuals and groups included in the qpWave analysis. Each line represents an individual, with colors indicating whether the date is radiocarbon-calibrated. Ia: Iron Age; em: Early Medieval

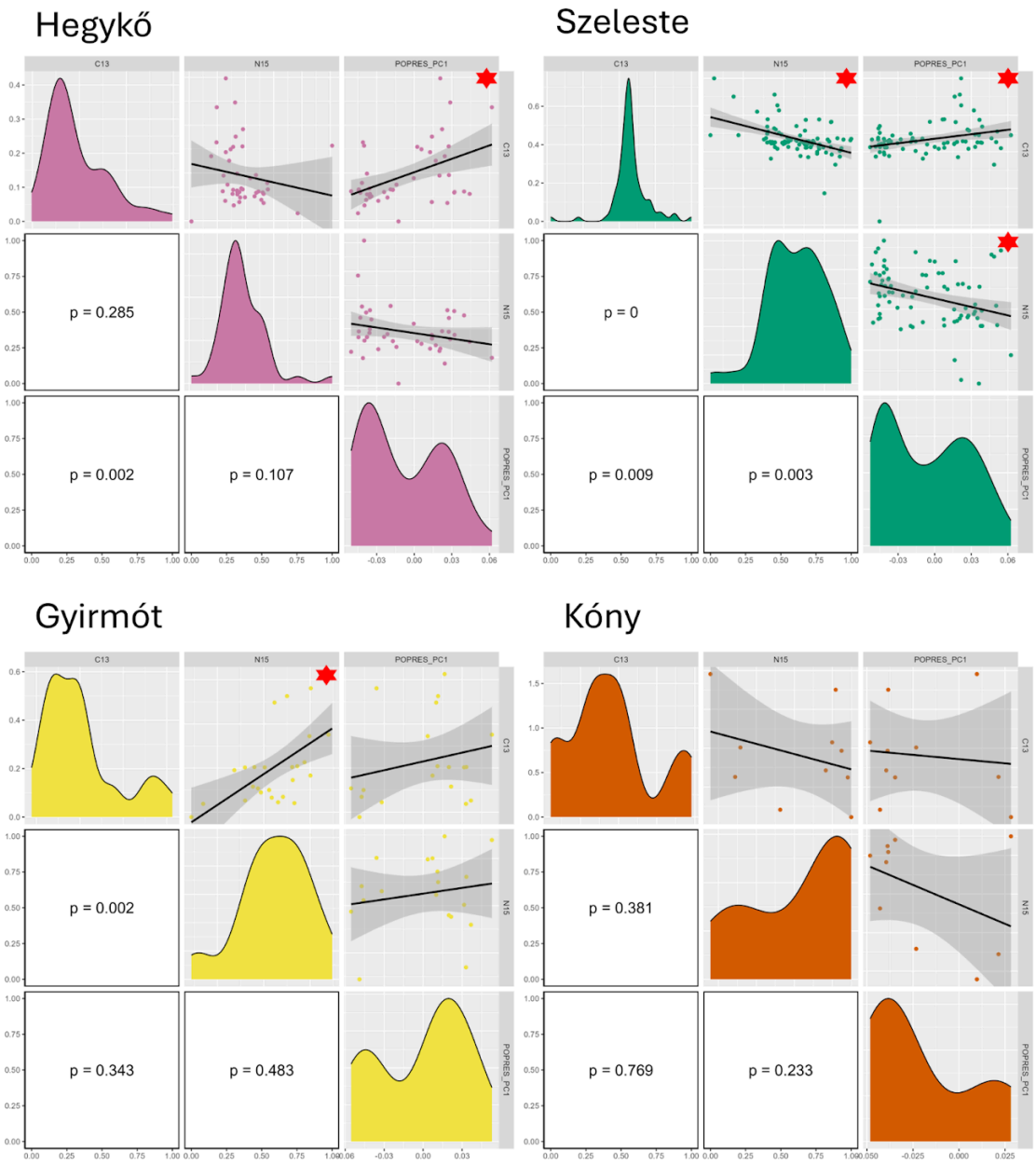


Fig. S24. Pairwise correlation matrix of isotopic and ancestry variables. This matrix plot, generated using the ggpairs() function (part of the GGally R package (*149*).), illustrates the relationships between $\delta^{13}C$, $\delta^{15}N$ and PC1 (Using POPRES dataset as the reference). The figure is organized into three distinct components: Diagonal Panels (Univariate Distribution): The plots along the diagonal (from top-left to bottom-right) represent the distribution of a single variable. The curves are kernel density estimates, which visualize the data's probability density and spread for each respective variable. Upper Triangle (Bivariate Relationships): The panels in the upper-right section display scatterplots for each pair of variables, overlaid with a linear regression line. Lower Triangle (Statistical Significance): The panels in the lower-left section

correspond directly to the scatterplots mirrored across the diagonal. Each box displays the statistical significance of the linear relationship between the two intersecting variables. Asterisks indicate significance ($p < 0.05$), with the exact p-values provided numerically. Points and curves are color-coded by Site, allowing for a visual comparison of isotopic and genetic clusters across the four geographic locations.

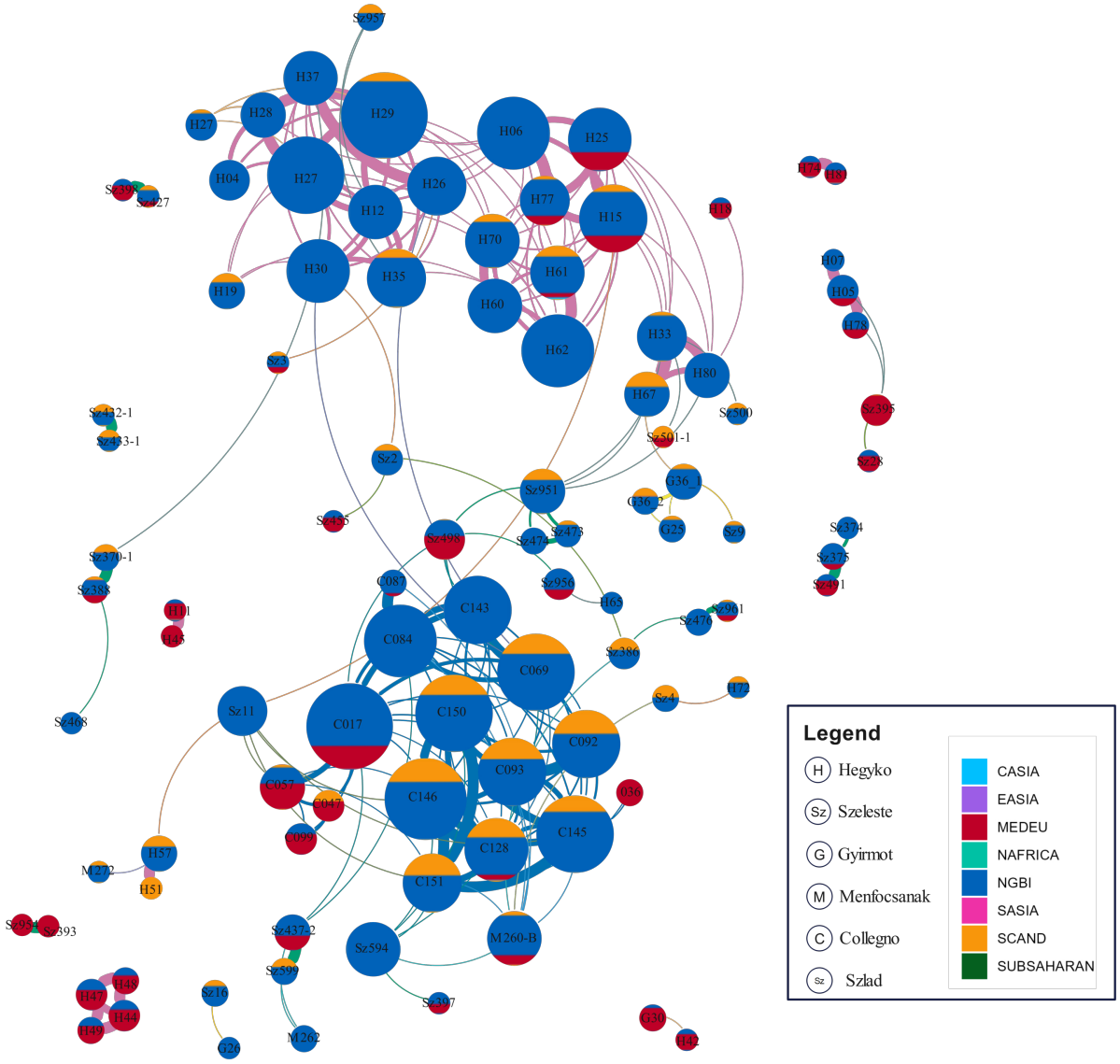


Fig. S25. The same IBD network as in Fig. 3C, but colored according to genetic ancestry inferred from fastNGSadmix results.

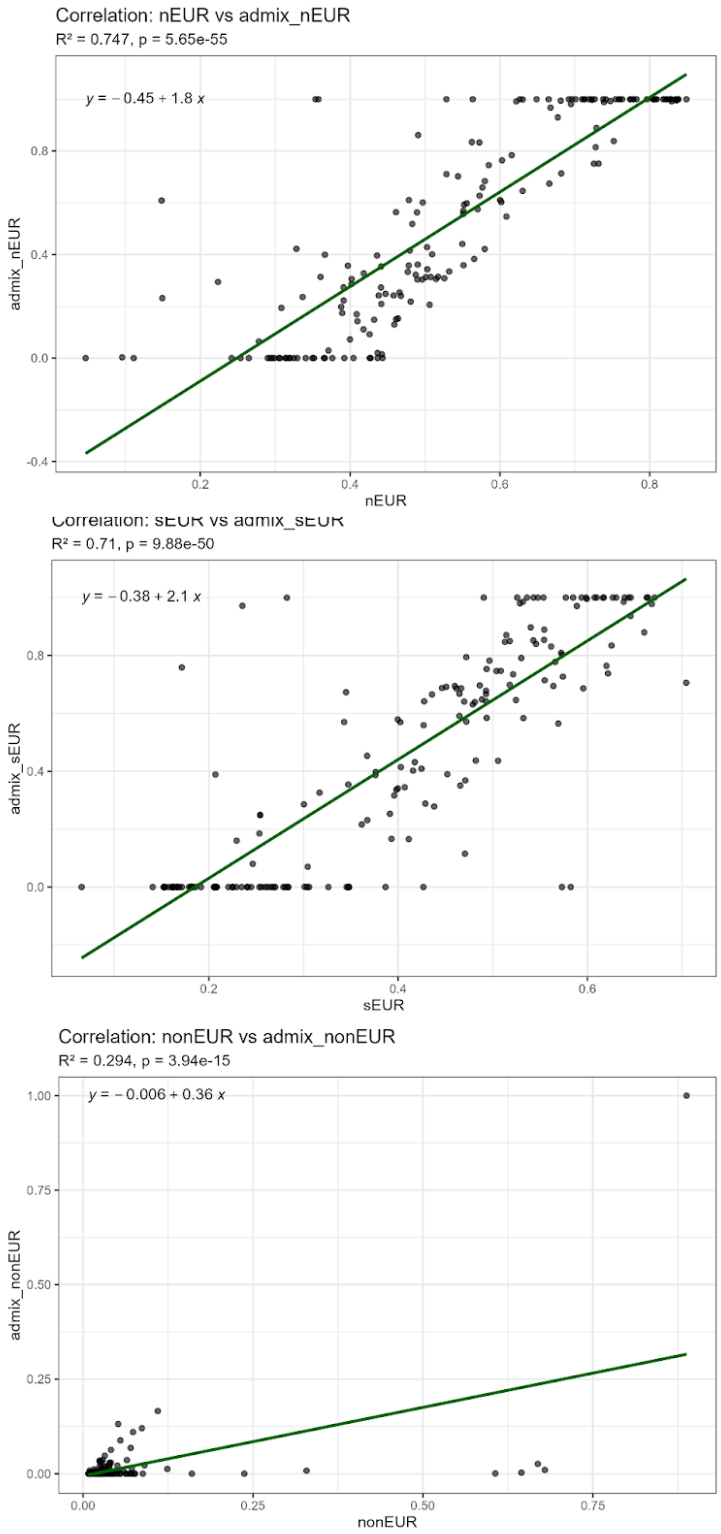


Fig. S26. Correlation and linear regression analyses between fastNGSadmix and Local Ancestry Inference results. nEUR - Northern European; sEUR - Southern European; nonEUR - non-European

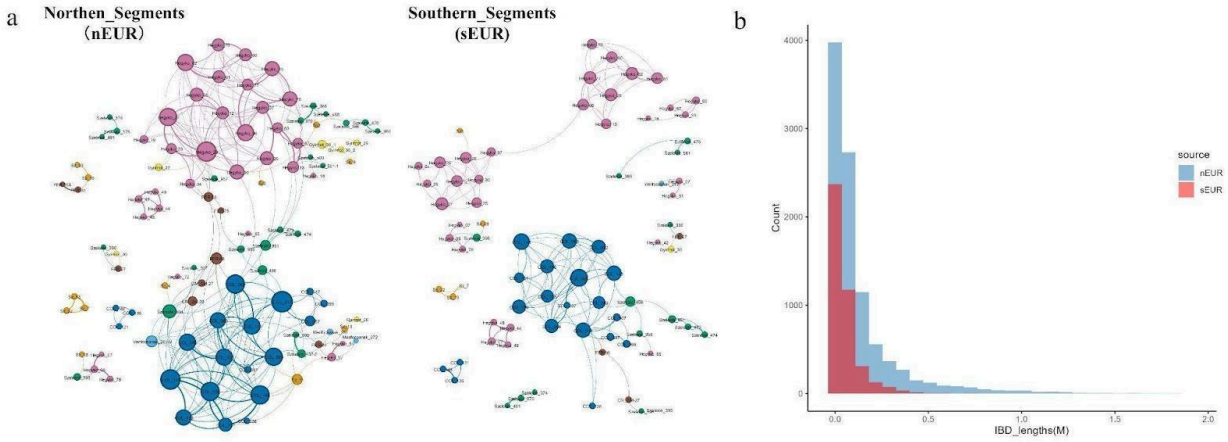
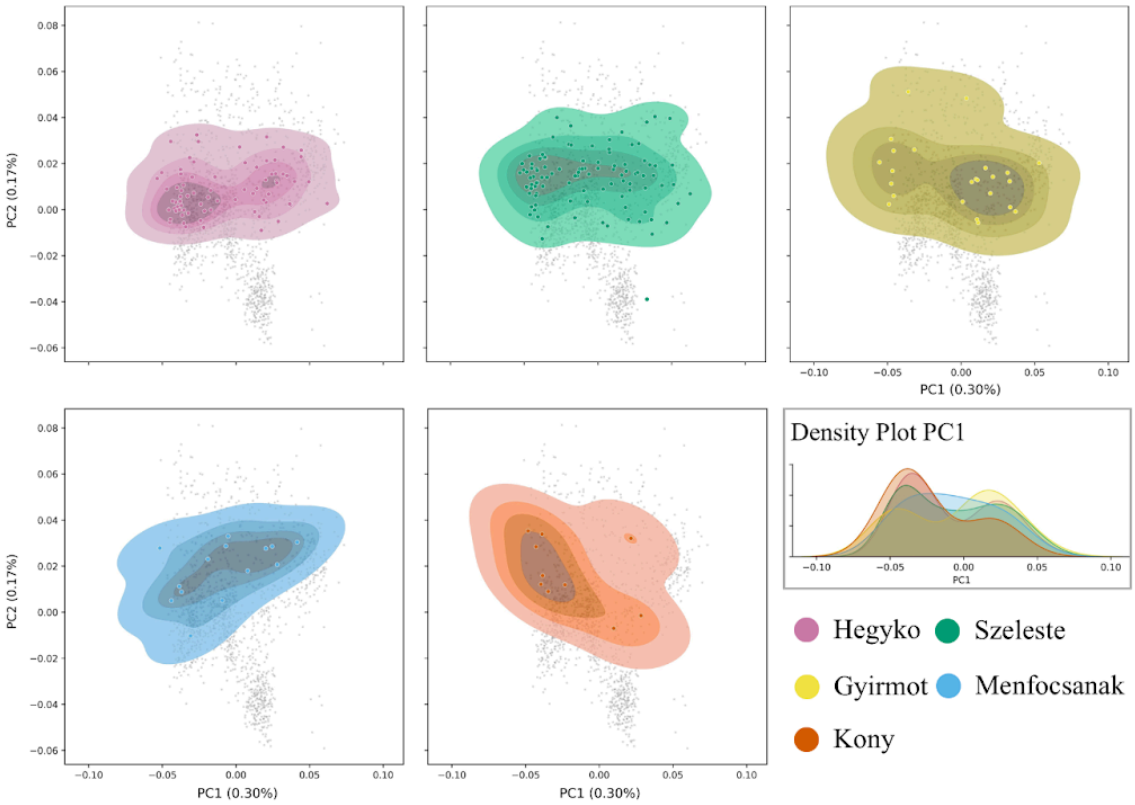


Fig. S27. Local Ancestry Inference results using FLARE. a, IBD network based on both Northern ancestry segments (nEUR) and Southern ancestry Segments (sEUR). b, The distribution of nEUR and sEUR.

a. PCA analysis for 5 post-Roman sites



b. PCA analysis for 5 post-Roman sites (unrelated individuals)

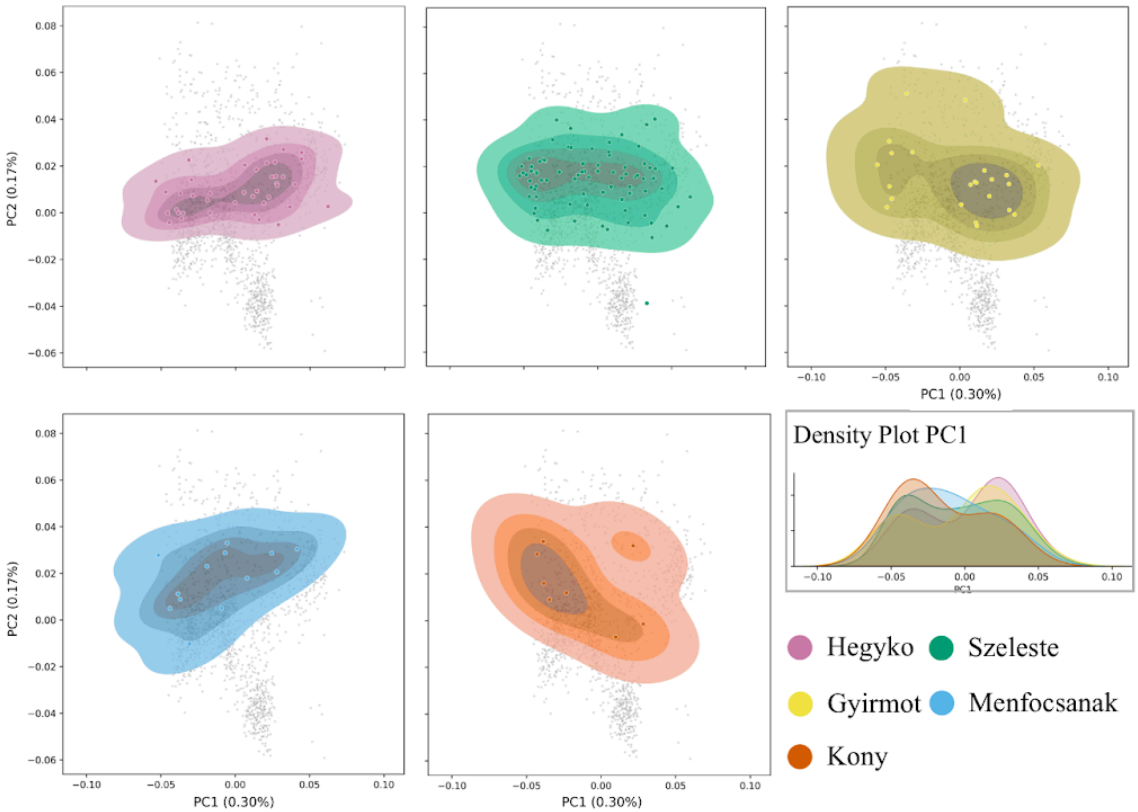


Fig. S28. Principal Component Analysis (PCA) of 6th-century CE populations. All samples from the five sites in the 6th century CE LHP are projected onto a POPRES reference panel using the methodology described in Materials and Methods. (a) PCA including all analyzed individuals. (b) PCA restricted to unrelated individuals, excluding those with biological relatedness up to the third degree.

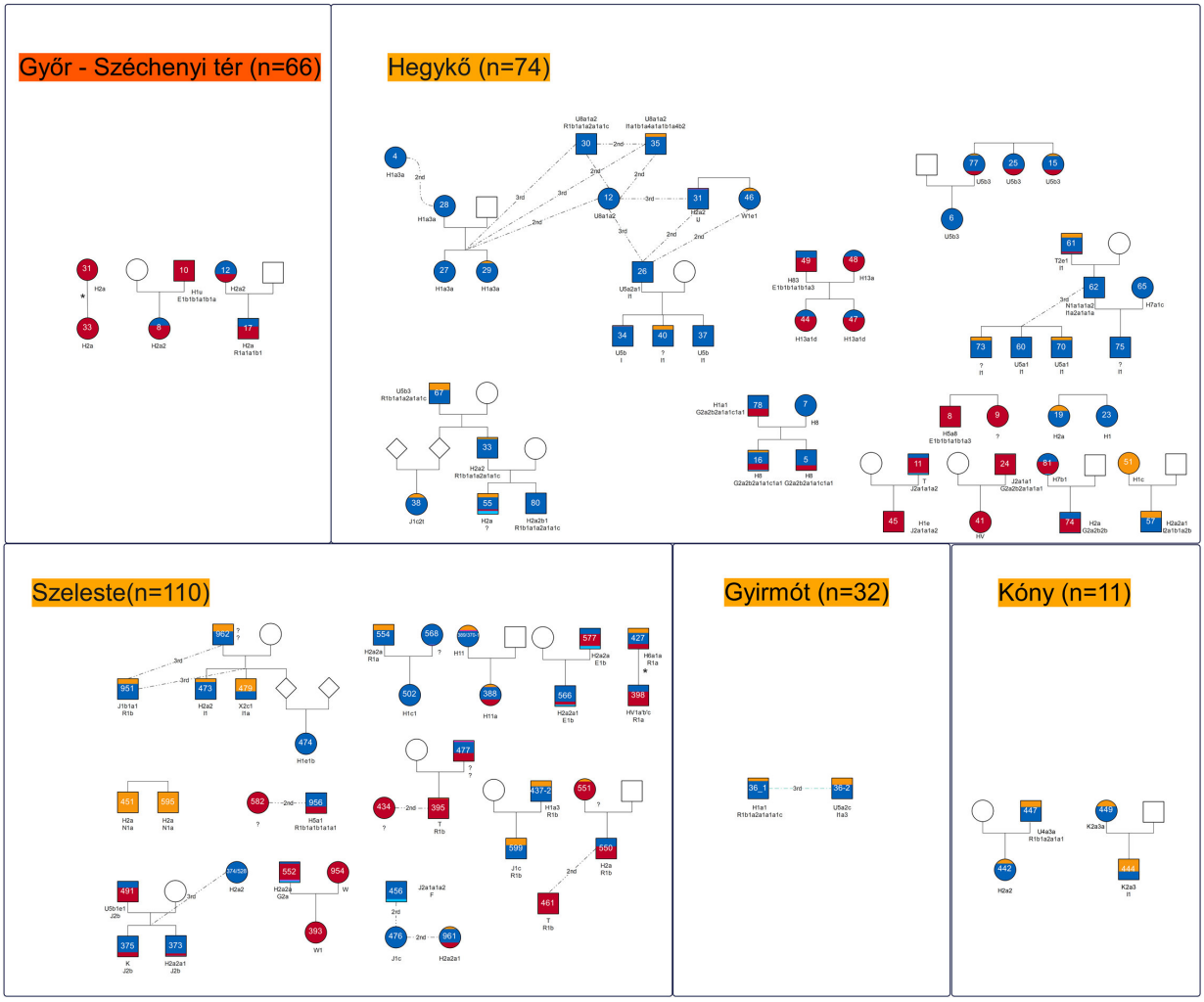


Fig. S29. Pedigrees identified across all LHP sites. Squares represent males and circles represent females. Fill colors indicate ancestry components inferred by fastNGSadmix using penecontemporaneous panels. Uniparental haplogroups are listed below each individual (mtDNA on top; Y-chromosome on bottom). Parent-offspring relationships with undetermined directionality are marked with an asterisk (*). Only relationships up to the third degree are displayed.

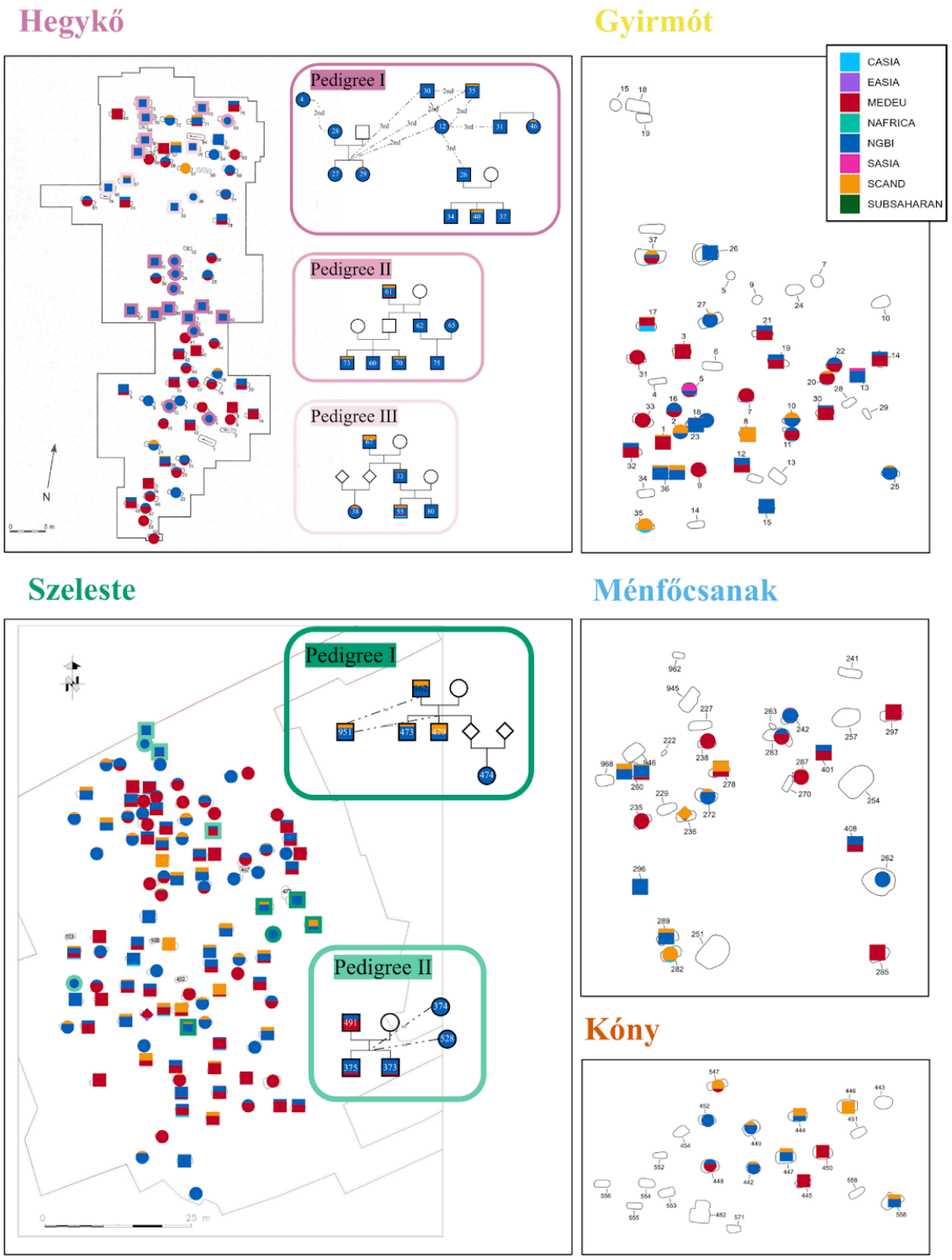


Fig. S30. Cemetery maps combined with genetic profiles for individuals in all the five 6th century CE sites. Burials are marked by genetic ancestries derived from fastNGSadmix analysis, with circles representing females and squares representing males. Large pedigrees (n>4) are highlighted, with scaled colors used to distinguish them within each cemetery map.

Supplementary Tables

Table S1. Meta information of newly reported data from all the sites in this study, including new aDNA and isotope results. (Excel file)
Table S2. Y haplogroup assignment for all the LHP males.(Excel file)
Table S3. Reference individuals used in qpAdm, qpWave and ancIBD analysis. (Excel file)
Table S4. FastNGSadmix point estimate and bootstrap results. (Excel file)
Table S5. Successful models from qpAdm analysis, including one-source and two-source models. (Excel file)
Table S6. Summary of qpAdm results for all newly reported individuals in this study. The source populations are the same as those used in the FastNGSadmix analysis. (Excel file)
Table S7. qpWave results for all the newly reported individuals (with coverage > 0.01x) from the 3rd-5th (Roman period) century CE. We used nine sources here. (Excel file)
Table S8. qpWave results for all newly reported individuals (with coverage > 0.01x) from the 6th century CE (post-Roman period). The analysis included the nine sources used for Roman-period individuals, supplemented with two additional sources. (Excel file)
Table S16. (Excel file) Measurement of environmental samples in this study. (Excel file)
Table S17. IBD connections identified in this study. Only connections including at least one segment greater than 12 cM are retained. (Excel file)
Table S18. Summary of the IBD connections identified in this study. (Excel file)
Table S21. lcMLkin results. (Excel file)
Table S22. KIN results and comparison with lcMLkin results. In the column lcMLkin_compare, a value of '1' indicates that the first-guess relatedness result matches the lcMLkin estimate. If not, the differing lcMLkin result or the reason for the discrepancy is reported. Comparisons were restricted to first-guess relatedness assignments within the third degree. (Excel file)

Mann-Whitney pairwise p=0.05 (red-after sequential Bonferroni significance)	Győr	Gyirmót	Hegykő	Kóny	Szeleste
Győr		3.652E-05	0.02548	2.356E-06	2.707E-09
Gyirmót	3.652E-05		0.0002664	0.1106	0.836
Hegykő	0.02548	0.0002664		1.809E-06	4.737E-08
Kóny	2.356E-06	0.1106	1.809E-06		0.04209
Szeleste	2.707E-09	0.836	4.737E-08	0.04209	

Table S9. Paired Mann-Whitney tests on $\delta^{13}C$ values between 5 sites

Mann-Whitney pairwise p=0.05 (red-after sequential Bonferroni significance)	Győr	Gyirmót	Hegykő	Kóny	Szeleste
Győr		1.641E-09	1.403E-14	0.005602	9.056E-13
Gyirmót	1.641E-09		0.02863	0.0003826	0.5206
Hegykő	1.403E-14	0.02863		2.284E-06	0.0001492
Kóny	0.005602	0.0003826	2.284E-06		0.000595
Szeleste	9.056E-13	0.5206	0.0001492	0.000595	

Table S10. Paired Mann-Whitney tests on $\delta^{15}N$ values between 5 sites.

Mann-Whitney pairwise p=0.05 (red-after sequential Bonferroni significance)	Hegykő-F	Hegykő-M	Szólád-F	Szólád-M	Szeleste-F	Szeleste-M	Kóny-F	Kóny-M	Gyirmót-F	Gyirmót-M
Hegykő-F		0.9436	0.0185	0.002005	0.0001	0.001367	0.04633	0.0009911	0.04712	0.01196
Hegykő-M	0.9436		0.02127	0.003707	0.0001627	0.00155	0.04506	0.001398	0.0614	0.01357
Szólád-F	0.0185	0.02127		0.8483	0.1736	0.571	0.4299	0.00742	0.9752	0.5926
Szólád-M	0.002005	0.003707	0.8483		0.1773	0.702	0.4269	0.009701	0.7896	0.9173
Szeleste-F	0.0001	0.000162 7	0.1736	0.1773		0.409	0.969	0.06572	0.2805	0.4472
Szeleste-M	0.001367	0.00155	0.571	0.702	0.409		0.6464	0.04992	0.7308	0.8695
Kóny-F	0.04633	0.04506	0.4299	0.4269	0.969	0.6464		0.1207	0.6671	0.6094
Kóny-M	0.0009911	0.001398	0.00742	0.009701	0.06572	0.04992	0.1207		0.05694	0.06269
Gyirmót-F	0.04712	0.0614	0.9752	0.7896	0.2805	0.7308	0.6671	0.05694		0.9529
Gyirmót-M	0.01196	0.01357	0.5926	0.9173	0.4472	0.8695	0.6094	0.06269	0.9529	

Table S11. Paired Mann-Whitney tests conducted on $\delta^{13}C$ values among five sites. focusing on adult males and females.

Tukey's Q pairwise p=0.05	Hegykő-F	Hegykő-M	Szólád-F	Szólád-M	Szeleste-F	Szeleste-M	Kóny-F	Kóny-M	Gyirmót-F	Gyirmót-M
Hegykő-F		0.0435	0.07774	1.528E-05	0.0207	0.002522	0.03201	3.344E-05	0.8707	0.07071
Hegykő-M			1	0.312	1	1	0.9454	0.1093	0.9894	1
Szólád-F				0.5574	1	1	0.9795	0.2165	0.9832	1
Szólád-M					0.1183	0.2755	1	0.995	0.08415	0.5092
Szeleste-F						0.9998	0.874	0.04531	0.995	1
Szeleste-M							0.961	0.1005	0.944	1
Kóny-F								0.9794	0.6356	0.9748
Kóny-M									0.02737	0.1919
Gyirmót-F										0.9845
Gyirmót-M										

Table S12. Paired Mann-Whitney tests conducted on $\delta^{15}N$ values among five sites. focusing on adult males and females

Mann-Whitney pairwise p=0.05 (red-after sequential Bonferroni significance)	Szólád-weapons	Szólád-no weapons	Hegykő-weapons	Hegykő-no weapons	Szeleste-weapons	Szeleste-no weapons
Szólád-weapons		0,9058	0,06559	0,000836	0,3448	0,4877
Szólád-no weapons	0,9058		0,1093	0,0005762	0,3216	0,328
Hegykő-weapons	0,06559	0,1093		0,07024	0,01614	0,04464
Hegykő-no weapons	0,000836	0,0005762	0,07024		8,564E-05	7,58E-06
Szeleste-weapons	0,3448	0,3216	0,01614	8,564E-05		0,8122
Szeleste-no weapons	0,4877	0,328	0,04464	7,58E-06	0,8122	

Table S13. Paired Mann-Whitney tests conducted on $\delta^{13}C$ values among three sites, focusing on males with weapons and other adults without weapons.

Tukey's Q pairwise p=0.05	Szólád-weapons	Szólád-no weapons	Hegykő-weapons	Hegykő-no weapons	Szeleste-weapons	Szeleste-no weapons
Szólád-weapons		0,04374	0,7297	2,384E-07	0,5012	0,001409
Szólád-no weapons			0,727	0,01849	0,7386	0,9902
Hegykő-weapons				0,000413	1	0,2576
Hegykő-no weapons					4,849E-05	0,004596
Szeleste-weapons						0,1713
Szeleste-no weapons						

Table S14. Paired Tukey's Q tests conducted on $\delta^{15}N$ values among three sites, focusing on males with weapons and other adults without weapons.

Sites	Age	Material	Type	Feature	87Sr/86Sr	
Kóny 85 Enese	TLBK	human bone	Femur	56	0.70984	0.00001
Kóny 85 Enese	no data	shell	Gastropoda	505/491 (Bag: 1125)	0.71056	0.00004
Kóny 85 Enese	no data	shell	Bivalvia	547/533 (Bag: 1427)	0.71087	0.00002
Kóny 85 Enese	no data	shell	Bivalvia	56/55 (Bag: 167)	0.71095	0.00005
Kóny 85 Enese	no data	shell	Bivalvia	300/286 (Bag: 560)	0.70975	0.00006
Kóny 85 Enese	no data	animal enamel	Sus domesticus	642/609 (Bag: 1059)	0.70989	0.00002
Kóny 85 Enese	no data	animal enamel	Sus domesticus	776 / 741 (Bag: 2158)	0.70998	0.00002
Kóny 85 Enese	no data	animal enamel	Sus scrofa	642 / 609 (Bag: 1059)	0.70990	0.00003

Table S15. ^{87}Sr /^{86}Sr values from the site Kóny 85 Enese

Group1	Group2	mtDNA		Y	
		P_Value	P_Adj_FDR	P_Value	P_Adj_FDR
Roman	Gyirmót	0.379962	0.379962	0.254375	0.479015
Roman	Hegykő	0.011299	0.158984	0.0016	0.023998
Roman	Kóny	0.20198	0.310469	0.058094	0.254975
Roman	Ménfőcsanak	0.132887	0.310469	0.450155	0.568693
Roman	Szeleste	0.361164	0.379962	0.10199	0.254975
Gyirmót	Hegykő	0.066993	0.261724	0.637036	0.682539
Gyirmót	Kóny	0.316168	0.36481	0.972203	0.972203
Gyirmót	Ménfőcsanak	0.069793	0.261724	0.255474	0.479015
Gyirmót	Szeleste	0.206979	0.310469	0.528947	0.610324
Hegykő	Kóny	0.168883	0.310469	0.422958	0.568693
Hegykő	Ménfőcsanak	0.265873	0.332342	0.083692	0.254975
Hegykő	Szeleste	0.021198	0.158984	0.020498	0.153735
Kóny	Ménfőcsanak	0.154085	0.310469	0.293171	0.488618
Kóny	Szeleste	0.166183	0.310469	0.454955	0.568693
Ménfőcsanak	Szeleste	0.254675	0.332342	0.09819	0.254975

Table S19. Pairwise Fisher's exact test results for mtDNA and Y-chromosome haplotypes across the LHP dataset. Note that the two Roman period sites were merged due to small sample size. P_Adj_FDR: p-values corrected for False Discovery Rate.

Group1	Group2	mtDNA		Y	
		P_Value	P_Adj_FDR	P_Value	P_Adj_FDR
Roman	Gyirmót	0.283472	0.327083	0.308569	0.473803
Roman	Hegykő	0.246675	0.308344	0.044796	0.262174
Roman	Kóny	0.094291	0.245761	0.081392	0.262174
Roman	Ménfőcsanak	0.166683	0.277806	0.443856	0.512141
Roman	Szeleste	0.642236	0.642236	0.071893	0.262174
Gyirmót	Hegykő	0.245775	0.308344	0.618338	0.662505
Gyirmót	Kóny	0.110089	0.245761	1	1
Gyirmót	Ménfőcsanak	0.012199	0.182982	0.286071	0.473803
Gyirmót	Szeleste	0.063894	0.245761	0.30317	0.473803
Hegykő	Kóny	0.137386	0.257599	0.426457	0.512141
Hegykő	Ménfőcsanak	0.371463	0.397996	0.315868	0.473803
Hegykő	Szeleste	0.114689	0.245761	0.052695	0.262174
Kóny	Ménfőcsanak	0.075992	0.245761	0.294471	0.473803
Kóny	Szeleste	0.044496	0.245761	0.415058	0.512141
Ménfőcsanak	Szeleste	0.20338	0.305069	0.087391	0.262174

Table S20. Pairwise Fisher's exact test results for mtDNA and Y-chromosome haplotypes across the LHP dataset, restricted to non-related individuals. Note that the two Roman period sites were merged due to small sample size. P_Adj_FDR: p-values corrected for False Discovery Rate.

	Szeleste (n=110)	Hegykő (n=74)	Szólad (n=36)	Gyirmót (n=32)	Ménfőcsanak (n=19)	Kóny (n=11)
Szeleste	NA	0	0	0.884	0.89	0.06
Hegykő	NA	NA	0.02	0.018	0.042	0.564
Szólad	NA	NA	NA	0.002	0.038	0.938
Gyirmót	NA	NA	NA	NA	1	0
Ménfőcsanak	NA	NA	NA	NA	NA	0
Kóny	NA	NA	NA	NA	NA	NA

Table S23. Pairwise comparison between 6th century sites including Szólád. Each cell displays the empirical p value derived from the resampling analysis.